Department of Applied Physics

Modelling design basis accidents LOCA and RIA from the perspective of single fuel rods

Asko Arkoma

Aalto University

DOCTORAL DISSERTATIONS

Aalto University publication series
DOCTORAL DISSERTATIONS 26/2018
VTT SCIENCE 170

Modelling design basis accidents LOCA and RIA from the perspective of single fuel rods

Asko Arkoma

A doctoral dissertation completed for the degree of Doctor of Science (Technology) to be defended, with the permission of the Aalto University School of Science, at a public examination held at the lecture hall H304 of the school on 8 March 2018 at 1 p.m.

Aalto University
School of Science
Department of Applied Physics

Supervising professor
Professor Filip Tuomisto, Aalto University, Finland

Thesis advisor
Dr. Anitta Hämäläinen, VTT Technical Research Centre of Finland Ltd

Preliminary examiners
Dr. Lars Olof Jernkvist, Quantum Technologies AB, Sweden
Dr. Joshua Kaizer, United States Nuclear Regulatory Commission, USA

Opponent
Dr. Inmaculada C. Sagrado García, Centro de Investigaciones Energéticas, Medioambientales y Tecnológicas, Spain

Aalto University publication series
DOCTORAL DISSERTATIONS 26/2018

VTT SCIENCE 170

ISBN 978-952-60-7846-5 (printed)
ISBN 978-952-60-7847-2 (pdf)
ISSN-L 1799-4934
ISSN 1799-4934 (printed)
ISSN 1799-4942 (pdf)
http://urn.fi/URN:ISBN:978-952-60-7847-2

ISBN 978-951-38-8617-2 (printed)
ISBN 978-951-38-8616-5 (pdf)
ISSN-L 2242-119X
ISSN 2242-119X (printed)
ISSN 2242-1203 (pdf)
http://urn.fi/URN:ISBN:978-951-38-8616-5

Unigrafia Oy
Helsinki 2018

Finland

NORDIC ECOLABEL
441 697
Printed matter

Author
Asko Arkoma

Name of the doctoral dissertation
Modelling design basis accidents LOCA and RIA from the perspective of single fuel rods

Publisher School of Science

Unit Department of Applied Physics

Series Aalto University publication series DOCTORAL DISSERTATIONS 26/2018

Field of research Engineering Physics

Manuscript submitted 12 September 2017 **Date of the defence** 8 March 2018

Permission to publish granted (date) 22 November 2017 **Language** English

☐ **Monograph** ☒ **Article dissertation** ☐ **Essay dissertation**

Abstract

When designing a nuclear power plant and its fuel, certain accidents are postulated to occur with a predetermined low frequency. The consequences of these accidents are mitigated by various passive and active safety features, and an adequate safety level is implemented by the regulatory authority in the safety requirements.

The dissertation considers computational modelling of two main design basis accidents in current light water reactors: loss-of-coolant accident (abbreviated LOCA) and reactivity initiated accident (RIA). The applied computer programmes are designed for modelling the behaviour of a single fuel rod in transient and accident conditions.

LOCA modelling is focused on developing a statistical analysis methodology for the evaluation of fuel failures in LOCA. The statistical system is applied to a large break LOCA in an EPR type reactor, and fulfilment of the regulations included in the Regulatory Guides on nuclear safety set by the Finnish nuclear safety authority STUK is studied. In order to determine the underlying factors affecting the fuel rod failures, a sensitivity analysis is performed. A systematic multistage procedure is developed for the sensitivity analysis.

RIA modelling focuses on adaptation of the single rod RIA modelling code SCANAIR for boiling water reactor (BWR) conditions. The SCANAIR code, developed by the French research organisation Institut de Radioprotection et de Sûreté Nucléaire (IRSN), is specifically designed for modelling RIAs in pressurized water reactors (PWRs). In this dissertation, the code is adapted to take into account BWR specific properties and conditions.

Keywords loss-of-coolant accident, reactivity initiated accident, fuel rod modelling

ISBN (printed) 978-952-60-7846-5 **ISBN (pdf)** 978-952-60-7847-2

ISSN-L 1799-4934 **ISSN (printed)** 1799-4934 **ISSN (pdf)** 1799-4942

Location of publisher Helsinki **Location of printing** Helsinki **Year** 2018

Pages 148 **urn** http://urn.fi/URN:ISBN:978-952-60-7847-2

Aalto-yliopisto

Tiivistelmä

Aalto-yliopisto, PL 11000, 00076 Aalto www.aalto.fi

Tekijä
Asko Arkoma

Väitöskirjan nimi
Suunnitteluperusteisten onnettomuuksien (LOCA ja RIA) mallinnus yksittäisten polttoainesauvojen näkökulmasta

Julkaisija Perustieteiden korkeakoulu

Yksikkö Teknillisen fysiikan laitos

Sarja Aalto University publication series DOCTORAL DISSERTATIONS 26/2018

Tutkimusala Teknillinen fysiikka

Käsikirjoituksen pvm 12.09.2017 **Väitöspäivä** 08.03.2018

Julkaisuluvan myöntämispäivä 22.11.2017 **Kieli** Englanti

☐ **Monografia** ☒ **Artikkeliväitöskirja** ☐ **Esseeväitöskirja**

Tiivistelmä

Ydinvoimalaitoksen ja siellä käytettävän polttoaineen suunnittelussa on oletettu tiettyjen onnettomuuksien esiintyvän ennalta määritetyllä harvalla tapahtumataajuudella. Erilaiset passiiviset ja aktiiviset turvallisuusominaisuudet lieventävät näiden oletettujen onnettomuuksien seurauksia, ja säteilyturvaviranomaisen turvallisuusvaatimukset toimeenpanevat riittävän turvallisuustason.

Väitöskirjassa käsitellään nykyisten kevytvesireaktoreiden suunnitteluperusteisten onnettomuuksien kahden päätyypin laskennallista mallintamista: jäähdytteenmenetysonnettomuus (lyhennettynä LOCA) ja reaktiivisuusonnettomuus (RIA). Käytettävät tietokoneohjelmat on suunniteltu mallintamaan yksittäisen polttoainesauvan käyttäytymistä transientti- ja onnettomuustilanteissa.

LOCA-mallinnus keskittyy tilastollisen analyysimenetelmän kehittämiseen LOCA:ssa vaurioituvien polttoainesauvojen arvioimiseksi. Tilastollista menetelmää sovelletaan EPR-tyyppisen reaktorin isoon jäähdytteenmenetysonnettomuuteen, ja tutkitaan Suomen säteilyturvaviranomaisen STUKin asettamien ydinturvallisuusohjeiden täyttämistä. Polttoainesauvojen rikkoutumisten taustatekijöiden selvittämiseksi tehdään herkkyysanalyysi. Herkkyysanalyysille on kehitetty monivaiheinen systemaattinen menetelmä.

RIA-mallinnus keskittyy RIA-polttoainekoodi SCANAIR:n mukauttamiseen kiehutusvesireaktorin (BWR) olosuhteisiin. Ranskalaisen Institut de Radioprotection et de Sûreté Nucléaire (IRSN) -organisaation kehittämä SCANAIR-koodi on suunniteltu erityisesti RIA:n mallinnukseen painevesireaktoreissa (PWR). Tässä väitöskirjassa mallinnuskoodi on mukautettu ottamaan huomioon BWR:n ominaisuudet ja olosuhteet.

Avainsanat jäähdytteenmenetysonnettomuus, reaktiivisuusonnettomuus, polttoainemallinnus

ISBN (painettu) 978-952-60-7846-5 **ISBN (pdf)** 978-952-60-7847-2

ISSN-L 1799-4934 **ISSN (painettu)** 1799-4934 **ISSN (pdf)** 1799-4942

Julkaisupaikka Helsinki **Painopaikka** Helsinki **Vuosi** 2018

Sivumäärä 148 **urn** http://urn.fi/URN:ISBN:978-952-60-7847-2

Acknowledgments

The research presented in this dissertation was carried out under the auspices of the Finnish Research Programmes on Nuclear Power Plant Safety – SAFIR2010, SAFIR2014 and SAFIR2018, in the projects POKEVA, PALAMA, PANCHO and USVA. A VTT grant was used for finalizing the compiling part of the dissertation. The statistical LOCA analysis presented in Publication **II** was delivered to the Finnish nuclear safety authority STUK under the contract 5/2600/2013.

IRSN, the developer and owner of the SCANAIR software, is gratefully acknowledged for granting VTT the right to use SCANAIR for the RIA studies.

I would like to thank Professor Filip Tuomisto for supervising the thesis, and Professor Emeritus Rainer Salomaa who was the first supervising professor. Research team leader Dr. Anitta Hämäläinen, acting as a thesis advisor, gave guidance to thermal hydraulics modelling which is very important in both LOCA and RIA fuel performance simulations. The research work was carried out in projects led by Mr. Seppo Kelppe, Dr. Ville Tulkki and Dr. Timo Ikonen, and they also instructed the research work. I express my gratitude to the preliminary examiners, Dr. Lars Olof Jernkvist and Dr. Joshua Kaizer, for providing valuable comments and suggestions how to improve the summary part of the dissertation.

I would also like to thank all the co-authors of the publications included in this thesis. Mr. Jukka Rintala created the basis for the statistical system presented and applied in the LOCA simulations. Concerning Publication **II**, the boundary conditions for the LOCA fuel performance simulations originated from system code simulations carried out by Dr. Markku Hänninen, and Mr. Joona Kurki improved the system code model for this work. The reactor physics calculations needed for Publication **II** were performed by Dr. Karin Rantamäki. All the co-authors gave valuable comments in order to improve the manuscript of Publication **II**. In the peer-review process of that article, the two anonymous reviewers gave many constructive comments, and as a result, several additions were implemented to the manuscript. Concerning Publication **III**, Dr. Timo Ikonen instructed the research work, and had a substantial contribution to the writing. Dr. Alain Moal and Dr. Vincent Georgenthum from IRSN instructed the research work presented in Publication **V**. I thank IRSN for the opportunity to perform the studies of Publication **V** at IRSN in Cadarache, France, during my six-month researcher posting.

The language of the summary part of the dissertation has been checked by the company Semantix.

Espoo, 23 January 2018,

Asko Arkoma

List of publications

This thesis is based on the following original publications which are referred to in the text as I–VI. The publications are reproduced with kind permission from the publishers.

I Arffman, A. (currently Arkoma, A.), Rintala, J., 2011. Statistical analysis of fuel failures in accident conditions. In proceedings of: Water Reactor Fuel Performance Meeting/LWR/TopFuel, Chengdu, China, September 11-14, 2011, Paper T3-028.

II Arkoma, A., Hänninen, M., Rantamäki, K., Kurki, J., Hämäläinen, A., 2015. Statistical analysis of fuel failures in large break loss-of-coolant accident (LBLOCA) in EPR type nuclear power plant. Nuclear Engineering and Design, Vol. 285, pp. 1–14.

III Arkoma, A., Ikonen, T., 2016. Sensitivity analysis of local uncertainties in large break loss-of-coolant accident (LB-LOCA) thermo-mechanical simulations. Nuclear Engineering and Design, Vol. 305, pp. 293-302.

IV Arkoma, A., Ikonen, T., 2016. Statistical and sensitivity analysis of failing rods in EPR LB-LOCA. In proceedings of: TopFuel 2016, Boise, Idaho, USA, September 11-15, 2016, Paper 17570.

V Arffman, A. (currently Arkoma, A.), Moal, A., Georgenthum, V., 2012. Evaluation and adaptation of the RIA code SCANAIR for modelling BWR fuel and conditions. In proceedings of: TopFuel 2012, Manchester, United Kingdom, September 2-6, 2012, Paper A0089.

VI Arkoma, A., 2017. Extending the reactivity initiated accident (RIA) fuel performance code SCANAIR for boiling water reactor (BWR) applications. Nuclear Engineering and Design, Vol. 322, pp. 192–203.

Author's contributions

Publication I: Statistical analysis of fuel failures in accident conditions

The author is the primary author of the manuscript, and he conducted the research work presented in the peer-reviewed conference paper.

Publication II: Statistical analysis of fuel failures in large break loss-of-coolant accident (LBLOCA) in EPR type nuclear power plant

The author is the primary author of the manuscript, and he conducted the statistical fuel behaviour simulations presented in the article.

Publication III: Sensitivity analysis of local uncertainties in large break loss-of-coolant accident (LB-LOCA) thermo-mechanical simulations

The author is the primary author of the manuscript, and he conducted the studies presented in the article. The author wrote the initial version of the paper.

Publication IV: Statistical and sensitivity analysis of failing rods in EPR LB-LOCA

The author is the primary author of the manuscript.

Publication V: Evaluation and adaptation of the RIA code SCANAIR for modelling BWR fuel and conditions

The author is the primary author of the manuscript, and he conducted the research work presented in the peer-reviewed conference paper.

Publication VI: Extending the reactivity initiated accident (RIA) fuel performance code SCANAIR for boiling water reactor (BWR) applications

The author is the only author of the manuscript.

Contents

List of symbols

β	confidence level
γ	probability content
ΔT_L	Leidenfrost temperature difference
δ_i	Borgonovo's delta (for the i:th input variable)
ε	strain
ρ	Pearson linear correlation coefficient
σ	stress; standard deviation
$coeff_{assembly}$	fuel assembly power coefficient
E, E_{X_i}	expectation value
e_0	as-fabricated cladding thickness
e_{ZrO_2}	zirconia layer thickness
F	hydrogen pick-up
H	hydrogen
N	number of simulations
$P_{assembly}$	fuel assembly power
$P_{channel}$	coolant channel power in APROS
R^2	squared Pearson correlation coefficient; coefficient of determination (Section 3.2.1)
$R_{p0.2}$	0.2% offset yield strength
S_i	first order Sobol' sensitivity index (for the i:th input variable)
T_{sat}	saturation temperature
X_i	i:th input variable
Y	output parameter

1. Introduction

The fissile material in current nuclear reactors is in the form of ceramic uranium dioxide or mixed oxide pellets that are stacked in hermetically sealed corrosion-resistant tubes, i.e. cladding. Fuel rods are then grouped into fuel assemblies (Bailly et al., 1999; Rahn et al., 1984). To prevent the radioactive material from being released to the coolant, the integrity of the cladding tube should be ensured. This assessment is supported by simulations performed with designated computer programmes, herein “codes”. The range of calculation tools varies from system codes modelling even the operation of the whole nuclear power plant, to neutronics codes and thermal hydraulics codes designated for more specialized functions. In addition to these, the entity of a single fuel rod in conjunction with the thermal hydraulics of the surrounding coolant forms a basic unit for fuel performance modelling.

In addition to normal operation, the design basis scenarios of a nuclear reactor include anticipated operational occurrences, postulated accidents, and so-called design extension conditions (STUK, 2013). Postulated accidents are defined to be off-normal events that occur less often than once in a hundred operating years, and that do not cause severe fuel failure (STUK, 2013). When considering the fuel behaviour, there are two main types of postulated design basis accidents of interest: loss-of-coolant accidents (abbreviated as LOCA) and reactivity initiated accidents (RIA).

Postulated accidents and transients naturally cannot be studied in-situ in power reactors. Therefore, various test reactors and separate effects programmes designed for special purposes, for example to study fuel mechanical properties or coolant behaviour, have been realized. When conducting in-reactor tests in research reactors, new information and understanding concerning the fuel behaviour is gained. However, the set-up and the conditions in a test reactor differ from those in a power reactor. Therefore, transient fuel performance codes are important tools in transforming the integral and separate effect test results into the expected outcomes of transients and postulated accidents in commercial reactors. With the combination of testing and simulations, the safe operation of nuclear reactors can be ensured in all design situations.

In order to acquaint the reader with the design basis accidents discussed in this thesis, the basics of LOCA and RIA are next described. More information can be

found from the latest state-of-the-art reports on LOCA (OECD/NEA, 2009b) and RIA (OECD/NEA, 2010).

1.1 Loss-of-coolant accidents

In LOCAs, cooling of the reactor core is diminished by a break in a coolant pipe of a coolant circulation loop. For each main reactor type, distinct design scenarios of LOCA may be defined. Furthermore, LOCAs may be categorized into small break (SB-LOCA) and large break LOCAs (LB-LOCA) based on the break size; for example, a small break LOCA in a pressurized water reactor (PWR) has a break size typically less than 1 ft^2 (0.093 m^2) (OECD/NEA, 2009b). The emergency cooling systems are designed to mitigate the effects of LOCAs, so that the radiological consequences would be minimized.

After the break in a coolant loop, the system pressure decreases and reactor scram occurs. The impaired cooling causes the temperature to rise, and consequently, the fuel rod internal pressure increases. The elevated temperature may also cause the gaseous fission products inside the fuel matrix to be released to the gas gap between the pellet and cladding, further increasing the rod internal pressure. As the coolant pressure drops, the fuel rod internal pressure becomes considerably higher than the surrounding pressure. Consequently, the cladding may undergo non-reversible plastic deformation, that is, it may balloon outwards and eventually burst.

As a consequence of the temperature transient, the zirconium cladding alloy may go through a phase transformation from alpha to beta phase. However, the dissolved oxygen stabilizes part of the alpha phase, resulting in a brittle structure. In addition, the cladding metal is consumed by the high temperature oxidation occurring at the cladding outer surface, and the remaining metal suffers from hydrogen pickup, which further embrittles the cladding. If the fuel rod survives the high temperature phase without bursting, the embrittled cladding may still fail during or after the rewetting due to stresses caused by the quenching (OECD/NEA, 2009b).

1.2 Reactivity initiated accidents

In RIA, the reactivity of the core or part of it is abruptly increased, inducing a sharp power pulse which may cause fuel rod failures and consequent release of radioactive material to the coolant. The shattered fuel pellet fragments give rise to steam generation, and in the worst case this initiates a pressure pulse which can damage the surrounding fuel assemblies and possibly the whole core.

There are distinct initializing events of an RIA in different light water reactor (LWR) types. In a boiling water reactor (BWR), a control rod drop causes a sudden increase in reactivity, and in a PWR, the same happens if the control rod ejects from the core. The cause of these accidents is a mechanical fault in the drive mechanism or housing of the control rods, and as a result, the control rod assembly drops out of the core by gravity in a BWR or ejects by pressure in a PWR. Another postulated

cause of reactivity insertion is the so-called boron dilution accident. Boron has a high thermal neutron absorption cross-section, and therefore boric acid is added to the coolant water in PWRs for chemical shim. If the borated water is somehow diluted with pure water, conditions for an RIA may become possible.

In modern LWRs, RIAs are prevented primarily by a built-in safety feature: increase in fuel temperature induces a negative reactivity feedback which limits the peak power. In addition, the plant design, including both automation and operation procedures, averts the accident.

The extremely narrow time scale of the reactivity initiated accident sets additional demands on the fuel modelling code. The thermo-mechanical models need to be adapted for fast transient conditions.

1.3 Objectives and scope

The research theme of this dissertation is to develop and apply enhanced methods for computational modelling of design basis accidents in LWRs. The dissertation covers the two main design basis accidents, LOCA and RIA.

The LOCA part of the dissertation is focused on development and application of a statistical methodology for core-wide fuel performance code simulations of an LB-LOCA. There are two research questions related to the performed LOCA modelling. Does the number of failing fuel rods in LB-LOCA of an EPR type reactor remain below the 10% limit set by the safety authority? How can the factors affecting the fuel rod failures in an LB-LOCA be disclosed based on the simulation results from a complex calculation chain of several codes? Publications **I-IV** address these questions. The developed statistical LOCA method is described in Publication **I**, and an application of the method is presented in Publications **II** and **IV**. It is also important to bring out the underlying factors affecting the rod failures, and therefore a sensitivity analysis procedure is outlined and adopted (Publications **III** and **IV**). Prior to this dissertation, there has not been any systematic statistical method in Finland to confirm that the safety regulations (STUK, 2013) are fulfilled.

In RIA modelling, the focus is on adaptation of the single rod RIA modelling code SCANAIR for BWR fuel and conditions. The SCANAIR code, developed by the French research organization Institut de Radioprotection et de Sûreté Nucléaire (IRSN), is specifically developed for modelling RIAs. Due to the fact that the whole nuclear fleet in France consists of PWRs, the code has been developed and tuned for that reactor type. Which modifications to the code are needed in order to be able to model BWR RIA with SCANAIR? How well does SCANAIR perform in modelling BWR RIAs? These matters are discussed in Publications **V** and **VI**. Cladding material properties, cladding failure estimations, and the thermal hydraulics are considered. Cladding yield strength correlations for BWR fuel cladding are developed based on experimental data, and implemented into SCANAIR (Publication **V**). The capability of SCANAIR to predict BWR cladding low temperature failures is estimated, and the uncertainty of the results is brought out (Publication **VI**). The standard thermal hydraulics model in SCANAIR is not suitable for the simulation of a

BWR RIA, as it is one-dimensional and able to model single phase coolant only. In order to address this issue, SCANAIR is here coupled with the general thermal hydraulics code GENFLO developed at VTT, and the first results are presented (Publication **VI**). The RIA topic is important in general terms, as few or none of the transient fuel behaviour codes can handle excessive steam generation in BWR RIA (Marchand et al., 2016), and domestically, as there are two operating BWR units in Finland.

1.4 Structure of the dissertation

The statistical and sensitivity analyses of LB-LOCA are presented in Section 2, and the RIA studies in Section 3. Within both subject areas, the background and state-of-the-art of research are brought out. A separate sub-section is devoted to each research problem, i.e. the statistical LOCA analysis, sensitivity analysis of LOCA, BWR cladding material properties in RIA, BWR cladding low temperature failure estimation, and the thermal hydraulics modelling in BWR RIA. In each of these sub-sections, the research contribution, results and discussion are presented. Finally, the overall conclusions and the consequential proposals for prospective future work for both LOCA and RIA modelling are presented in Section 4.

2. Statistical and sensitivity analysis of loss-of-coolant accidents (LOCA)

2.1 Background

The Regulatory Guides on nuclear safety set by the Finnish nuclear safety authority STUK introduce a number of design criteria that the fuel must fulfil in accident conditions (STUK, 2013). Among others, the following criteria are applicable in LOCA conditions: less than 10% of the rods in the reactor may fail (herein failure means the loss of fuel rod integrity), and the peak cladding temperature should not exceed 1200 ºC. The estimation of the fraction of failing rods is traditionally based on conservative analyses, but this approach has several downsides. Sometimes it is hard to judge whether the assumptions are conservative because the phenomena in the reactor are highly non-linear. Additionally, conservative methods often lead to excessive margins and in this way to economic losses.

As a result, statistical best-estimate methods have acquired an established position during recent decades. The development started worldwide when the United States Nuclear Regulatory Commission (U.S.NRC) revised its rules in 1988 (U.S.NRC, 1988) and allowed realistic Best Estimate Plus Uncertainty (BEPU) methods alongside the old conservative approach. In Finland, the accepted methods are the conservative analysis method supplemented with sensitivity studies, or alternatively, the best estimate method supplemented with uncertainty analysis (STUK, 2013).

Statistical best-estimate methods are based on the selection and variation of parameters that are important in accident conditions. The accident scenario is simulated with a designated computer programme several times with different parameter values between the simulations, and in this way an estimation of the number of failed rods is obtained. In order for the results to be statistically reliable, an enormous number of simulation runs is needed. Thus, the analysis requires considerable computational resources, which has been a limiting factor for the breakthrough of statistical methods. Various approaches have been used to reduce the number of simulation code calculations.

BEPU methods have been used both in licensing and in safety analyses. Recent fuel or thermal hydraulics -related uncertainty and/or sensitivity studies have been made, for example, by Bouloré et al. (2012), Di Maio et al. (2014), Feria and Herranz (2015), Freixa et al. (2012), Gamble and Swiler (2016), Keresztúri et al. (2016), Klouzal et al. (2016), Li et al. (2015), Marcum and Brigantic (2015), Pourgol-Mohammad et al. (2016), Queral et al. (2015), Sagrado and Herranz (2013), Trivedi et al. (2012), Wang et al. (2013), Wanninger et al. (2016), Zhao and Mousseau (2012), Zio and Pedroni (2012). The uncertainty and sensitivity analysis is, or has been, an integrated part of the recent OECD Nuclear Energy Agency's (NEA) benchmark programmes: UAM (Blyth et al., 2012), BEMUSE (de Crécy et al., 2008; OECD/NEA, 2007, 2009a; Perez et al., 2011) and RIA codes benchmark Phase II (OECD/NEA, 2017).

2.1.1 Statistical analysis

Code, Scaling, Applicability, and Uncertainty (CSAU) methodology (TPG, 1989) was the first systematic procedure for conducting BEPU analyses, and variations of the methodology are still widely used, e.g in the BEMUSE programme (de Crécy et al., 2008). The first uncertainty analysis made with the CSAU was performed by Boyack et al. (1990), Lellouche et al. (1990), Wilson et al. (1990), and Wulff et al. (1990). With the contribution of U.S.NRC, a group of experts developed this three-step method to meet the new regulations. In the first phase, the accident scenario is divided into distinct segments by place and by the course of the accident, and then important phenomena and the corresponding parameters are recognized for each place and time. The second phase consists of evaluation of the fuel performance code and its ability to model the identified phenomena. In addition, the distributions of the related parameters are qualified. The third phase is to combine the uncertainty distributions with a chosen method.

Depending on the method of the last phase of the CSAU process, the number of varied input parameters may need to be limited. In the original CSAU procedure, the use of a polynomial surrogate model, i.e. response surfaces, was demonstrated to be suitable for combining the uncertainties. Response surfaces are still widely in use, and were recently applied e.g. by Feria and Herranz (2015), Keresztúri et al. (2016), and Wang et al. (2013). It is a parametric method, and only a limited number of input parameters may be used for fitting the model. By contrast, with the so-called nonparametric statistics, the number of input parameters is not limited. In addition, more advanced surrogate methods may be applied, such as neural networks, applied e.g. by Bouloré et al. (2012) and Secchi et al. (2008), and support vector machines. After building a surrogate model with the help of a limited amount of calculations with the simulation code, a large number of Monte Carlo sampled values may be fed through the model with little computational cost. Surrogate models are used in both uncertainty and sensitivity analyses.

The selection of parameters is often carried out with the Phenomena Identification and Ranking Table (PIRT) (TPG, 1989). There are numerous sources of uncertainties in fuel behaviour modelling. In addition to uncertainties in input and model parameters and in initial and boundary conditions, uncertainties stem from numerical parameters such as nodalization and convergence criteria, the use of alternative models in codes, and various user effects. In many cases the latter ones are not considered in uncertainty analyses (de Crécy et al., 2008).

Even setting the input parameter nominal values, not to mention defining their distributions, is not an easy task. As an example, the pre- and post-test thermal hydraulic analysis performed by Freixa et al. (2012) highlights the difficulty in setting the input parameter values in blind calculations. In pre-test simulations, the output uncertainty bands did not manage to capture the experimental results, but after small changes in the nodalization, modification of one input parameter value, and activating a certain model, good agreement with the experimental results was obtained. Thus, it should be kept in mind that most often not all the sources of uncertainties are included in the analysis.

The uncertainty distributions may be defined by various methods, for example based on measurements, experiments, or expert judgment. Inverse methods, in which the model parameter uncertainties are defined in such a way that the result leads to the known output uncertainty interval (Bouloré et al., 2012), are also applicable. Another type of method is the Input Parameter Range Evaluation Methodology (IPREM) developed at the University of Pisa (Kovtonyuk et al., 2017).

Various sampling techniques are available for extracting the values from the distributions; e.g. random sampling, Latin hypercube sampling, orthogonal sampling, and quasi-random sampling methods such as Sobol' sequences (Sobol', 1967). Most often, the two first mentioned are used in this context. Unlike in random sampling, in Latin hypercube sampling it must be decided in advance how many sample points are used, and a record must be kept of the points already sampled (Roberts and Sanders, 2013).

Gesellschaft für Anlagen- und Reaktorsicherheit (GRS) introduced (Hofer et al., 1985) the use of the Wilks' theorem (Wilks, 1941, 1942) to determine the minimum number of required simulations. In conjunction with the tolerance interval theory (order-statistics, nonparametric statistics), the Wilks' formula provides a way to determine the number of simulations that are needed for the statistical analysis when the probability content and the confidence level are predetermined. For example, the nuclear industry companies Westinghouse (Frepoli, 2008; Frepoli and Ohkawa, 2011; Frepoli et al., 2004, 2010) and Areva (Abdelghany and Martin, 2010; Martin and O'Dell, 2008) have both developed statistical methods based on the CSAU procedure, with the results of nonparametric statistics chosen to be the final step to combine the uncertainty distributions.

In brief, the number of calculations can be solved as follows. To start with, *N* sets of initial parameter values are sampled from their corresponding distributions. The distribution of the result parameter is an unknown function, here denoted by *f(y)*. With the tolerance interval method, the upper and lower limits in the distribution *f(y)* are chosen in such a way that a given probability content γ would be inside those limits with a confidence level β. This is expressed as (Guba et al., 2003; Panka and Keresztúri, 2007):

$$P\left(\int_L^U f(y)dy > \gamma\right) = \beta. \qquad (2.1)$$

A set of result parameter values picked from the unknown distribution *f(y)* is arranged in ascending order. When the minimum value is marked with index *r* and the maximum value with index *s*, Eq. (2.1) may be written:

$$\beta = 1 - \sum_{j=s-r}^{N} \binom{N}{j} \gamma^j (1-\gamma)^{N-j}. \qquad (2.2)$$

In the case of a one-sided tolerance interval, the lower bound *L* is chosen to be $-\infty$ (*r=0*) and the upper bound *U* is the highest value (in first order formulation) in the random sample picked from the distribution (*s=N*). Thus, inserting *r=0* and *s=N* into Eq. (2.2), one gets the relation known as the Wilks' formula:

$$\beta = 1 - \gamma^N. \quad (2.3)$$

This equation is nowadays widely used by the nuclear community. When Eq. (2.3) is applied to safety evaluations, the generally acceptable level is 95% probability with 95% confidence that the number of failed rods would not overstep the permitted limit. These figures are also stated in the Finnish Regulatory Guides on nuclear safety, guide B.3 (STUK, 2013). When the corresponding values are inserted into Eq. (2.3), the number of cases comes out as 59. The number of calculations is independent of the number of initial parameters included in the analysis. Furthermore, the figure is valid for one output quantity, and in the analysis presented in this dissertation, only one output is of interest, i.e. the total number of failing rods.

Taking the highest value gives the first order estimation, but if one can afford more simulations, taking into account the computational burden, one can select the second highest value (or third highest, etc.). The numbers of simulations in the first, second, third and fourth order are 59, 93, 124 and 153, respectively. As the number of simulations increases, the conservatism in the estimated tolerance limit decreases (Arimescu, 2012; Martin and Nutt, 2011). The unnecessary amount of conservatism in the lowest number of simulations may be seen as a disadvantage (Abdelghany and Martin, 2010). Another benefit of using higher order methods is that a certain number of failed simulations is allowed, that is, one failed simulation for the second order method, two for the third order, etc. (OECD/NEA, 2007). For example at the Korea Institute of Nuclear Safety (KINS), BEPU and sensitivity analyses have been applied to both LOCA (Kang, 2016; Lee and Woo, 2013, 2014) and RIA (Lee, 2016; Lee and Woo, 2015) by using one-sided, third order Wilks' formula with 124 simulations.

In addition to Wilks' method, other order-statistics methods also exist, as pointed out by Martin and Nutt (2011). These are the Wald and Guba method, Tukey method, bracketing method, and Wallis and Nutt testing method. Another type of approach has been developed at the University of Pisa and applied in the BEMUSE programme (de Crécy et al., 2008; OECD/NEA, 2011). This method extrapolates the differences between the code predictions and the experiments, and makes use of a large experimental database.

2.1.2 Sensitivity analysis

Sensitivity analysis methods are classified into three types: local, regional and global (Saltelli et al., 2000). Local sensitivity of the output is obtained when one input parameter is perturbed at a time, while others remain in their reference values. Global sensitivity takes into account all the uncertain input parameters simultaneously. Regional sensitivity is calculated by reducing the input uncertainty ranges, and by studying how this affects the output uncertainty (Di Maio et al., 2014; Pourgol-Mohammad et al., 2016). Unlike local and regional sensitivity analysis, global sensitivity analysis is capable of handling non-linear and non-monotone models

(Saltelli et al., 2008). However, global methods have higher computational cost (Di Maio et al., 2014).

The available sensitivity analysis methods were elaborated by Iooss and Lemaître (2015), Borgonovo and Plischke (2016), and Ikonen (2015, 2016). There are various ways to categorize the sensitivity analysis methods. Borgonovo (2006) categorized uncertainty indicators into nonparametric techniques, screening methods, variance-based methods, and moment independent approaches. In addition, Di Maio et al. (2014) cited other global sensitivity analysis methods: the response surface methodology and the Fourier Amplitude Sensitivity Test (FAST). In FAST, a Fourier series surrogate model is composed, and its coefficients and frequencies may be used to estimate the partial variances of the individual input parameters (Di Maio et al., 2014).

Next, the available screening methods and the most common quantitative sensitivity indices are introduced.

2.1.2.1 Screening methods

In screening analysis, the most influential input parameters to the output are identified (Wanninger et al., 2016). Information on the nature of the dependency between the input and the output is also gained. Various screening methods exist, but most of them would require performing new sets of simulations, and many are computationally expensive (Iooss and Lemaître, 2015). The screening methods mentioned are (Iooss and Lemaître, 2015):

- One At a Time (OAT): one input is varied at a time and other inputs are fixed.
- Morris method: classification of inputs into three groups based on significance/linearity/interactions (Iooss and Lemaître, 2015). Morris' elementary effects method is an OAT design, and it helps to determine which factors have linear and additive effects, nonlinear and interaction effects, or no effects (Wanninger et al., 2016).
- Supersaturated design, Screening by groups, or Sequential bifurcation method: these may be applied if the number of code runs is smaller than the number of inputs.

A cobweb graph (Cooke and van Noortwijk, 2000; Iooss and Lemaître, 2015) may be used for visualizing and screening the input variables that lead to extreme values of a selected output parameter. In the graph, the values of the input parameters are scaled to the range 0...1, and the values associated with a single simulation are connected with lines. The simulations that exceed a certain criterion are plotted with a different colour than the rest of the simulations.

2.1.2.2 Sensitivity indices

Probably the simplest way to perform a sensitivity analysis is to calculate correlation coefficients between the input and output parameters. Correlation coefficients may

be divided into simple, rank and partial coefficients. Simple correlation calculated with the Pearson linear correlation coefficient is one of the most widely used sensitivity indicators. It is calculated by using covariance (*cov*) and standard deviations (σ) of the input parameter X_i and the output parameter Y:

$$\rho_i = \frac{cov(Y,X_i)}{\sigma_X \sigma_Y}. \quad (2.4)$$

Rank correlation is calculated by Spearman's rank correlation coefficient. It is calculated similarly to the Pearson coefficient, except that the input and output values are replaced by their ranks. Occasionally, it is more suitable to use partial correlation coefficients: these are constructed from Pearson and Spearman correlation coefficients by removing the linear effects resulting from other input variables (OECD/NEA, 2017). Another commonly used coefficient is the (standardised) (rank) regression coefficient (Borgonovo and Plischke, 2016; de Crécy et al., 2008; Perez et al., 2011).

As the correlation coefficients can detect only linear or monotonic relationships, variance-based indices, i.e. Sobol' indices (Sobol', 1993), have become popular in nuclear fuel related sensitivity studies. Sobol' index gives the share of variance of the output that is due to a given input, or combination of inputs (Iooss and Lemaître, 2015; Saltelli et al., 2000). Variance-based sensitivity indices may be divided into main effects and total effects indices. The main effects indices give the fraction of uncertainty in the output associated with a single input. In total effects indices, interactions between input parameters are considered.

The Sobol' sensitivity index S_i for an input parameter X_i and output Y is formally defined as the ratio between the variance of the conditional expectation value (*E*) and unconditional variance (*var*) as:

$$S_i = var\big[E[Y|X_i]\big] \,/\, var[Y]. \quad (2.5)$$

Borgonovo (2007) introduced a new kind of measure: the δ-measure, which is a so-called moment independent uncertainty importance measure. The measure evaluates the change in the output when the uncertainties are eliminated in an input parameter, i.e. a normalized expected shift in the output distribution given by input parameters. In Borgonovo and Plischke (2016), this measure was categorized to belong to a family of Csiszar divergences, together with Kullback-Leibler divergence. The Borgonovo's delta is defined for the input variable X_i as:

$$\delta_i = 0.5\, E_{X_i}\big[\int |f_Y(y) - f_{Y|X_i}(y)| dy\big]. \quad (2.6)$$

The term in the square brackets is the shift between the probability density function of an output and the probability density function of a conditional output with the value of X_i fixed. E_{X_i} stands for expectation value. With both sensitivity measures S_i and δ_i, the range of the indices is 0-1; zero means that the output is independent of the input parameter in question.

Instead of using only one type of sensitivity measure, an ensemble of indices may be calculated. In studies by Di Maio et al. (2014, 2016), three global sensitivity analysis methods, namely input saliency, Hellinger distance and Kullback–Leibler divergence, were used for identifying the input variables that most affect the thermal hydraulic code output. Using a combination of indices allows the construction of more reliable and robust rankings of important parameters (Di Maio et al., 2014). This approach is especially useful with thermal hydraulics analyses, in which the computational cost is high. However, Pourgol-Mohammad et al. (2016) pointed out the difficulties that the ensemble approach might entail. In their study, four sensitivity indices suggested by Plischke (2010, 2012), Plischke et al. (2013), and Baucells and Borgonovo (2013), were used: Borgonovo's delta, first order Sobol' index, EASI and BETA. In a thermal hydraulic analysis with a hundred LOCA simulations, the indices resulted in diverging outcomes, and were inconsistent from the phenomenological point of view.

2.2 Statistical analysis of LOCA

2.2.1 Applied codes

The primary calculation tool in the statistical analysis is the coupled fuel performance – thermal hydraulics code FRAPTRAN-GENFLO. FRAPTRAN is a single-rod transient fuel performance code developed by Pacific Northwest National Laboratory (PNNL) for U.S.NRC (Geelhood et al., 2011b). FRAPTRAN has been coupled (Hämäläinen et al., 2001) with the general thermal hydraulics code GENFLO (Miettinen and Hämäläinen, 2002), developed at VTT, to improve the thermal hydraulics modelling in LOCA.

The default LOCA cladding failure criterion in FRAPTRAN is applied in rod failure predictions, explained as follows. The ballooning model of FRAPTRAN assumes that local non-axisymmetric cladding ballooning begins when the effective plastic strain in any axial segment of the cladding exceeds the instability strain given by the material properties package MATPRO (Hagrman, 1993). FRAPTRAN predicts the fuel rod failure in the ballooned region when the calculated true hoop stress in the cladding exceeds an empirical limit, or when the cladding plastic hoop strain exceeds a strain limit (Geelhood et al., 2011b). In the stress calculations, FRAPTRAN takes into account the thinning of the cladding resulting from the high temperature oxidation. The Cathcart-Pawel (Cathcart et al., 1977; Pawel et al., 1979) best-estimate oxidation model is chosen for these simulations; it is activated in FRAPTRAN once the cladding temperature exceeds 800 °C.

For each time-step and axial segment, GENFLO calculates the coolant temperature and the clad-to-coolant heat transfer coefficients. GENFLO contains a five-equation thermal hydraulics model (two energy and mass equations, one momentum equation) with drift-flux phase separation. GENFLO is fast running due to a non-iterative solution of the field equations. When GENFLO is coupled to a fuel performance code, it solves the thermal hydraulics only once during a given instant of

time. The code is able to simulate the long-lasting reversed core flow which is possible in EPR.

The steady-state initializations of the transient calculations are performed with the U.S.NRC/PNNL FRAPCON code (Geelhood, 2011a), with statistical features introduced at VTT (Stengård and Kelppe, 2003). For the FRAPCON simulations, the steady-state power histories of all the rods in the reactor are needed. SIMULATE 3 (Studsvik Scandpower Inc., 2003) was used to simulate the core and to obtain the power histories.

In order to obtain the boundary conditions for the fuel performance code calculations, the progress of the accident was simulated 59 times with the system code APROS (www.apros.fi), developed jointly by VTT and Fortum. The applied dynamic one-dimensional two-phase flow model of APROS simulates the behaviour of a system containing liquid and gas phases, covering all heat transfer modes. The system is governed by six partial differential equations, from which pressures, void fractions and phase velocities and enthalpies are solved. The phases are coupled to each other with empirical friction and heat transfer terms.

Sampling of parameter values is conducted with the SUSA software (Kloos, 2008) developed by the German research organization GRS. Simple random sampling is applied.

2.2.2 Calculation system

The calculation system is presented in Fig. 2.1. The developed method employed in this dissertation makes use of the first order Wilks' formula with 59 instances of the accident sequence. A neural network surrogate model is also tested to complement the analysis (Publication **II**). The neural network analysis is conducted using a MATLAB (MathWorks, 2017a) built-in neural network software package, the Neural Network Toolbox™ (MathWorks, 2017b).

The initial parameters of the statistical analysis can be divided into two groups by their range. Global parameters have an effect on all the rods in the reactor, whereas local parameters bring variation only to individual rods. For example, the model parameters of a fuel performance code are global, whereas fuel manufacturing parameters are local. The above-mentioned 59 transient simulation cases are constructed in such a way that selected model parameters in the codes, and the FRAPTRAN-GENFLO boundary conditions, are different between the scenarios. The values for fuel manufacturing parameters are random sampled from their distributions; these have the same values in each global scenario. The uncertainties related to the neutronics calculations used to produce the base irradiation pin power histories are left outside this study. No model parameters are varied in FRAPTRAN as there is no statistical version of FRAPTRAN available at the moment.

When applying the first order Wilks' formula to this problem, all the 63 865 rods in an EPR should be simulated 59 times, with variations between each of the 59 scenarios. Then, if the number of failed rods in the worst case would be below the permitted limit, the safety requirements are met with a probability of 95% and with

a confidence level of 95%. As this number of transient fuel performance code simulations is out of reach of currently available computer resources, some other method or approach is needed alongside, in order to reduce the number of simulations.

In the approach introduced in Publication **I**, a limited number of random sampled rods are simulated for each global scenario. The number of simulated rods is chosen to be 1000, in order to keep the computation time reasonable (less than two weeks with 25-32 simultaneous simulations in the cluster), and yet the number of simulations sufficient. In order to be able to pinpoint the worst global scenario unambiguously, the same rods are simulated in each global scenario. The number of failed rods in the worst global case can then be directly scaled to determine the number of failed rods in the whole reactor. This approach is on the conservative side, because with a smaller number of included rods, the deviation of the number of failures grows. Therefore, the highest failure number is likely to be higher than it would have been if all the rods had been calculated.

In a thorough analysis, the rest of the rods among the global scenarios would be taken into account by fitting a neural network for each global scenario by using the limited data from the 1000 simulated rods per scenario. The trained network could then be applied to reduce the deviation resulting from the extrapolation (examined in Publication **II**). Additionally, once the worst global scenario is identified based on the 59 000 simulations, all the rods in the reactor during this particular scenario may be simulated, as was also done in Publication **II**. Additional simulations reduce the conservatism of the result.

For comparison, a similar kind of approach was adopted for example by Kereszt-úri et al. (2016). They applied FRAPTRAN in statistical LOCA analysis by training a response surface surrogate model with FRAPTRAN results, and then feeding the data from all the rods in the reactor 59 times through the surrogate model.

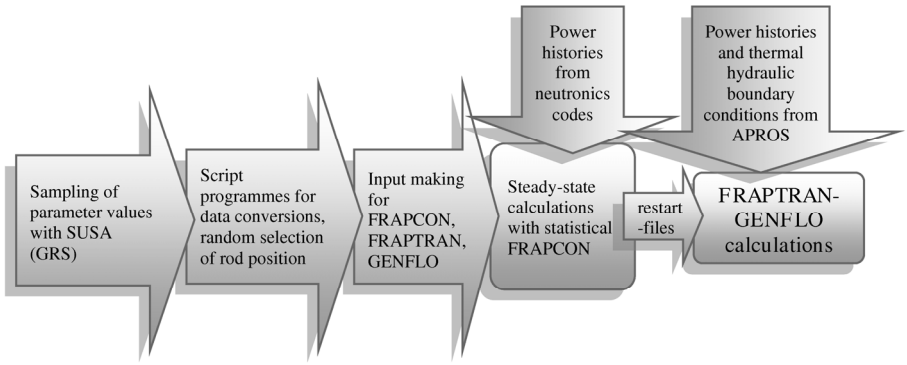

Figure 2.1. Flowchart of the calculation system.

2.2.3 Accident sequence, varied parameters and boundary conditions

The studied conservative accident sequence in EPR is chosen based on regulatory requirements, and may be summarized as follows (Publication **II**). As an initiating event, a double-ended break in a cold leg opens. Due to pressure decrease, reactor and turbine trips follow. Simultaneously with the turbine trip, the offsite power is lost and the main recirculating coolant pumps start to coast down. The core is uncovered. The content of the accumulators is injected to the primary loop when the accumulator pressure is reached. After a delay, the diesel generators are started and the medium head safety injections, and later on, the low head safety injections start operation, and the core is quenched.

In the LOCA scenario now considered, the accident occurs at the end of the 4th irradiation cycle. At the end of cycle 4, there are five different fuel assembly types in the core. These types vary in U-235 enrichment, the number of urania-gadolinia rods in the assembly, and the Gd_2O_3 content in the urania-gadolinia rods. About half of the assemblies have been in the core only for the cycle 4. The rest have been irradiated for two cycles: one assembly during cycles 1 and 4, and all the others during cycles 3 and 4. The cycle lengths for cycles 1, 3 and 4 are 18, 24 and 24 months, respectively.

The parameters chosen to be varied have been collected into Table 2.1. The parameters that are important regarding the whole core are varied in APROS, and those that are important in fuel behaviour analysis are varied in fuel performance codes. Generally, the parameters affecting the thermal hydraulics are varied in APROS. However, the parameters now varied in GENFLO cannot be currently varied in APROS and therefore these are taken into consideration in GENFLO. Meanwhile, fuel-related parameters are kept at their best-estimate values in APROS and varied only in the fuel performance codes.

The parameters and their ranges used in the APROS analysis are based mainly on the BEMUSE programme data (OECD/NEA, 2007, 2009a), but other publicly available data has also been used (Freixa et al., 2010, 2011). The varied model parameters and their ranges in FRAPCON and GENFLO are based on previous analyses carried out at VTT. Normal distribution is used for the fuel manufacturing parameters, but the applied mean and standard deviation values are proprietary.

The relevant boundary conditions obtained from APROS are the enthalpy and the mass flows of both liquid and vapour at the channel inlet and outlet, the coolant pressure and the rod power evolution. Axial power profiles are also provided by APROS.

In APROS, the reactor core is divided into 20 axial nodes for the solution of thermal hydraulics and neutronics. The core is further divided into 17 thermal hydraulic channels. The locations of the thermal hydraulic channels in relation to the fuel assemblies are presented in Fig. 2.2. As there are no shrouds around the fuel assemblies in EPR, there are cross flows in the core. A single FRAPTRAN-GENFLO simulation is performed for a closed subchannel, and thus the cross flows cannot explicitly be taken into account. However, as the core is divided in APROS into thermal

hydraulic channels consisting of several fuel assemblies instead of only one assembly per channel, the cross flows are taken into account in the boundary conditions produced for FRAPTRAN-GENFLO.

Table 2.1. Varied parameters and their distributions.

Global parameters	***Distribution[1]***	***Min.***	***Max.***	***Global scenario #47[2]***
APROS				
Containment pressure [MPa]	N (0.250)	0.200	0.300	0.263
Pump1 inertia [kgm^2]	N (5210.0)	5157.9	55262.1	5247.2
Pump2,3,4 inertia [kgm^2]	N (5210.0)	5105.8	5314.2	5164.9
Decay heat of normal [%]	N (100.0)	92.0	108.0	95.1
Accu2,3,4 pressure [MPa]	N (4.9800)	4.7800	5.1800	4.9484
Accu2,3,4 level [m]	N (4.4600)	4.3600	4.5600	4.5124
Emergency water temperature [°C]	N (50.0)	10.0	50.0	21.4
Emergency water flow [%]	N (100.00)	95.00	105.00	97.47
CCFL parameter	N (1.0000)	0.6900	1.0350	0.9232
Discharge coefficient, RPV side	N (0.8750)	0.7500	1.0000	0.8202
Discharge coefficient, pump side	N (0.8750)	0.7500	1.0000	0.9383
Upper plenum temperature [°C]	N (336.0)	331.0	341.0	332.9
FRAPCON				
Swelling parameter	N (1.0; 0.000144)	not defined		0.995770
Creep rate parameter	N (1.0; 0.25)	0.6	1.1	0.881100
Fission gas parameter	N (0.0; 0.25)	-1	1	0.363080
Thermal conductivity parameter	N (1.0; 0.01)	not defined		1.015300
Cladding corrosion parameter	N (1.0; 0.0004)	0.6	1.4	1.016000
GENFLO				
Basic drift flux velocity	Tri (1.2)	1.13	1.2	1.154200
Drift flux separation constant	Tri (1.1)	1.1	1.2	1.122200
Interphasial heat transfer tuning factor	Tri (0.3)	0.1	0.33	0.183950
Film boiling heat transfer tuning factor	Tri (0.2)	0.08	0.22	0.187390
Transition boiling heat transfer tuning factor	Tri (0.2)	0.18	0.22	0.192250
Local parameters FRAPCON and FRAPTRAN	N			
Cladding inner diameter, Fuel pellet diameter, Cladding wall thickness, Cold plenum length, Fuel pellet density, Bottom plenum volume, Internal fill pressure				

[1]N=Normal (μ,σ^2) or (μ); Tri=Triangular (mode)
[2]Values in global scenario #47 which turned out to be the worst case

The linear power histories and thermal hydraulic boundary conditions are available for 17 channels, except for the inlet enthalpy for liquid and vapour, which are given for eight sectors. The eight sectors take into account the asymmetric temperature distribution in the core resulting from the break in one of the cold legs. The axial power profiles are available for all the 241 fuel assemblies. The same static beginning-of-transient axial power profiles are used in all the 59 global scenarios. The linear power histories available for the channels are further refined for each fuel assembly by using a normalized multiplier defined from an APROS output file. The multiplying coefficients are defined using the average power (*P*) in an APROS channel:

$$coeff_{assembly} = P_{assembly} \frac{total\ number\ of\ assemblies\ in\ APROS\ channel}{P_{channel}} \quad (2.7)$$

The channel power is obtained by adding up the assembly powers in that particular coolant channel. An approximation has to be made regarding the transient power evolutions in fuel rods: as the transient pin power is not known but only the assembly power, the latter is used in FRAPTRAN-GENFLO simulations as pin power. Similarly, the assembly axial power profile is used as pin axial profile.

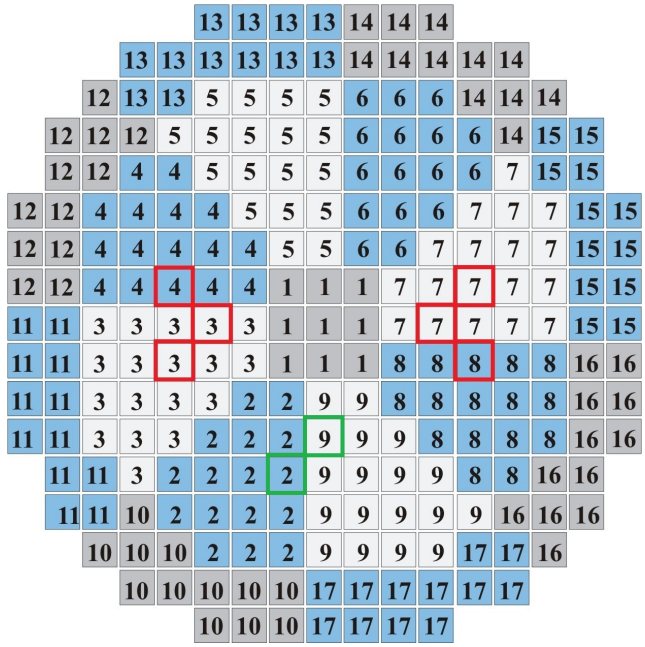

Figure 2.2. Division of the core into 17 coolant channels in APROS.

2.2.4 Results of the statistical analysis

The numbers of rods that failed in each global scenario are shown in Fig. 2.3. The highest number of failures, 14 rods out of 1000, occurred in global scenario #47. Thus in the worst case, 1.4% of the rods failed. In each scenario, the same 1000 rods were simulated, and consequently in many cases, the same rods failed in various global scenarios. Some of the simulations were not successfully terminated; in scenario #3, a total of 62 simulations ended with an error, 58 of which were due to GENFLO. With respect to errors, this was the worst case. If all the erroneous simulations were conservatively assumed to represent a rod failure, the total portion would be 6.6%, and the safety criterion is still easily met. The global parameter values applied in scenario #47 are presented in Table 2.1.

The evolutions of selected output parameters in the global scenario #47 have been plotted in Fig. 2.4 (left-hand side). The curves corresponding to the failed rods are indicated with markers. In each global scenario, the highest peak cladding temperatures occurred soon after the beginning of the accident, and were at the same level in all global variations, around 900 ºC.

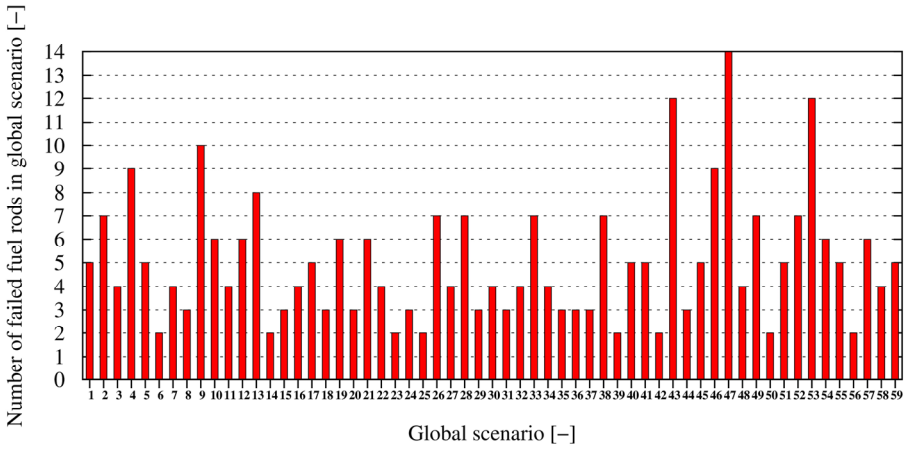

Figure 2.3. Numbers of failed fuel rods in each global scenario (Publication **IV**). 1000 rods were simulated per scenario.

In Publication **IV**, updated results yield a few units higher numbers of failed rods in almost all the scenarios compared to those in Publication **II**. The reason is that a different cladding yield strength correlation in FRAPTRAN is applied between the analyses. The default model is used in Publication **IV**, and an older model was applied in Publications **II** and **III**. The older model was used in the first analysis, as it had proved to give the best results in modelling Halden IFA-650 LOCA series with FRAPTRAN-GENFLO. In addition, a bug in FRAPTRAN was corrected between the two analyses: in previous simulations, false indications of rod failures were given by the low-temperature PCMI cladding failure model during the high temperature phase in LOCA. However, the vast majority of the rods that were predicted to fail in

the first analysis were also predicted to fail in the updated analysis. Therefore, those rods clearly had a tendency to face a simulated cladding failure in LOCA.

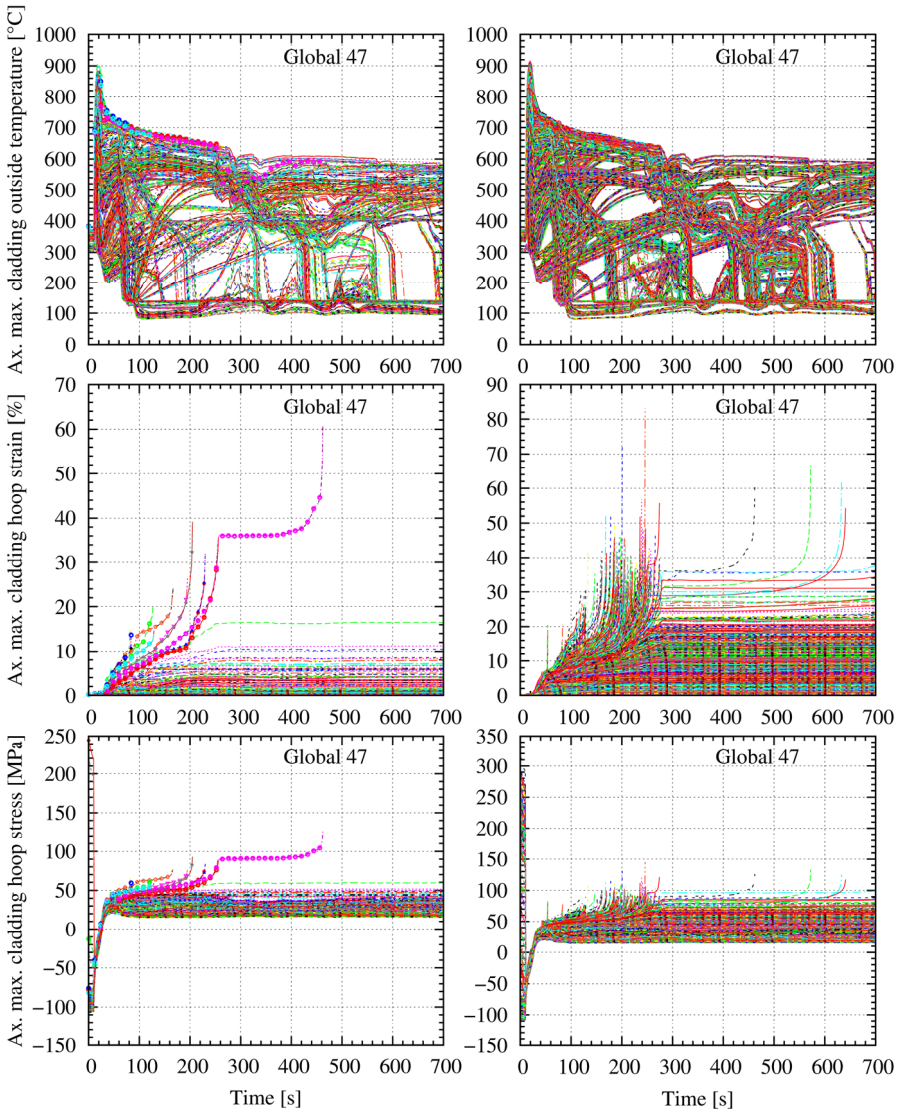

Figure 2.4. Evolutions of key output parameters in FRAPTRAN-GENFLO simulations in the worst global scenario with respect to the number of failing fuel rods (Publication **IV**). First, 1000 rods were simulated (left-hand side), and then all the rods that had been in the reactor during cycles 3 and 4 (right-hand side).

Among the analysed global scenarios, all the failed rods had been in the reactor during both the 3rd and the 4th cycles (Publication **II**). In other words, no failures were simulated in the rods that had been in the reactor only during the 4th cycle, or during

the 1st and 4th cycle. Therefore, by applying the boundary conditions and the global parameter values of the worst global scenario (in terms of the number of failed rods), all the rods in the loading pattern that had been in the reactor during the 3rd and the 4th cycles were simulated with FRAPTRAN-GENFLO (Publication **IV**). In this smart sample, 1.96% of rods were simulated to end up in fuel rod failure, and 0.44% of simulations crashed. Thus even in the whole reactor scale, taking into account the most limiting rods, the safety criterion is met. The evolutions of the output parameters of 3rd and 4th cycle rods are presented in Fig. 2.4 (right-hand side).

Preliminary testing of neural networks was carried out in Publication **II**. Neural networks are used to complement the analysis: the initial data from all the rods in the reactor may be fed through the surrogate model. A network was trained using the 1000 simulations from the worst global scenario. The network predictions were then compared to FRAPTRAN-GENFLO results of all the rods in the reactor. It was discovered that the rods calculated by FRAPTRAN-GENFLO to survive were well predicted by the network to survive. However, a significant number of rods calculated to fail were not correctly predicted by the network. This can be explained by the fact that the number of failing rods used in teaching the network was very limited.

The number of failing rods was found to be in the same range as in FRAPTRAN-GENFLO simulations, but the prediction is not very accurate. However, neural networks may be used for a cursory glance at the number of failing rods. Suggestions to improve the predictions are given in Section 4.3.1.

2.2.5 Discussion

By applying the calculation system for statistical fuel failure analysis introduced in Publication **I**, the number of failed fuel rods in LB-LOCA in an EPR was estimated in Publications **II** and **IV**. The number of failing fuel rods in 59 simulated global scenarios ranged from 2 to 14 rods per 1000 simulations. Thus, in the worst case, 1.4% of the simulated rods failed. It can be concluded that according to the statistical analysis of the chosen conservative accident sequence, the requirement that less than 10% of rods may fail is met. The highest peak cladding temperatures in all global variations were around 900 ºC, and the requirement concerning the highest peak cladding temperature, 1200 ºC, is thereby met. The high temperature oxidation was not a concern in this analysis due to the relatively moderate and short-duration peak cladding temperatures.

The weakness of the current analysis is that no model parameters are varied in FRAPTRAN, as statistical features have not been incorporated into that code. This deficiency will be corrected in future analyses.

2.3 Sensitivity analysis of local uncertainties

The fuel rod failures in an LB-LOCA are usually affected by many interconnected phenomena. Thermal hydraulic conditions in the rod's location during a LOCA play an important role, as does the decay heat power during the transient. On the local

level, the rod's irradiation history prior to the accident and the resulting state of the rod also have an effect. Furthermore, fuel rod design parameters such as enrichment and gadolinia content and tolerances in the fuel manufacturing parameters may make a contribution. In order to determine the relevant factors affecting fuel rod failures, and to quantify their relative importance, a sensitivity analysis was performed (Publication **III,** updated in Publication **IV**), using the data from the statistical analysis introduced in Publication **II**.

The sensitivity analysis was made using the data of all those rods that had been in the core during cycles 3 and 4, i.e. those rods that were found to be more susceptible to failure. In this analysis, only one global scenario, the worst, is considered. The effect and importance of various local parameters to the outcomes of chosen output parameters were studied. In the future, the analysis will be extended to other global scenarios, which will shed some light on the effects of the global parameters and enable comparison with similar studies made e.g. in the BEMUSE programme (OECD/NEA, 2009a).

2.3.1 The developed sensitivity analysis procedure

The number of sensitivity analysis methods that are suitable for this problem is limited because the dataset is given, which excludes methods that take advantage of efficient sampling techniques (Saltelli et al., 2008). In addition, the influential input parameters are highly correlated. This results from the facts that, firstly, the phenomena in a nuclear reactor are highly interlinked, and secondly, the data used for the sensitivity analysis originates from a complex calculation system consisting of several codes. If parameters are selected from successive phases of the calculation chain, their effect may be taken into account more than once when performing the sensitivity analysis. The analysis is further complicated by the differences in the level of detail in modelling in various codes.

Because the data used in the sensitivity analysis is complex, even defining the input parameters is not straightforward. To tackle the problem, a multistage procedure was developed. In the first phase, all the potentially important sampled or calculated input parameters of the LOCA analysis are distinguished. This phase also includes condensing the time series data into scalar form. To help identify the relevant parameters, a cobweb graph (Cooke and van Noortwijk, 2000; Iooss and Lemaître, 2015) is used to visualize the input variables that lead to high hoop strains in the LOCA calculations. In LOCA analysis, the cladding ballooning is a key result and may be represented by the cladding plastic hoop strain. Therefore, the simulations in which the plastic hoop strain is equal or exceeds a chosen limit, fixed in this analysis to be 20% (Publication **IV**), are highlighted in the cobweb graph. In the first sensitivity analysis (Publication **III**), the strains were lower due to the different cladding yield strength correlation, and there a limit of 5% was used in the cobweb graph.

Finally, sensitivities are quantified by calculating various sensitivity indices. The Borgonovo's delta (Borgonovo, 2007) and Sobol' indices (Sobol', 1993) are chosen, as they can be evaluated from pre-existing data. The first order Sobol' sensitivity

index was chosen for its simplicity, and the Borgonovo's delta is applied because it is a more comprehensive measure. Squared Pearson correlation coefficients, i.e. the R^2 values, are also calculated for comparison whenever possible. The present study involves data presented as ordinal numbers (the coolant channel number) that cannot be analysed with correlation coefficients.

The calculation of the indices was carried out with two MATLAB scripts by Plischke (2014). Usually, calculation of the Sobol' index is performed with a specific sampling design (Saltelli et al., 2008), which is very efficient but cannot be used in the case of pre-existing data. Instead, the numerical estimation of Sobol' index follows the discrete cosine transformation method. The numerical estimation of Borgonovo's delta is accomplished using a Gaussian kernel estimator with Kolmogorov-Smirnov filtering to reduce spurious correlations (Plischke et al., 2013).

Compared to other studies, the chosen approach of calculating multiple indices resembles the ensemble approach used by Di Maio et al. (2014, 2016), and the division into qualitative and quantitative parts is the same as applied by Pourgol-Mohammad et al. (2016). The sensitivity analysis procedure follows the path also proposed in Iooss and Lemaître (2015): first, screening out the non-influential parameters, and then proceeding with more advanced and costly sensitivity analysis methods.

2.3.2 Data pre-processing and preliminary screening

Part of the data is scalar, whereas some is in the form of time series. The latter include transient power histories, thermal hydraulic boundary conditions, and steady-state power histories. In order to perform the sensitivity analysis, the time series data needs to be simplified. Some of the thermal hydraulic boundary conditions of the 17 coolant channels vary significantly during the transient, and therefore condensing the boundary conditions into scalars was not attempted. Instead, the 17 thermal hydraulic boundary conditions are treated by the sequence number of the particular channel in the APROS model.

When comparing the steady-state power histories during both of the cycles, it is seen that within a cycle the power evolutions are quite steady. The exceptions are the gadolinia-doped rods in which the power increases during the first cycle. Due to the simplicity of the histories, average values for power are calculated for each rod for both cycles.

The decay heat during the transient is directly proportional to the power prior to the transient, and therefore the transient power histories may be represented by the pre-transient steady-state power values obtained from APROS. However, here the power coefficients for the fuel assemblies are considered instead of the actual transient power. This choice is made because in this way the channel power may be grouped together with the thermal hydraulics boundary conditions, which are also given per channel. The normalized assembly power coefficients are calculated through Eq. (2.7).

The rod failure criterion in FRAPTRAN for ballooning in LOCA is based on empirical stress and strain limits. In the sensitivity analysis, the maximum values of

cladding plastic hoop strain, hoop stress and outer surface temperature are used instead (maximum relative to time and axial position). This makes the analysis more general and independent of the particular failure criterion adopted in FRAPTRAN. The continuous output is also easier to analyse statistically than the binary failed/non-failed output of the rod failure model.

2.3.3 Results of the sensitivity analysis

The cobweb graph is shown in Fig. 2.5. Parameter values of all the rods that have been irradiated during cycles 3 and 4 are plotted with red colour and the simulations with equal to or higher than 20% plastic hoop strain are plotted with black. Fuel enrichment and gadolinia content are not shown in the figure for reasons of confidentiality.

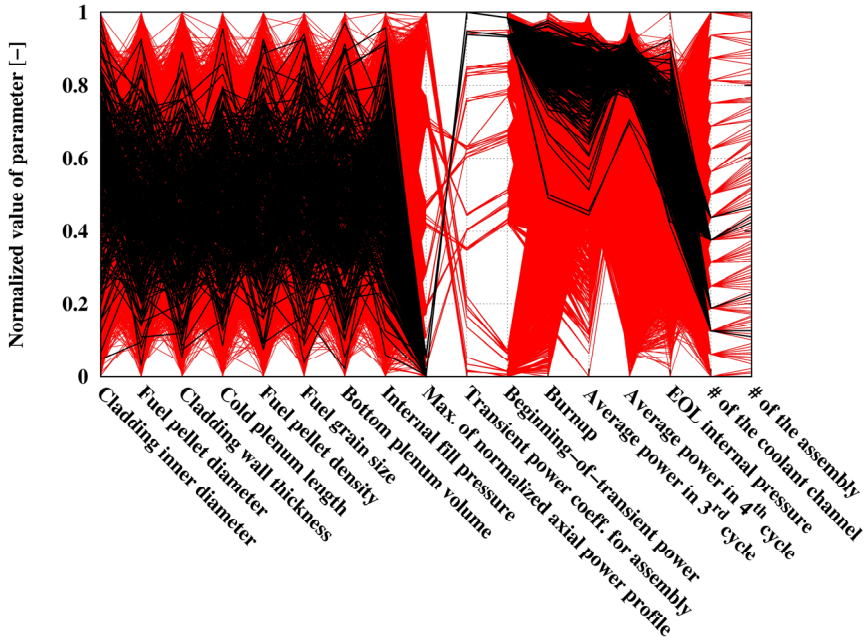

Figure 2.5. Cobweb graph used for screening the most important input parameters (Publication **IV**).

The following conclusions can be made based on the cobweb graph:

- Tolerances in fuel manufacturing parameters do not significantly affect the transient strain.
- Average steady-state power during the 4th cycle is more strongly correlated with high strains than the 3rd cycle power.
- High burnup is related to high strain, but the range of burnups in the high strain rods is relatively large.

- The range of end-of-life (EOL) internal pressures resulting in high strains is wide, but high strains are not reached in rods with the EOL internal pressure in the lower third.
- The distinction between the beginning-of-transient power and the transient power coefficients for the fuel assemblies is seen: highest strains are achieved with the highest power coefficients but not with the highest beginning-of-transient powers. Strong correlation with the high hoop strain is seen in both.
- High strains are associated with distinct coolant channels and fuel assemblies.

When comparing the cobweb graph with the locations of the fuel assemblies and coolant channels in the core (Fig. 2.2), it can be seen that the rods with the highest permanent hoop strain (>20%) are located in the assemblies that are situated in the middle circle of coolant channels in the APROS model, namely in channels 3, 4, 7 and 8. Again, these rods are located in six assemblies, marked with red squares in Fig. 2.2 (according to FRAPTRAN, a few rods also failed in two more assemblies with less than 20% strain, marked with green squares in Fig. 2.2). This is explained by the fact that the powers in the outer circle channels are significantly lower compared to the middle circle and the central channel. In the central channel, the highest powers do not reach the level of those in the middle circle channels, and therefore the hoop strains are not high in that channel.

Next, the parameters to be included in the quantitative sensitivity analysis are chosen. The cobweb graph showed that the rod manufacturing tolerances are almost insignificant, but the indices for these are calculated for comparison. Some of the input parameters are screened out due to their strong mutual correlation, whereas some dependent parameters cannot be excluded, such as burnup and transient power. The following are screened out: gadolinia content, as it is associated with the U-235 enrichment; end-of-life internal pressure, strongly correlated with burnup; average steady-state power in both cycles, correlated with burnup and decay heat; beginning-of-transient power, partly included in the channel number through the average channel power.

The sensitivity indices are presented in Fig. 2.6 for the chosen inputs and the output maximum value of cladding plastic hoop strain. It can be seen that the most relevant parameters, in order of importance, are the decay heat power during the transient represented by the fuel assembly power coefficient, the steady-state irradiation history of the rod represented by the rod burnup, and the thermal hydraulic boundary conditions plus the coolant channel power in the rod's location as represented by the coolant channel number. Fuel enrichment also has a non-zero effect. Meanwhile, the tolerances in fuel manufacturing parameters have practically negligible effects, even though the delta indices are not exactly zero. As the inputs are not independent, caution should be used with further interpretation of the indices. A similar study was conducted for the two other outputs, maximum stress and temperature, and the conclusions were the same (Publication **III**).

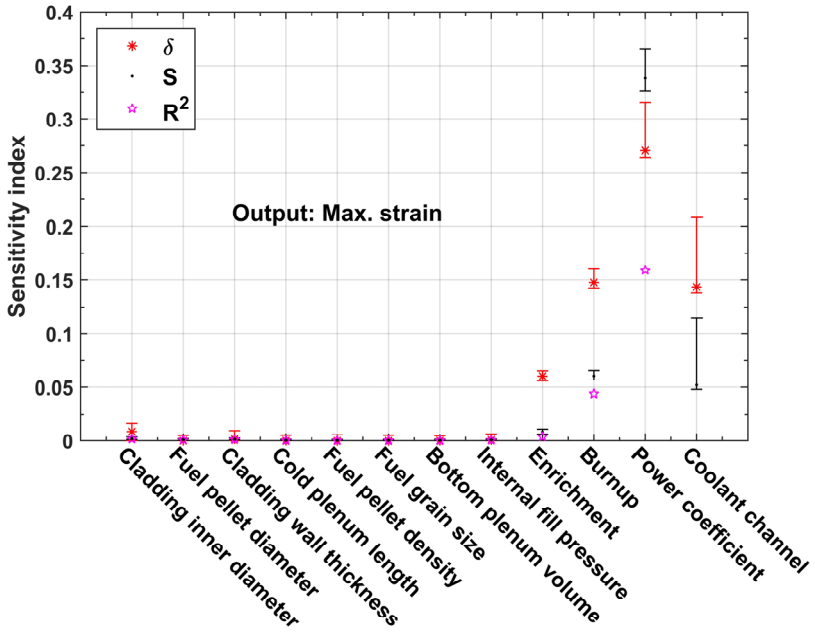

Figure 2.6. Calculated sensitivity indices (Publication **IV**). δ = Borgonovo's delta measure, S = first order Sobol' index, R^2 = squared Pearson correlation coefficient.

The effect of coolant channel thermal hydraulics is hard to distinguish from the effect of coolant channel power, and it may only be seen indirectly. Based on the high power, at least some of the rods located in channel 5 should reach high strains, but this is not observed. Furthermore, the coolant channel power in that channel is higher than in those where the high strains are reached. According to the cobweb graph and the calculated sensitivity indices, the explanation for the lower strains in that channel remains to be searched from among the rod burnup and the coolant channel thermal hydraulics. Similar burnups are observed in channel 5 as in the channels where the strains are high, which excludes the burnup as the sole explaining factor. Therefore, it may be concluded that the thermal hydraulic effects dominate over the effect of the coolant channel power.

2.3.4 Discussion

A sensitivity analysis was performed in order to discover the most influential input parameters in the worst global scenario. A systematic sensitivity analysis procedure consisting of several stages was developed. Both visual and numerical methods were applied. A cobweb graph was used both to visually interpret the data and to perform final screening of the input variables. For example, the rod manufacturing parameters were identified as almost non-influential already using the cobweb graph. The burnup, the power coefficient during the transient and the coolant chan-

nel number were chosen for further numerical analysis. For comparison, the manufacturing parameters were also chosen to be included in the last stage. The results of the numerical analysis supported the conclusions made concerning the importance of the three key parameters.

It should be borne in mind that the conclusions of the sensitivity analysis with respect to the most influential input parameters are naturally always dependent on the data used for the analysis. If for example the power evolutions and the axial power profiles during the transient would be known at the pin instead of the fuel assembly level, the relative importance of the most significant input parameters might be different.

The present work is not limited to the analysis of rod failures in a LOCA. The outlined analysis procedure is general, and could be useful in analysing other types of complex calculation sequences or simulations that produce correlated and sparse data. Since many such simulations are very time consuming, it is often not possible to generate additional data solely for the purpose of sensitivity analysis. The procedure used in this work uses only data that was available from a previous uncertainty analysis, and is therefore generally applicable to the analysis of pre-existing simulation data.

3. Reactivity initiated accidents (RIA) in boiling water reactors (BWR)

The main issues to be considered in order to be able to model a BWR RIA with SCANAIR are firstly the Zircaloy-2 (Zry-2) cladding material properties and mechanical behaviour, i.e. elastic, plastic and viscoplastic models, and secondly the BWR thermal hydraulics modelling in RIA conditions. In SCANAIR, the available material properties and the thermal hydraulics model are for PWR fuel and coolant conditions, respectively, but the code did not have similar models for BWRs. Prior to the studies presented in Publication **V**, the only Zry-2 models implemented into the code were yield strength (YS) and ultimate tensile strength (UTS) correlations of irradiated cladding from a bibliographic study, and the laws had not been validated with SCANAIR.

Ring tensile tests for fresh and irradiated Zry-2 cladding made as part of the French PROMETRA (TRAnsient MEchanical PROperties) programme (Cazalis et al., 2007) were utilized in fitting new YS (0.2% offset, $R_{p0.2}$) and UTS correlations (Publication **V**). This improves the accuracy of cladding plastic behaviour modelling. After implementing these laws into SCANAIR, comparative simulations were performed by applying the old and the new correlations to BWR fuel tests LS-1 and FK-1 performed in the Nuclear Safety Research Reactor (NSRR) in Japan at room temperature and atmospheric pressure conditions. The effect of the new models on cladding strain energy density (SED) and failure propensity was investigated (Publication **V**). The ability to predict Zry-2 low temperature failures was further evaluated by simulating the whole FK test series, eleven tests in total (Publication **VI**).

As the standard thermal hydraulics model in SCANAIR is one-dimensional and able to model single phase coolant only, the simulation of an RIA in a BWR is not possible when the bulk boiling regime is reached. In Publication **VI**, the code's application field was broadened to consider bulk boiling. In the chosen approach, SCANAIR was coupled with an external thermal hydraulics code. For this purpose, VTT's in-house general thermal hydraulics code GENFLO was used. The first demonstration results were introduced (Publication **VI**).

3.1 Background

3.1.1 Applied modelling codes

SCANAIR

The SCANAIR code (Moal et al., 2014), developed by IRSN, is designed for modelling the behaviour of a single fuel rod in fast transient and accident conditions during an RIA in PWRs. It considers the fuel rod thermo-mechanical behaviour, fission gases, and the thermal hydraulics of the surrounding coolant. The current SCANAIR version is V_7, with various subversions. The SCANAIR subversions applied here are V_7_2 in fitting the YS and UTS correlations and in the low temperature failure estimations, and V_7_4 in the high temperature thermal hydraulics analysis.

GENFLO

The thermal hydraulic solution principles and models in GENFLO are based on VTT's SMABRE code (Miettinen, 2000) for LOCAs. In the past, GENFLO has been used for a wide range of applications, but during recent years the sole application has been in the coupling with the FRAPTRAN code for statistical LOCA simulations (Publications **I-IV**).

The applied heat transfer correlations in each phase of the boiling curve were described in detail by Miettinen and Hämäläinen (2002). Many of the heat transfer correlations in GENFLO are not standard in the field, but are fitted based on typical correlations.

In GENFLO, a superposition of the various heat transfer mechanisms is assumed both in pre- and post- critical heat flux (CHF) conditions. More precisely, the clad-to-coolant heat transfer along the GENFLO boiling curve is described as follows. In pre-saturation, forced convection into liquid is considered. Between the saturation temperature and the critical temperature, nucleate boiling plus convection both into liquid and vapour are taken into account as separate components. Beyond the critical temperature, heat transfer into liquid and vapour are calculated separately with film boiling and convection correlations, respectively, and summed up with the radiation heat transfer into liquid. Transition boiling phase is described only during the rewetting. Film boiling phase is initiated when the cladding temperature exceeds $T_{sat} + \Delta T_L$, where the ΔT_L is the Leidenfrost temperature difference, set to be 160 °C. For comparison, in SCANAIR, transition begins earlier, at T_{sat} + 55 °C in PWR conditions (Bessiron, 2007), and film boiling starts at a minimum stable film boiling temperature determined experimentally. In addition to the clad-to-coolant heat transfer, interfacial heat transfer is taken into account in GENFLO.

FRAPCON and VTT-ENIGMA

The base irradiation initialization prior to an RIA is not performed by SCANAIR, but the relevant data is calculated with an external code, or known from the experiments, and inserted into the SCANAIR input deck. In simulations presented in Section 3.3, FRAPCON code (Geelhood et al., 2011a) has been used for the initializations. As an alternative, VTT-modified ENIGMA v5.9 steady-state fuel performance code (Kilgour et al., 1992) is also used, and applied here in BWR simulations presented in Section 3.4.

3.1.2 Cladding mechanical properties

As the cladding strain rates during an RIA can be around 1 s^{-1}, the mechanical properties tests have to be specifically designed for reaching high strain rates. The French PROMETRA programme is internationally the most extensive series of mechanical tests on PWR cladding materials under RIA loading conditions, but there had not been any tests on Zry-2 cladding before the tests utilized here. Other mechanical tests on Zry-2 reported in open literature are GNF mechanical tests on

Zry-2 under RIA conditions at room temperature (Nakatsuka, 2004), and NFD and Studsvik tests on irradiated and un-irradiated Zry-2 (Jernkvist et al., 2004).

The integral effect test data on BWR fuel mainly comes from the NSRR facility. Tests on BWR fuel have also been made in the SPERT facility in USA: ten tests were made during 1969-1970 on low burnup fuel, in ambient temperature and pressure conditions. The rodlets tested in SPERT were of different design than the current BWR fuel rods (OECD/NEA, 2010).

Zry-2 cladding elastic behaviour, enthalpy, conductivity and thermal expansion are reported (Hagrman, 1993) to be similar to those of Zircaloy-4 (Zry-4) alloy used in PWRs. Furthermore, the transition between the alpha and beta phases is similar to Zry-4. There is no viscoplastic model available in the open literature specifically for Zry-2 in RIA conditions, but it is expected that the high temperature viscoplastic behaviour of Zry-2 is similar to that of Zry-4, as the differences in the heat treatment during the manufacturing process no longer play any role at high temperatures.

In contrast to the stress relieved annealing (SRA) heat treatment typical for Zry-4 cladding, heat treatment of Zry-2 is typically recrystallization annealing (RXA). This difference affects the ductility degradation of the cladding as hydrogen is picked up by the metal during the fuel rod lifetime and brittle zirconium hydrides are formed. In RXA cladding, there are more radially oriented grains, and as the hydrides preferably precipitate along the grain boundaries, the RXA cladding has more radial hydrides (OECD/NEA, 2010). It is especially the radial hydrides that make the cladding vulnerable to a pellet-cladding mechanical interaction (PCMI) induced rupture when there is a strong tensile stress in the circumferential direction.

3.1.3 Cladding low temperature failure predictions

There are three methods in SCANAIR for the evaluation of cladding low temperature failure (Moal et al., 2014). These are the strain energy density (SED), fracture mechanics, and plastic hoop strain based approaches. The fracture mechanics approach is well applicable for PWR fuel (Georgenthum et al., 2014), but would require adaptation in order to be used with BWR claddings, as discussed in Publication **V**. Of the two applicable failure analysis methods, the SED approach was chosen for the study presented in this thesis.

The SED is an integral of the product of stress and strain, and it can be used to measure the potential of the cladding to fail. Mechanical SED is formulated in SCANAIR as follows (Moal et al., 2014):

$$SED = \int_0^{\varepsilon} \sigma d\varepsilon. \tag{3.1}$$

Here ε is the total mechanical strain, consisting of elastic, plastic and viscoplastic components. Local stress and strain components in hoop, radial and axial directions are considered (Bernaudat et al., 2009).

In cladding failure analysis, the SED is compared to a critical value of SED, the critical strain energy density (CSED) (Rashid et al., 2000). A correlation for the

CSED may be developed by using the results of mechanical tests. Material anisotropy, multiaxial stress state and strain rate must be considered when formulating a CSED criterion from the test data (EPRI, 2015). In general, the CSED depends on the cladding hydrogen content and the morphology, cladding outer surface oxide layer, fast fluence, cladding temperature and the loading rate (EPRI, 2015). In addition to Electric Power Research Institute (EPRI, 2015), the CSED approach has been applied e.g. by Bernaudat et al. (2009) and Georgenthum et al. (2014), but the validity of the approach has also been criticized (Motta, 2004).

As discussed in Publication **V**, EPRI had formulated a CSED criterion for Zry-2 cladding failure due to PCMI (EPRI, 2010; Liu et al., 2010). This correlation is applied in Publication **V** for FK-1 and LS-1 tests. Later on, EPRI has slightly tuned the correlation coefficients (EPRI, 2015) by using new data from EPRI's modified burst tests (Yueh et al., 2016). In the former study (EPRI, 2010), two CSED correlations were suggested: an ambient temperature correlation, and a scaled-up version for temperatures higher than 80 °C, to take into account the improved cladding ductility due to the higher temperature. However, in the latter report (EPRI, 2015), it was concluded that RXA Zry-2 is not susceptible to failure due to PCMI when the temperature is higher than 85 °C and the pulse width is greater than 15 ms, and when the injected enthalpy is less than 150 cal/g (Alvis et al., 2016; EPRI, 2015). Instead, the scaling is conducted for the CSED derived for 5 ms pulse width, to obtain another correlation for the more BWR-relevant 15 ms pulse. The CSED correlation for room temperature and 5 ms pulse as a function of cladding hydrogen content *H* is expressed as (EPRI, 2015):

$$CSED[\tfrac{MJ}{m^3}] = 38.0\exp(-0.0114\,H[ppm]) + 5.0. \qquad (3.2)$$

There are numerous factors causing uncertainty in the calculated SED, resulting from uncertainties in the code input parameters, models chosen and assumptions made, not to mention the uncertainties coming from the base irradiation simulation. It is known that the initial gap size prior to an RIA has an impact on the calculated SEDs, but due to complex phenomena such as fuel relocation and swelling and cladding creep during the base irradiation, modelling the gap size accurately is rather difficult. For example in FRAPCON, a coarse approximation is applied (Geelhood et al., 2011a, 2015): the relocation of the cracked fuel is taken into account in the thermal calculations by 100% (thermal gap), but the fuel-cladding mechanical contact is limited to take place only after the fuel swelling and thermal expansion have recovered 50% of the calculated fuel radial relocation (mechanical gap). In reality, the gap size may be somewhere between these two extremes.

If the hydrogen content is not known from the measurement, it may be estimated from the outer oxide layer with a correlation (Aufore, 1997; Desquines, 2007):

$$H[ppm] = \frac{271\,F[\%]\,e_{ZrO_2}[\mu m]}{e_0[\mu m] - 0.65\,e_{ZrO_2}[\mu m]} + H_0[ppm] \qquad (3.3)$$

Here H is the cladding hydrogen content, F is the hydrogen pick-up, 10% for Zry-2 (Desquines, 2007), e_{ZrO_2} is the zirconia layer thickness, e_0 is the as-fabricated thickness of the cladding, and H_0 is the initial hydrogen content. A value of 26 ppm (Desquines, 2007) may be used for H_0.

3.1.4 Thermal hydraulics modelling

In the high temperature regime, in which the cladding temperature is strongly affected by the thermal hydraulics, there is still plenty of room for improvements in modelling. One of the outcomes in the OECD/NEA RIA codes benchmark Phase II (OECD/NEA, 2016, 2017) was that the calculated cladding temperatures had very large dispersion among the various RIA fuel codes if the boiling crisis is reached. Poorly modelled cladding temperature evolution also affects many other output parameters of the simulations, undermining the reliability of the results. The difficulty in the RIA thermal hydraulics modelling is that the heat transfer in fast transients differs significantly from that in steady-state or slow transients. The lack of relevant experimental results, and the difficulty to experimentally measure thermal hydraulics phenomena in fast transient conditions, are identified problems (OECD/NEA, 2016).

The pursuit of improved thermal hydraulics modelling in RIA fuel behaviour analyses has intensified during recent years in many organizations worldwide. In the Japan Atomic Energy Agency (JAEA), improvements in the thermal hydraulics modelling of the RANNS code have been accomplished based on old NSRR RIA test data from an already dismantled water loop with versatile thermal hydraulic conditions (Udagawa et al., 2013). Quantum Technologies has developed for the Swedish Radiation Safety Authority SSM a simple homogeneous equilibrium model for the two-phase water coolant (Jernkvist, 2016; OECD/NEA, 2016). It is intended for BWR RIA applications, and implemented into SCANAIR. MTA-EK has built an online coupling between the fuel performance code FRAPTRAN and VTT-originated hot-channel code TRABCO, to be applied in RIAs (Keresztúri et al., 2013). In Utah State University, internal coupling of the BISON fuel performance code has been created with the thermal hydraulics code RELAP5 for RIA applications (Folsom et al., 2016).

In SCANAIR, the single-phase coolant is described with two conservation equations, mass and energy (2-equation model). The code has two established sets of thermal hydraulics model parameters. The first set of parameters is intended for PWR hot zero power (HZP) conditions (inlet temperature 280 °C, flow rate 4 m/s, coolant pressure 15.5 MPa), and it is fitted with the data from the out-of-reactor PATRICIA experimental programme (Bessiron, 2007). The second set, intended for interpretation of the results from pool test reactors, is fitted using the data from NSRR: stagnant water coolant at room temperature and atmospheric pressure (Bessiron et al., 2007).

Cold zero power (CZP, coolant at ~20-30 °C, 0.1 MPa) conditions are considered to be the worst initial state of an RIA in BWR because of the highest reactivity addition and the highest content of undissolved radial hydrides in the cladding

(OECD/NEA, 2010). In principle, the parameters tuned for the NSRR are applicable for a BWR rod drop accident initiating from CZP conditions. In practice, however, the excessive steam generation at atmospheric pressure may cause the current models in RIA codes to be non-adequate in these conditions (Marchand et al., 2016; OECD/NEA, 2016).

3.2 Zircaloy-2 material properties

3.2.1 New yield strength and UTS correlations

The PROMETRA data on Zry-2 originates from twelve tensile tests on ring specimens of irradiated cladding, and from nine tests on fresh cladding specimens. The irradiated cladding material (LK3 with inner liner) has been base-irradiated seven cycles up to the rod discharge burnup of ~58 MWd/kgU during the years 1998-2005.

The corresponding PROMETRA test matrix is presented in Table 3.1. The strain rate in the tests has been 1.0 s^{-1}, but one test with fresh and one with irradiated specimen has been made using a strain rate of 0.001 s^{-1}. The strain rate effect with the irradiated specimens is found to be insignificant.

Table 3.1. PROMETRA test matrix for Zry-2 cladding ring tensile tests.

		Furnace heating					Induction heating	
T [°C]		25	50	150	280	480	600	800
strain rate [s^{-1}]	Fresh fuel							
		1			0.001	1	1	1
		1					1	1
								1
	Irradiated fuel							
			1	1	1	1	1	1
			1	1	0.001	1	1	1

Some measurements in Table 3.1 are excluded from the final fitting of the new correlations. With the fresh fuel samples, when including the measurement point of deviant (0.001 s^{-1}) strain rate, the best-fit curve may be significantly different compared to that obtained if this point is excluded. More measurements in the temperature range 200-300 °C would be needed in order to verify the corresponding values of YS and UTS. Here the point is excluded from the fits. With the irradiated samples, the transition from furnace heating to induction heating may induce too low values

with two measurements prior to the transition. The same samples also showed macroscopic deformation. These measurements are excluded from the fits.

As there are no measurement points above 800 °C for Zry-2, points from Zry-4 mechanical tests are added to the high temperature region in the fits.

Different forms of correlations are tested in order to find the best fit with the measured points. First, the same formulation is tried as with the irradiated Zry-4, M5 and Zirlo claddings, presented in Eq. (3.4). This is also the correlation for Zry-2 YS and UTS already in SCANAIR:

$$\sigma[MPa] = \frac{a+b\,T[^{\circ}\mathrm{C}]}{1+e^{c(T[^{\circ}\mathrm{C}]-d)}}. \tag{3.4}$$

The other correlations that were tested are a second-order polynomial for the fresh fuel points, and a linear fit for the irradiated case. The most suitable correlation is searched by means of the highest coefficient of determination, R^2 (Brown, 2001):

$$R^2 = 1 - \frac{\sum_i (y_i - f_i)^2}{\sum_i (y_i - \bar{y})^2}. \tag{3.5}$$

Here, y_i:s are the measured YS and UTS values, $\bar{y}$ is the mean, and f_i:s are the YS and UTS values predicted with a correlation. For the irradiated Zry-2, Eq. (3.4) gives the highest R^2 values, 0.9984 (YS) and 0.9970 (UTS), while the R^2 values of the linear fit are 0.9972 (YS) and 0.9920 (UTS). For the irradiated Zry-2 cladding, the linear fit is thus almost as good as Eq. (3.4).

The polynomial fit is better for the fresh Zry-2 cladding: the R^2 values of Eq. (3.4) are 0.9681 (YS) and 0.9486 (UTS), and for the polynomial fit those are 0.9740 (YS) and 0.9642 (UTS). However, to be consistent, Eq. (3.4) is also used with fresh Zry-2, as the differences in the R^2 values between the two fits are not significant.

The fitted curves are presented in Fig. 3.1. For the latest SCANAIR releases, the YS and UTS laws have been slightly modified in the high temperature range in order to ensure the convergence (Moal, 2016).

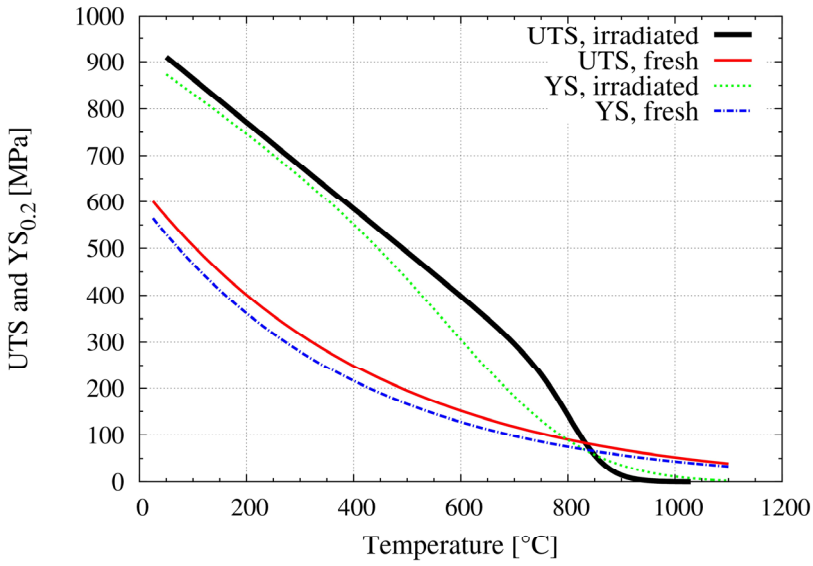

Figure 3.1. $YS_{0.2}$ and UTS of fresh and irradiated Zry-2.

3.2.2 Demonstration of the new correlations

The performance of the new correlations is evaluated by comparative simulations with the old and the new correlations. For this, the LS-1 and FK-1 tests on irradiated BWR fuel performed in NSRR are used. Both pool tests were carried out at room temperature and atmospheric pressure. The burnups of the rodlets were 69 (LS-1) and 45 MWd/kgU (FK-1).

With the LS-1 test, according to the base irradiation calculation with VTT-ENIGMA, the gap is closed prior to the transient, whereas with FK-1 there is a gap of 76 µm (according to FRAPCON 3.4). The gap size has a very large impact on the calculated SED, as can be seen in Fig 3.2a (see the small figure). If the gap is closed (LS-1), the calculated cladding mechanical SED increases by about 3 MJ/m³ when using the new correlations. If the gap is open (FK-1), the maximum mechanical SED remains unchanged. In both cases, there is no significant impact on cladding outer temperatures whether one uses the old or the new correlations. Thus, these simulations suggest that the effect of the new correlations on cladding failure estimation may be considered to be small.

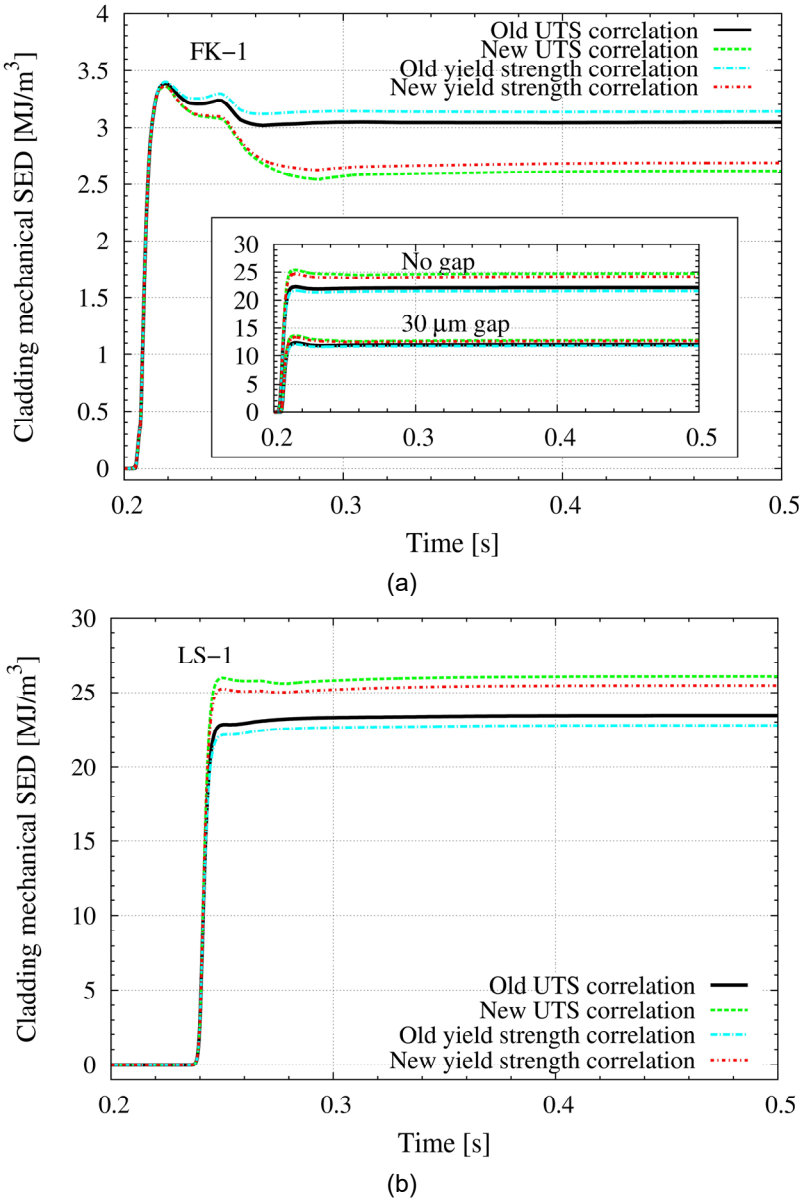

Figure 3.2. Cladding mechanical SED in FK-1 (a) and LS-1 (b) tests with the old and the new YS and UTS correlations in SCANAIR.

3.3 Cladding low temperature failure estimation

3.3.1 Simulation cases and the applied model

A number of RIA tests performed in NSRR on pre-irradiated BWR fuel are available for cladding low temperature failure evaluations (OECD/NEA, 2010; Udagawa et al., 2014b). In order to make a comprehensive review of the capability of SCANAIR to predict Zry-2 cladding failures, the complete FK test series was calculated in Publication **VI** with SCANAIR, eleven tests in total (Nakamura et al., 2002, 2004; Sugiyama et al., 2004). The pressure and the coolant temperature in the FK series were ambient, except in FK-10 and FK-12, in which the temperatures were 80 and 85 °C, respectively. The pulse widths in the FK test series range from 4.3 to 7.3 ms (OECD/NEA, 2010), and therefore the correlation in Eq. (3.2) may be used for these tests.

As stated in Section 3.1.3, the uncertainty in the simulated gap width causes uncertainty in the calculated SEDs. To study the effect of initial gap size on the calculated SEDs, the SCANAIR calculations are performed with various gap widths. The default cases are simulated using the FRAPCON mechanical gap (see Section 3.1.3). As a variation, smaller thermal gap values are applied. In addition, zero gap widths are used in high burnup tests (FK-6 – FK-12), in which the gap is closed according to the post-test examinations but still open according to the FRAPCON simulations.

Another factor causing uncertainty in the failure predictions with Eq. (3.2) is the applied hydrogen content. If the hydrogen content is not known from the measurement, an estimation must be used. To show the significance of this kind of approximation for the failure prediction, the CSED is calculated here in two ways from Eq. (3.2): by using the maximum values of the measured hydrogen contents, and by estimating the hydrogen content from Eq. (3.3).

3.3.2 Results

The cladding failure analysis results are presented in Table 3.2. The SED values calculated with SCANAIR are now conservatively compared with the minimum of the CSEDs calculated with the two methods explained above. The SEDs calculated by EPRI with the FALCON code (Alvis et al., 2016; EPRI, 2015) are also shown in Table 3.2. In most of the cases, the SEDs calculated with SCANAIR are comparable to the SEDs calculated with FALCON.

In Table 3.2, the mispredictions regarding the PCMI failure or non-failure are underlined. It can be seen that with tests FK-6 – FK-12, the use of the smaller gap width (thermal gap) gives fewer mispredictions than the mechanical gap. The small gap also gives good predictions for the other tests except for FK-3, which is mispredicted in this case. However, if the SED is compared to the CSED calculated directly from the maximum hydrogen content, FK-3 is also correctly predicted to survive

when applying the small gap. Test FK-4 is incorrectly predicted to fail by both SCANAIR and FALCON.

Table 3.2. SCANAIR calculations of mechanical SED in FK tests vs. the CSED. Basic case: FRAPCON mechanical gap is used as such; small (thermal) gap: gap width is reduced by adding the remaining 50% of the fuel relocation term to the pellet radius; zero gap: zero gap (post-test examination result) is used with SCANAIR. SED values are compared with the minimum (shown in bold) of the CSEDs calculated in two ways: directly using the measured maximum hydrogen content, or using hydrogen content determined from the outer oxide layer with a correlation. Mispredictions are underlined. Failure enthalpies are given in parentheses.

	SED				CSED					
	Max. mechanical SED by SCANAIR [MJ/m^3]			Max. calc. SED by FALCON (EPRI, 2015) [MJ/m^3]	CSED from Eq. (3.2), hydrogen content evaluated from clad oxide layer with Eq. (3.3)	CSED from Eq. (3.2), max. measured hydrogen content used	Survived (S) / Failed (F), failure enthalpy [cal/g]			
							Test result (OECD/NEA, 2010)	SCANAIR		
Test	Basic case	Small gap	Zero gap					Basic case	Small gap	Zero gap
FK-1	5.5	12.3	-	13	**17.9**	21.7	S	S	S	-
FK-2	0.30	0.40	-	2.1	**16.7**	21.7	S	S	S	-
FK-3	9.9	16.9	-	16	**16.0**	21.7	S	S	F (141)	-
FK-4	21.9	29.8	-	20.2	**17.6**	19.9	S	F (139)	F (120)	-
FK-5	0.58	3.7	-	7.4	**17.6**	19.9	S	S	S	-
FK-6	19.1	27.0	29.1	19	14.2	**8.1**	F (70)	F (106)	F (77)	F (68)
FK-7	17.5	25.1	27.0	19.3	14.2	**8.1**	F (62)	F (106)	F (77)	F (69)
FK-8	0.79	4.7	6.4	5.1	14.2	**11.2**	S	S	S	S
FK-9	3.9	10.8	12.6	12	14.2	**11.2**	F (86)	S	S	F (84)
FK-10	6.1	13.3	15.2	13.3	14.2	**8.1**	F (80)	S	F (81)	F (72)
FK-12	3.0	9.5	11.3	10.3	14.2	**8.1**	F (72)	S	F (82)	F (73)

The deviations between the calculated and observed failure enthalpies in the cases of mechanical gap initializations are 36 – 44 cal/g (with the cases that were correctly predicted to fail), with small gap 1 – 15 cal/g, and with zero gap 1 – 8 cal/g. Thus, in high burnup fuel (FK-6 – FK-12), the zero gap produces the best estimates with regard to failure enthalpy.

It should be remarked that the values for maximum enthalpy increase and failure enthalpy have been re-evaluated with a new method (Udagawa et al., 2014b) for several high burnup NSRR test series. In the tests with BWR fuel, the new values are slightly changed but are considered to be “similar” (Udagawa et al., 2014b) compared to the previous evaluations. Taking into account that the new method seems less important for BWR tests compared to PWR, and that there are difficulties in the

new method when applying it to BWR fuel (Udagawa et al., 2014b), the original values have been maintained in the current analysis.

3.3.3 Discussion

Despite the uncertainty resulting from the gap size, SCANAIR's SED approach applied with EPRI's CSED criterion is found to give correct predictions with reasonably good accuracy when applied to a larger dataset of several tests. However, if considering only a single test and applying a given gap width, it is easy to obtain false predictions. The applied hydrogen content in the CSED criterion brings another factor of uncertainty to the predictions. For these reasons, the SED approach should be applied with caution.

3.4 Thermal hydraulics in BWR RIA

3.4.1 SCANAIR-GENFLO coupling

The interface between SCANAIR and GENFLO codes is set at the cladding outer surface. SCANAIR serves as a master code and calls for GENFLO. A schematic presentation of the most important parameters passed between the codes during each time-step is shown in Fig. 3.3.

The coupling is made by introducing a new thermal hydraulics option in the driver subroutine of the SCANAIR thermal solver. An interface subroutine is coded for data exchange between the codes.

GENFLO has an own simple fuel rod thermal behaviour model, in which the cladding temperature is solved. As GENFLO is non-iterative, attention is paid to ensure that the rod thermal solutions in both codes are close to each other. Therefore, similar correlations for thermal conductivities and specific heat capacities of UO_2 and Zircaloy are used in SCANAIR and in GENFLO. The reduction of the coolant channel flow area, caused by the cladding ballooning, is transferred to GENFLO. Furthermore, the gap width evolution calculated by SCANAIR is taken into consideration in GENFLO.

Some further modifications to GENFLO were made in order to ease the code-to-code comparisons, and to test various film boiling correlations. A possibility to use some existing film boiling correlations of SCANAIR was added to GENFLO: Bishop-Sandberg-Tong (BST) for PWR (Bishop et al, 1965) and Sakurai (Sakurai et al., 1990) for stagnant water conditions. Groeneveld-5.7 and -5.9 (Groeneveld, 1969) film boiling correlations were also coded into GENFLO. Groeneveld correlations are applicable in BWR pressure conditions.

Furthermore, in a benchmark case in which boiling was prevented by the power level, it was found out that the CHF correlation of GENFLO produced too low values, resulting in a boiling crisis. Therefore, the Babcock and Wilcox CHF correlation (Weisman and Bowring, 1975) was coded into GENFLO and applied for the PWR

cases. The same correlation is used in SCANAIR, but in SCANAIR it is modified to take into account kinetic effects (Moal et al., 2014).

To compare the transition in the rewetting phase, the quadratic interpolation used in SCANAIR for the transition heat flux was coded into GENFLO. GENFLO was also provided with the possibility to give the rewetting temperature as an input. For the demonstration simulations, the rewetting temperature recommended by IRSN for PWR is used.

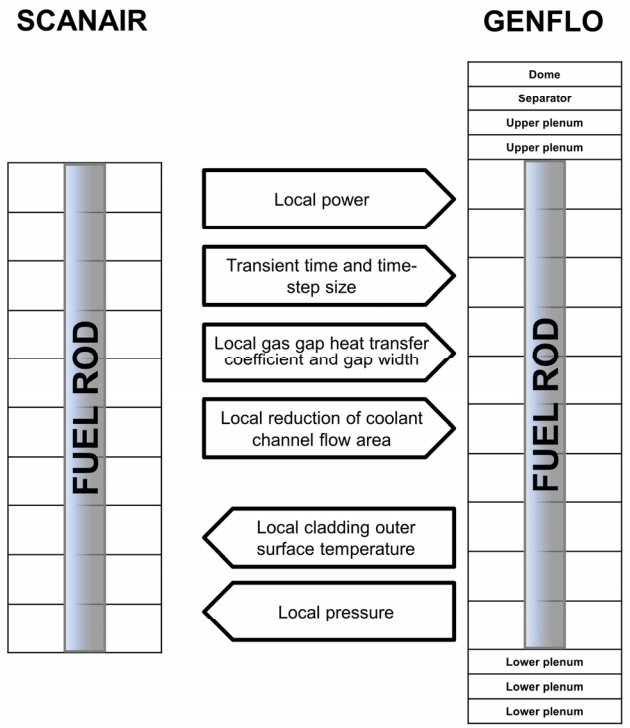

Figure 3.3. Schematic presentation of SCANAIR-GENFLO coupling.

3.4.2 Selected demonstration cases

To demonstrate the performance of the coupled code, generic RIA cases are simulated. Code-to-code comparisons using two recent OECD/NEA RIA codes benchmark Phase II cases in PWR conditions (OECD/NEA, 2016) are made. The coupling is further studied with a hypothetical BWR RIA case starting from hot full power (HFP).

The RIA benchmark cases are generic simplified cases with no measurements available for comparison. However, the simulation of the benchmark cases allows direct comparison with the other codes used internationally for modelling RIA fuel

behaviour. Comparison with the SCANAIR state-of-the-art model of PWR thermal hydraulics is also then possible. To better identify the differences in modelling between the stand-alone SCANAIR and SCANAIR-GENFLO, similar modelling assumptions and heat transfer correlations are used in simulations as much as possible. The benchmark cases, named Case 4 and 5 in the benchmark specifications, are fresh fuel cases but with zero initial gas gap, and initiate at HZP conditions. The fuel stack height is 10 cm, and the cladding material is standard Zry-4. The input definitions are the same in both cases, except for the maximum power during the RIA pulse: 0.4 MW in Case 4 in order to prevent boiling, and 1.0 MW in Case 5 to allow boiling. The power pulse is triangular, and the Full Width at Half Maximum (FWHM) is 30 ms. Case 5 has been used as a reference case in a detailed uncertainty and sensitivity analysis (OECD/NEA, 2017).

In the hypothetical BWR RIA case, the FWHM of the pulse is 30 ms, and the pulse shape is the same as that used in the CABRI reactor (Bessiron, 2007). The injected energy is chosen so that the maximum radially averaged enthalpy is well below the fuel failure limit, 140 cal/g, set by the Finnish safety authority (STUK, 2013). The base irradiation is simulated with the VTT-ENIGMA code. The main pre-transient parameters are as follows: 63.5 MWd/kgU average discharge burnup, 15 kW/m average pre-transient power, 3.5 m rod length and 20.0 µm cladding outer oxide layer. For simplicity, flat axial power profile during the transient is assumed. The analysed case does not reflect any real postulated scenario; for example, the pulse width in BWR HFP might be wider and the axial power profile is not flat in high burnup fuel.

3.4.3 Results

RIA benchmark cases

The calculated cladding surface temperature evolutions in the two benchmark cases are shown in Fig. 3.4. In Fig. 3.4a, it is seen that Case 4 without boiling is similarly modelled by SCANAIR and SCANAIR-GENFLO. This is an expected result, as both codes apply the Dittus-Boelter (Dittus and Boelter, 1930) heat transfer correlation for the forced convection into liquid.

In Fig. 3.4b, the cladding temperature evolutions in Case 5 may be compared with the temperatures produced by the other participants of the RIA codes benchmark Phase II (Marchand et al., 2016), shown as approximate envelope curves. The difference in the calculated maximum cladding temperatures between SCANAIR and SCANAIR-GENFLO results from the fact that the transition boiling in the heat-up phase is not modelled in GENFLO. The transition during the rewetting is described in GENFLO with the quadratic interpolation as in SCANAIR. If the original transition boiling correlation of GENFLO is used, it is necessary to use a higher value for the multiplying coefficient compared to the nominal value of 0.2 (Miettinen and Hämäläinen, 2002; Table 1 in Publication **VI**); for example, a value of 2.5 results in as fast transition as with the quadratic interpolation.

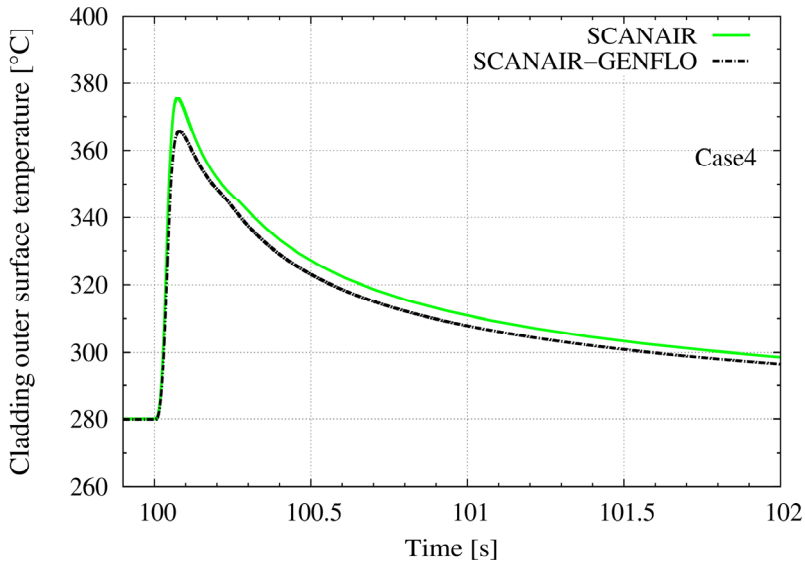

(a)

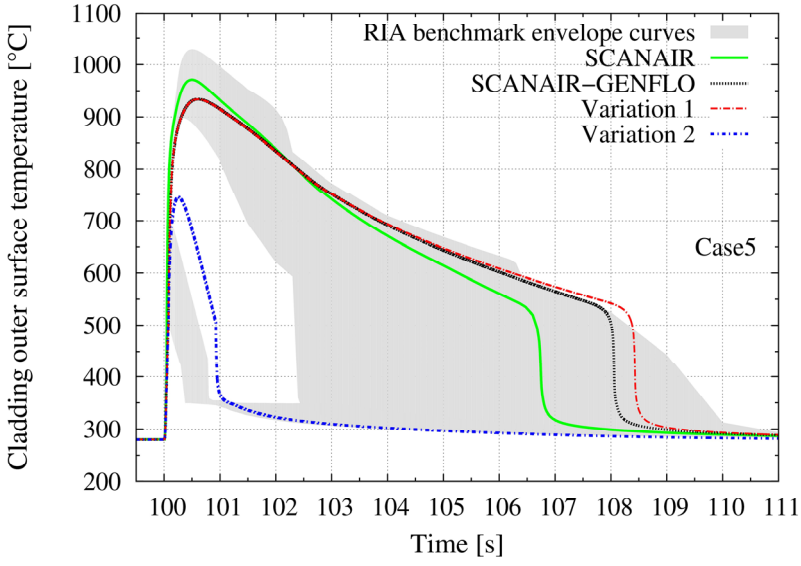

(b)

Figure 3.4. SCANAIR-GENFLO and stand-alone SCANAIR cladding outer surface temperatures (axially at the middle of the rodlet) in two benchmark cases defined in OECD/NEA (2016). Case 4 (a) without boiling, and Case 5 (b) with boiling.

In the film boiling phase, the BST heat transfer correlation is applied in GENFLO. The heat transfer coefficient calculated with the steady film boiling BST correlation is almost constant, and therefore the original film boiling correlation of GENFLO

(Miettinen and Hämäläinen, 2002; Table 1 in Publication **VI**) produces rather similar temperature evolution if a value 10.97 is used for the multiplying coefficient instead of the nominal value 0.2, as shown in "Variation 1" in Fig. 3.4b. The cladding cool-down rates differ somewhat during the film boiling while using the same BST correlation both in SCANAIR and SCANAIR-GENFLO. As a result, the rewetting occurs more than one second later with SCANAIR-GENFLO.

It can be seen in Fig. 3.4b that there are two groups of codes with respect to the duration of the high temperature phase and the maximum cladding temperature (Marchand et al., 2016). The first group produces short duration and lower maximum temperatures, and the other group long duration and higher temperatures. The first group contains many contributions calculated with FRAPTRAN. JAEA's RANNS code with its improved thermal hydraulics modelling also belongs to the first group. Both SCANAIR and SCANAIR-GENFLO results are within the envelopes of the higher temperature group. In order to explain the distinction between the two groups, and why SCANAIR-GENFLO belongs to the higher temperature group, "Variation 2" (Fig. 3.4b) is calculated with SCANAIR-GENFLO. In this variation, only convection into liquid (when $T_{clad} < T_{sat} + 160$ °C) and nucleate boiling (when $T_{clad} > T_{sat}$) are considered without entering into the film boiling regime. Furthermore, if only the convection into liquid is considered, approximately the lowest envelope curve is obtained. Therefore, it may be stated that in the lower envelope group in the benchmark Case 5, the extremely high clad-to-coolant heat transfer corresponds to the convective and nucleate boiling regime in GENFLO.

BWR case

Film boiling in BWR may be divided into two sub-regions separated by slug flow in the transition: inverted annular film boiling (IAFB) with vapour film separating the cladding surface and liquid coolant (in void fractions below ~40%), and dispersed flow film boiling (DFFB) with liquid droplets in vapour flow (IAEA, 2001). During RIA, DFFB dominates in the upper part of the rod, and in the lower section, the main clad-to-coolant heat transfer mode is IAFB. As explained in Section 3.1, superposition of the various heat transfer mechanisms is assumed in the GENFLO approach, with no sharp transition to another regime. When applying the GENFLO film boiling correlation (heat transfer into liquid), the value of that heat transfer component gradually decreases upwards in the coolant channel as a function of the void fraction, while the heat transfer component describing the convective heat transfer into steam increases.

Of the two film boiling modes, greater uncertainty is associated with the IAFB heat transfer in general (IAEA, 2001), and with BWR RIA heating conditions in particular. Therefore, the BWR RIA scenario is now calculated with two different film boiling correlations: GENFLO film boiling correlation with the same value for the multiplying coefficient, 10.97, as applied above in the RIA benchmark Case 5 (plots in the left-hand side in Fig. 3.5), and Groeneveld-5.7 (right-hand side in Fig. 3.5). In Fig. 3.5, axial evolutions of cladding outer surface temperature, coolant pressure and the dominating components of clad-to-coolant heat transfer coefficients are shown. As the Groeneveld correlation gives the overall heat transfer coefficient from

clad to fluid, the heat transfer to vapour in the upper part of the rod is effectively counted twice. However, in this case, this does not have a dramatic effect on the temperatures in the upper nodes, as the explicit convective heat transfer component dominates in this region (Fig. 3.5).

According to the AECL look-up table for fully developed film boiling heat transfer coefficients (IAEA, 2001), the coefficient increases when the quality increases upwards of the coolant channel, by taking into consideration the prevailing pressure, mass flux, and heat flux at various axial locations in this particular hypothetical BWR case. The results obtained with the Groeneveld correlation, suggesting that the surface temperatures in the upper part of the rod are lower than in the bottom part, are consistent with the trend seen in tabulated film boiling heat transfer coefficients. However, the overall heat transfer coefficient calculated with the Groeneveld correlation, added up with the convection into vapour, is underestimated, as the heat transfer coefficient from the AECL table would be around 700-1100 $W/m^2/K$ in the bottom part of the rod. Then again, the GENFLO correlation, tuned with the multiplier, overestimates the heat transfer in the bottom part. In reality, the heat transfer coefficients and the surface temperatures in the IAFB region might be somewhere between the two extremes shown in Fig. 3.5.

The radiation heat transfer becomes important in the film boiling phase when the cladding surface temperatures are higher than 700 °C (IAEA, 2001). Here, the default value for the multiplying coefficient in the radiation heat transfer correlation is applied (Miettinen and Hämäläinen, 2002; Table 1 in Publication **VI**). If a tenfold higher value is applied for the coefficient, and the Groeneveld film boiling correlation is used, the maximum cladding surface temperature in the bottom part of the rod decreases by about 60 °C and the quenching in that part occurs about 5 seconds earlier compared to the situation with the default coefficient. Thus, the effect of radiation heat transfer in this case is not very pronounced. It should be noted that by using a more realistic axial power profile instead of a flat one, the temperatures in the bottom end of the rod would naturally decrease.

The calculated coolant pressure evolutions shown in Fig. 3.5 present a sharp and relatively short pressure jump immediately after the power surge. In the rewetting phase, steam is generated when the liquid contacts the heated surface, increasing the void fraction. If the cladding rewetting occurs almost instantaneously along the whole rod, the pressure rise due to steam generation is significant, as seen in the left-hand side pressure plot in Fig. 3.5. However, instantaneous rewetting of the full-length rod may be considered highly unlikely.

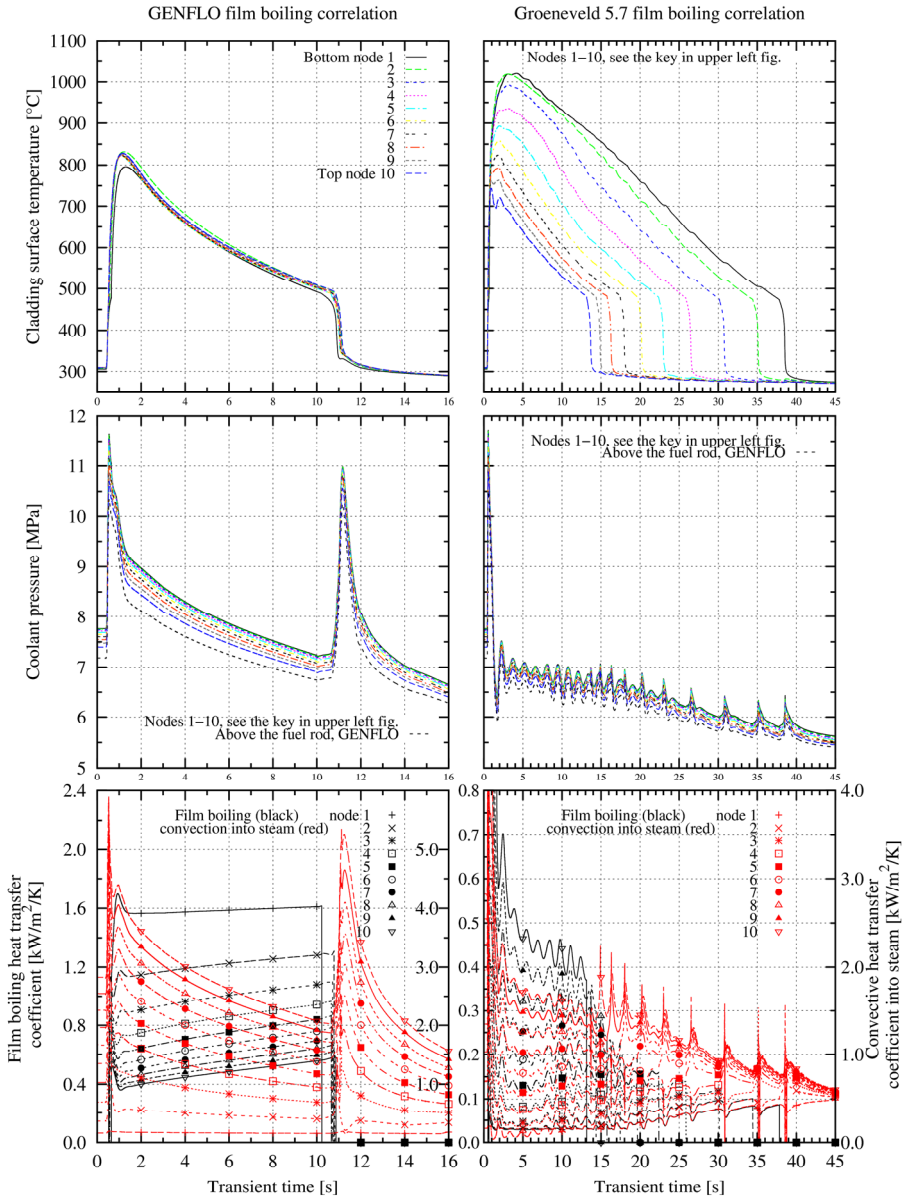

Figure 3.5. Axial evolutions of cladding outer surface temperature, coolant pressure and the dominating components of clad-to-coolant heat transfer coefficients in the hypothetical BWR HFP case. Figures on the left-hand side were calculated using the original film boiling correlation of GENFLO and a multiplication coefficient of 10.97. Figures on the right-hand side were calculated with the Groeneveld-5.7 (Groeneveld, 1969) film boiling correlation.

3.4.4 Discussion

Overall, the demonstration cases show that the coupling works as expected. In the benchmark case with PWR HZP conditions without boiling, the cladding temperatures are comparable with the stand-alone SCANAIR. The results are also in line with one of the conclusions of the RIA benchmark (Marchand et al., 2016), stating that relatively good agreement in cladding temperatures between various codes is observed when boiling crisis is not reached. In the second considered benchmark case with boiling, the cladding temperatures of SCANAIR-GENFLO match rather well with stand-alone SCANAIR, when similar assumptions and heat transfer correlations are used. The transition boiling during the heat-up would require a rigorous model to be implemented into GENFLO.

The advantages of using GENFLO are that, unlike in SCANAIR, the bulk boiling phenomena are considered, and the thermal hydraulics description is more detailed compared to homogeneous equilibrium models such as that included in FRAPTRAN (Geelhood et al., 2016). As the coolant pressure is not calculated in the standard SCANAIR thermal hydraulics model, and as the axial pressure evolution naturally affects the thermal hydraulics behaviour, it is a clear improvement that the pressure modelling is now considered.

A shortcoming of GENFLO regarding RIA modelling is that the code's heat transfer models are not specifically fitted for modelling fast transient conditions of an RIA, but are intended for steady-state and slow transients such as LOCA. However, this is not rare in this field of research, even if a small number of fuel performance codes have RIA-specific thermal hydraulics models. When new information on fast transient heat transfer becomes available, it will be easy to make changes to GENFLO. Not only the correlations, but also transitions between the boiling regimes in the boiling curve should be fitted in BWR RIA bulk boiling conditions. Based on the BWR thermal hydraulics analysis, it may by concluded that in order to improve the modelling, especially the IAFB region needs experimental results in prototypical BWR RIA thermal hydraulics conditions.

4. Conclusions

4.1 LOCA modelling

In this thesis, a new core-wide statistical approach was adopted for evaluation of the number of failing rods in a large break LOCA in an EPR type reactor. The fulfilment of the safety regulation was shown with a sound statistical method relying on the results of nonparametric statistics. A multistage calculation chain was required to consolidate the procedure. As an outcome, in the worst global scenario, 1.4% of the rods were simulated to fail. Therefore, it was concluded that the Finnish safety regulation with respect to the maximum permitted number of failing rods, 10%, was met.

In order to determine which initial parameters have significance for the risk of fuel failure, sensitivity analysis was performed. Due to the complexity of the existing data, a multistage sensitivity analysis methodology was developed. In the first phase, the relevant input parameters for the sensitivity analysis had to be specified. Data visualization with a cobweb graph was used for the screening. Then, selected sensitivity measures were calculated between the chosen input and output parameters. The sensitivity indices calculated were the Borgonovo's delta measure, the first order Sobol' sensitivity index, and squared Pearson correlation coefficient. The first mentioned is a novelty in this context.

As an outcome, the most relevant parameters with respect to the cladding integrity were determined to be the decay heat power during the transient, the thermal hydraulic conditions in the rod's location in the reactor, and the steady-state irradiation history of the rod as represented in this analysis by the rod burnup. Ultimately, when the factors affecting the fuel rod failures are known from the sensitivity analysis, this information could be used in diminishing the number of failing rods.

4.2 RIA modelling

The goal in RIA modelling was to adapt the French SCANAIR code, specifically developed for modelling RIAs in PWRs, to be able also to model BWR RIAs. New cladding yield strength correlations were fitted and implemented for better description of the plastic behaviour of BWR cladding during an RIA. The capability of SCANAIR to predict low temperature failures in BWR claddings was evaluated. SCANAIR was found to give correct predictions with reasonably good accuracy when applied to a larger dataset of several tests. The sensitivity of the failure predictions with respect to the initial gap size used as an input for SCANAIR was highlighted.

The thermal hydraulics of standard SCANAIR cannot handle bulk boiling phenomena, and therefore a coupling with an external thermal hydraulics code was introduced. The chosen thermal hydraulics code is VTT's in-house GENFLO code. The first demonstration simulations yielded promising results, and the coupling is now proceeding to the validation stage.

It should be noted that the work presented in this thesis is not limited to GENFLO, but it also demonstrates that any suitable subchannel thermal hydraulics code could be coupled with SCANAIR in a similar fashion.

Internationally, improving the thermal hydraulics modelling in RIA conditions is a very topical subject, but the lack of experimental thermal hydraulics results in prototypical BWR RIA conditions is a problem. This can be solved only by performing more instrumented separate effect or integral tests. When the test conditions and the materials are representative of those in a power reactor, the results may eventually be used for making improvements to the thermal hydraulic models and heat transfer correlations.

4.3 Future plans

4.3.1 Statistical and sensitivity analysis of LOCA

In the LOCA sensitivity analysis presented in this thesis, the influence of various local parameters was studied. In the future, global parameters will also be addressed. However, data from global scenarios other than the worst case is scarce, as only 1000 rods were simulated per scenario. Therefore, surrogate models are needed for making a thorough sensitivity analysis with the global parameters included.

Further development of the statistical and sensitivity analysis procedure has been started (Arkoma, 2017) by replacing the neural networks with support vector machines (SVMs) (James et al., 2013). SVMs have some advantages over neural networks; in this analysis, better performance in classification of the rods into failed/non-failed is seen as a possible advantage.

The problem with the neural network surrogate model (Publication **II**) was that a significant number of rods calculated to fail were not correctly predicted by the network. This could be explained by the fact that the number of failing rods used in teaching the network was very limited. To cure the problem in rod failure recognition caused by the imbalance between the number failing and surviving rods, an iterative solution was formulated: an SVM is trained with the existing small number of simulations, and then it is used in predicting a new set of rods that could possibly fail in LOCA. These rods are then simulated with the fuel performance code, and the resulting additional data is included in the training set of the SVM. It was demonstrated that the iterative procedure indeed improves the predictions of the surrogate model with moderate increase in the number of additional fuel code simulations (Arkoma, 2017).

The procedure has implications for the sensitivity analysis to be performed with the artificial data. When the accuracy of predictions is improved with the procedure described above, the accuracy of the sensitivity analysis is improved compared to the situation in which only the original 1000 simulations were used in the fitting.

The next step will be to apply SVMs for each global scenario to capture the global effects. An evaluation of the SVMs in the sensitivity analysis will be carried out, with

comparisons to the sensitivity analysis results of FRAPTRAN-GENFLO simulations (Publication **IV**).

4.3.2 BWR RIA modelling

Validation and further development of SCANAIR-GENFLO coupling will be carried out in the future. RIA tests in BWR conditions and/or with BWR fuel, performed in NSRR (Amaya et al., 2015; Sugiyama et al., 2010; Udagawa et al., 2013, 2014a), and in SPERT and PBF facilities in the USA (OECD/NEA, 2010), could be used for validation.

References

Abdelghany, J.M., Martin, R.P., 2010. Uncertainty analysis for containment response of U.S. EPR™ reactor to large break loss-of-coolant accidents. In proceedings of: ICAPP '10, San Diego, California, USA, June 12-17, 2010.

Alvis, J., Lyon, W., Yeuh, K., 2016. Using Falcon to develop an RIA PCMI failure criteria. In proceedings of: TopFuel 2016, Boise, Idaho, USA, September 11-15, 2016.

Amaya, M., Udagawa, Y., Narukawa, T., Mihara, T., Sugiyama, T., 2015. Behavior of high burnup advanced fuels for LWR during design-basis accidents. In proceedings of: TopFuel 2015, Zurich, Switzerland, September 13-17, 2015.

Arimescu, V.I., 2012. Quantifying uncertainties and best-estimate, realistic methods for LWR fuel mechanical analysis during steady-state and AOO transients. In proceedings of: TopFuel 2012, Manchester, United Kingdom, September 2-6, 2012.

Arkoma, A., 2017. Applying support vector machines (SVMs) to predict fuel failures in LOCA. VTT Research Report. VTT-R-00964-17.

Aufore, L., 1997. Etude du transport de l'hydrogene produit lors de la corrosion des gaines d'elements combustibles des reacteurs a eau sous pression dans la zircone et le zircaloy-4. Doctoral dissertation, Université de la Mediterranée, Aix-Marseille-II. FRCEA-TH--656. https://inis.iaea.org/search/search.aspx?orig_q=RN:30011301 (visited May 5, 2017).

Bailly, H., Menessier, D., Prunier, C., 1999. The nuclear fuel of pressurized water reactors and fast reactors. Design and behaviour. Le Commissariat à l'énergie atomique et aux énergies alternatives (CEA). Published by Intercept Ltd. 660 p.

Baucells, M., Borgonovo, E., 2013. Invariant probabilistic sensitivity analysis. Management Science, Vol. 59, pp. 2536-2549.

Bernaudat, C., Cambier, S., Guion, J., Benjamin, S., 2009. An analytical criterion to prevent PCMI fuel rod cladding failure during RIA transients. In proceedings of: TopFuel 2009, Paris, France, September 6-10, 2009.

Bessiron, V., 2007. Modelling of clad-to-coolant heat transfer for RIA applications. Journal of Nuclear Science and Technology, Vol. 44, pp. 211-221.

Bessiron, V., Sugiyama, T., Fuketa, T., 2007. Clad-to-coolant heat transfer in NSRR experiments. Journal of Nuclear Science and Technology, Vol. 44, pp. 723-732.

Bishop, A., Sandberg, R., Tong, L., 1965. Forced convection heat transfer at high pressure after the critical heat flux. American Society of Mechanical Engineers, ASME-65-HT-31.

Blyth, T., Avramova, M., Ivanov, K., Royer, E., Sartori, E., Cabellos, O., 2012. Benchmark of uncertainty analysis in modeling (UAM) for design, operation and safety analysis of LWRs, volume II: Specification and support data for the core cases (Phase II). Technical Report draft version 1.0, NEA/NSC/DOC(2012)?.

Borgonovo, E., 2006. Measuring uncertainty importance: investigation and comparison of alternative approaches. Risk Analysis, Vol. 26, pp. 1349-1362.

Borgonovo, E., 2007. A new uncertainty importance measure. Reliability Engineering and System Safety, Vol. 92, pp. 771-784.

Borgonovo, E., Plischke, E., 2016. Sensitivity analysis: a review of recent advances. European Journal of Operational Research, Vol. 248, pp. 869-887.

Bouloré, A., Struzik, C., Gaudier, F., 2012. Uncertainty and sensitivity analysis of the nuclear fuel thermal behaviour. Nuclear Engineering and Design, Vol. 253, pp. 200-210.

Boyack, B.E., Catton, I., Duffey, R.B., Griffith, P., Kastma, K.R., Lellouche, G.S., Levy, S., Rohatgi, U.S., Wilson, G.E., Wulf, W., Zuber, N., 1990. Quantifying reactor safety margins. Part 1: an overview of the code scaling, applicability and uncertainty evaluation methodology. Nuclear Engineering and Design, Vol. 119, pp. 1-15.

Brown, A.M., 2001. A step-by-step guide to non-linear regression analysis of experimental data using a Microsoft Excel spreadsheet. Computer Methods and Programs in Biomedicine, Vol. 65, pp.191-200.

Cathcart, J.V., Pawel, R.E., McKee, R.A., Druschel, R.E., Yurek, G.J., Campbell, J.J., Jury S.H., 1977. Zirconium metal-water oxidation kinetics IV, reaction rate studies. Oak Ridge National Laboratory, Oak Ridge, Tennessee. ORNL/NUREG-17.

Cazalis, B., Desquines, J., Poussard, C., Petit, M., Monerie, Y., Bernaudat, C., Yvon, P., Averty, X., 2007. The PROMETRA program: fuel cladding

mechanical behavior under high strain rate. Nuclear Technology, Vol. 157, pp. 215-229.

Cooke, R.M., van Noortwijk, J.M., 2000. Generic graphics for uncertainty and sensitivity analysis. In proceedings of: ESREL '99 - The 10th European conference on safety and reliability, Munich, Germany, September 13-17, 1999.

de Crécy, A., Bazin, P., Glaeser, H., Skorek, T., Joucla, J., Probst, P., Fujioka, K., Chung, B.D., Oh, D.Y., Kyncl, M., Pernica, R., Macek, J., Meca, R., Macian, R., D'Auria, F., Petruzzi, A., Batet, L., Perez, M., Reventos, F., 2008. Uncertainty and sensitivity analysis of the LOFT L2-5 test: results of the BEMUSE programme. Nuclear Engineering and Design, Vol. 238, pp. 3561-3578.

Desquines, J., 2007. Propriétés des gainages dans le cadre de leur transport : Zircaloy-2 (English title: Cladding properties for transportations: Zircaloy-2). Note Technique, SEMCA-2007-386. IRSN, Cadarache, France.

Di Maio, F., Bandini, A., Zio, E., Carlos Alberola, S., Sanchez-Saez, F., Martorell, S., 2016. Bootstrapped-ensemble-based sensitivity analysis of a trace thermal-hydraulic model based on a limited number of PWR large break LOCA simulations. Reliability Engineering and System Safety, Vol. 153, pp. 122-134.

Di Maio, F., Nicola, G., Zio, E., Yu, Y., 2014. Ensemble-based sensitivity analysis of a best estimate thermal hydraulics model: application to a passive containment cooling system of an AP1000 nuclear power plant. Annals of Nuclear Energy, Vol. 73, pp. 200-210.

Dittus, F.W, Boelter, L.M, 1930. Heat transfer in automobile radiators of the tubular type. University of California Publications in Engineering, Vol. 2, pp. 443-461.

EPRI, 2010. Fuel reliability program: proposed RIA acceptance criteria. Electric Power Research Institute, Palo Alto, California. Technical Report, final report, 1021036.

EPRI, 2015. Fuel reliability program: proposed reactivity insertion accident (RIA) acceptance criteria, revision 1. Electric Power Research Institute, Palo Alto, California. Technical Report, final report, 3002005540.

Feria, F., Herranz, L.E., 2015. Internal pressure of spent PWR fuel rod at high burnup: prediction enhancement through FRAPCON-3.5 uncertainty

analysis. In proceedings of: TopFuel 2015, Zurich, Switzerland, September 13-17, 2015.

Folsom, C.P., Jensen, C.B., Williamson, R.L., Woolstenhulme, N.E., Ban, H., Wachs, D.M., 2016. BISON modeling of reactivity-initiated accident experiments in a static environment. In proceedings of: TopFuel 2016, Boise, Idaho, USA, September 11-15, 2016.

Freixa, J., Kim, T.-W., Manera, A., 2010. Thermal-hydraulic analysis of an intermediate LOCA test at the ROSA facility including uncertainty evaluation. In proceedings of: The 8th international topical meeting on nuclear thermal-hydraulics, operation and safety, NUTHOS-8, Shanghai, China, October 10-14, 2010.

Freixa, J., Kim, T.-W., Manera, A., 2011. Post-test thermal-hydraulic analysis of two intermediate LOCA tests at the ROSA facility including uncertainty evaluation. In proceedings of: The 14th international topical meeting on nuclear reactor thermal hydraulics, NURETH-14, Toronto, Ontario, Canada, September 25-30, 2011.

Freixa, J., Kim, T.-W., Manera, A., 2012. Thermal-hydraulic analysis of an intermediate LOCA test at the ROSA facility including uncertainty evaluation. Nuclear Engineering and Design, Vol. 249, pp. 97-103.

Frepoli, C., 2008. An overview of Westinghouse realistic large break LOCA evaluation model. Science and Technology of Nuclear Installations, Vol. 2008, article ID 498737.

Frepoli, C., Chiang, J.S., Petzold, J.S., Olinski, D.C., 2010. Application and licensing of Westinghouse realistic large break LOCA evaluation model (ASTRUM) for Maanshan units 1 and 2 nuclear power plant. In proceedings of: PHYSOR 2010, Pittsburgh, Pennsylvania, USA, May 9-14, 2010.

Frepoli, C., Ohkawa, K., 2011. The development of a realistic LOCA evaluation model applicable to the full range of breaks sizes: Westinghouse Full Spectrum LOCA (FSLOCA™) methodology. In proceedings of: The 14th international topical meeting on nuclear reactor thermal hydraulics, NURETH-14. Toronto, Ontario, Canada, September 25-30, 2011.

Frepoli, C., Ohkawa, K., Kemper, R.M., 2004. Realistic large break LOCA analysis of AP1000 with ASTRUM. In proceedings of: The 6th international conference on nuclear thermal hydraulics, operations and safety, NUTHOS-6, Nara, Japan, October 4-8, 2004.

Gamble, K.A., Swiler, L.P., 2016. Uncertainty quantification and sensitivity analysis applications to fuel performance modeling. In proceedings of: TopFuel 2016, Boise, Idaho, USA, September 11-15, 2016.

Geelhood, K.J, Luscher, W.G., Beyer, C.E., 2011a. FRAPCON-3.4: A computer code for the calculation of steady-state, thermal-mechanical behavior of oxide fuel rods for high burnup. NUREG/CR-7022, Vol. 1, PNNL-19418, Vol. 1.

Geelhood, K.J, Luscher, W.G., Beyer, C.E., Cuta, J.M., 2011b. FRAPTRAN 1.4: A computer code for the transient analysis of oxide fuel rods. NUREG/CR-7023, Vol. 1, PNNL-19400, Vol. 1.

Geelhood, K.J, Luscher, W.G., Cuta, J.M., Porter, I.A., 2016. FRAPTRAN-2.0: A computer code for the transient analysis of oxide fuel rods. PNNL-19400, Vol.1, Rev.2.

Geelhood, K.J, Luscher, W.G., Raynaud, P.A., Porter, I.E., 2015. FRAPCON-4.0: A computer code for the calculation of steady-state, thermal-mechanical behavior of oxide fuel rods for high burnup. PNNL-19418, Vol.1, Rev.2.

Georgenthum, V., Moal, A., Marchand, O., 2014. SCANAIR a transient fuel performance code part two: assessment of modelling capabilities. Nuclear Engineering and Design, Vol. 280, pp. 172-180.

Groeneveld, D.C., 1969. An investigation of heat transfer in the liquid deficient regime. Atomic Energy of Canada Limited, AECL-3281.

Guba, A., Makai, M., Pál, L., 2003. Statistical aspects of best estimate method – I. Reliability Engineering and System Safety, Vol. 80, pp. 217-232.

Hagrman, D. T (editor), 1993. SCDAP/ RELAP5/MOD3.1 code manual volume IV: MATPRO – a library of materials properties for light-water-reactor accident analysis. NUREG/CR-6150, EGG-2720, Volume IV. Prepared for the U.S.NRC.

Hämäläinen, A., Stengård, J.-O., Miettinen, J., Kyrki-Rajamäki, R., 2001. Coupled code FRAPTRAN – GENFLO for analysing fuel behaviour during PWR and BWR transients and accidents. In proceeding of: Fuel behaviour under transient and LOCA conditions, technical committee meeting, Halden, Norway, September 10-14, 2001. IAEA-TECDOC-1320.

Hofer, E., Krzykacz, B., Ehrhardt, J., Fischer, F., Crick, M.J., Kelly, G.N., 1985. Uncertainty and sensitivity analysis of accident consequence submodels. In proceedings of: International topical meeting on probabilistic safety

methods and applications, San Francisco, California, USA, February 24 - March 1, 1985.

IAEA, 2001. Thermohydraulic relationships for advanced water cooled reactors. IAEA-TECDOC-1203.

Ikonen, T., 2015. Global sensitivity analysis in fuel performance modelling. In proceedings of: TopFuel 2015, Zurich, Switzerland, September 13-17, 2015.

Ikonen, T., 2016. Comparison of global sensitivity analysis methods – application to fuel behavior modeling. Nuclear Engineering and Design, Vol. 297, pp. 72-80.

Iooss, B., Lemaître, P., (Editors: Dellino, G., Meloni, C.), 2015. Uncertainty management in simulation-optimization of complex systems. Algorithms and applications. Springer. ISBN 978-1-4899-7546-1.

James, G., Witten, D., Hastie, T., Tibshirani, R., 2013. An introduction to statistical learning with applications in R. Springer Texts in Statistics. ISBN 978-1-4614-7138-7.

Jernkvist, L.O., Massih, A.R., Rudling, P., 2004. A strain-based clad failure criterion for reactivity initiated accidents in light water reactors. SKI Report 2004:32. Published by: Swedish Nuclear Power Inspectorate (SKI), Stockholm, Sweden.

Jernkvist, L.O., 2016. Uncertainty assessment of the SCANAIR V_7_5 computer program in analyses of BWR reactivity initiated accidents. 2016:04, ISSN: 2000-0456. Published by: Swedish Radiation Safety Authority SSM, Stockholm, Sweden.

Kang, D.G., 2016. Analysis of LBLOCA using best estimate plus uncertainties for three-loop nuclear power plant power uprate. Annals of Nuclear Energy, Vol. 90, pp. 318-330.

Keresztúri, A., Brolly, Á., Panka, I., Pázmándi, T., Trosztel, I., 2016. A methodology for the estimation of the radiological consequences of a LOCA event. In proceedings of: 26th Symposium of AER on VVER reactor physics and reactor safety, Helsinki, Finland, October 10-14, 2016.

Keresztúri, A., Panka, I., Molnár, A., Tóta, Á, 2013. Multi-physics development for the hot-channel calculation of fast reactivity transients. Progress in Nuclear Energy, Vol. 67, pp. 74-81.

Kilgour, W.J., White, R.J., Shea, J.H., Turnbull, J.A., 1992. The ENIGMA fuel performance code, code description, version 5.8d. Berkeley Nuclear Laboratories, TD/NS/REP/0035.

Kloos, M., 2008. SUSA version 3.6, user's guide and tutorial, software for uncertainty and sensitivity analyses. Gesellschaft für Anlagen- und Reaktorsicherheit (GRS) mbH.

Klouzal, J., Dostál, M., Matocha, V., 2016. Treatment of the uncertainties in fuel rod design analysis. In proceedings of: TopFuel 2016, Boise, Idaho, USA, September 11-15, 2016.

Kovtonyuk, A., Lutsanych, S., Moretti, F. D'Auria, F., 2017. Development and assessment of a method for evaluating uncertainty of input parameters. Nuclear Engineering and Design, Vol. 321, pp. 219-229.

Lee, J., 2016. Uncertainty evaluation for the realistic safety analysis methodology of RIA by utilizing experimental results. In proceedings of: TopFuel 2016, Boise, Idaho, USA, September 11-15, 2016.

Lee, J., Woo, S., 2013. Validation of gap conductance uncertainty for realistic evaluation methodology on LOCA analysis. In proceedings of: TopFuel 2013, Charlotte, North Carolina, USA, September 15-19, 2013.

Lee, J., Woo, S., 2014. Effects of fuel rod uncertainty on the LBLOCA safety analysis with limiting fuel burnup change. Nuclear Engineering and Design, Vol. 273, pp. 367-375.

Lee, J., Woo, S., 2015. Effects of fuel rod uncertainty in PWR HZP RIA analysis. In proceedings of: TopFuel 2015, Zurich, Switzerland, September 13-17, 2015.

Lellouche, G.S., Levy, S., Boyack, B.E., Catton, I., Duffy, R.B., Griffith, P., Katsma, K.R, May, R., Rohatgi, U.S., Wilson, G., Wulff, W., Zuber, N., 1990. Quantifying reactor safety margins. Part 4: uncertainty evaluation of LBLOCA analysis based on TRAC-PF1/MOD 1. Nuclear Engineering and Design, Vol. 119, pp. 67-95.

Li, W.Y., Chang, H.C., Chen, S.W., Wang, J.R., Shih, C., Lin, H.T., 2015. Fuel rod uncertainty analysis of Chinshan NPP spent fuel pool by TRACE and FRAPTRAN/DAKOTA/SNAP. In proceedings of: TopFuel 2015, Zurich, Switzerland, September 13-17, 2015.

Liu, W., Alvis, J., Montgomery, R., 2010. Analysis of high burnup fuel failures at low temperatures in RIA tests using CSED. In proceedings of: 2010 LWR fuel

performance meeting/TopFuel/WRFPM, Orlando, Florida, USA, September 26-29, 2010.

Marchand, O., Zhang, J., Cherubini, M., 2016. OECD RIA benchmark phase II - towards a better understanding of the RIA fuel modelling. In proceedings of: TopFuel 2016, Boise, Idaho, USA, September 11-15, 2016.

Marcum, W.R., Brigantic, A.J., 2015. Applying uncertainty and sensitivity on thermal hydraulic subchannel analysis for the multi-application small light water reactor. Nuclear Engineering and Design, Vol. 293, pp. 272-291.

Martin, R.P., Nutt, W.T., 2011. Perspectives on the application of order-statistics in best-estimate plus uncertainty nuclear safety analysis. Nuclear Engineering and Design, Vol. 241, pp. 274-284.

Martin, R., O'Dell, L., 2008. Development considerations of AREVA NP Inc.'s realistic LBLOCA analysis methodology. Science and Technology of Nuclear Installations, Vol. 2008, article ID 239718.

MathWorks, 2017a. www.mathworks.com/products/matlab.html (visited November 4, 2017).

MathWorks, 2017b. www.mathworks.com/products/neural-network.html (visited November 4, 2017).

Miettinen, J., 2000. Thermohydraulic model SMABRE for light water reactor simulations. Thesis for the degree of Licentiate of Technology, Helsinki University of Technology.

Miettinen, J., Hämäläinen, A., 2002. GENFLO - A general thermal hydraulic solution for accident simulation. VTT Research notes 2163, ISBN 951-38-6083-3, ISSN 1455-0865. www.vtt.fi/inf/pdf/tiedotteet/2002/T2163.pdf (visited May 5, 2017).

Moal, A., 2016. SCANAIR reference documentation, Version V_7_7. PSN-RES/SEMIA-2016-00358. IRSN, Cadarache, France.

Moal, A., Georgenthum, V., Marchand, O., 2014. SCANAIR: a transient fuel performance code: part one: general modelling description. Nuclear Engineering and Design, Vol. 280, pp. 150-171.

Motta, A.T., 2004. A review of the critical strain energy density (CSED) model to analyzing reactivity initiated accidents (RIA) in high burnup fuel. U.S. NRC ADAMS accession number: ML041030260. https://adams.nrc.gov/wba (visited November 9, 2017).

Nakamura, T., Fuketa, T., Sugiyama, T., Sasajima, H., 2004. Failure thresholds of high burnup BWR fuel rods under RIA conditions. Journal of Nuclear Science and Technology, Vol. 41, pp. 37-43.

Nakamura, T., Kusagaya, K., Fuketa, T., Uetsuka, H., 2002. High-burnup BWR fuel behavior under simulated reactivity-initiated accident conditions. Nuclear Technology, Vol. 138, pp. 246-259.

Nakatsuka, M., 2004. Mechanical properties of high burnup BWR fuel cladding tubes under simulated RIA conditions. In proceedings of: 2004 international meeting on LWR fuel performance, Orlando, Florida, September 19-22, 2004.

OECD/NEA, 2007. BEMUSE phase III report, uncertainty and sensitivity analysis of the LOFT L2-5 Test. NEA/CSNI/R(2007)4.

OECD/NEA, 2009a. BEMUSE phase V report, uncertainty and sensitivity analysis of a LB-LOCA in Zion nuclear power plant. NEA/CSNI/R(2009)13.

OECD/NEA, 2009b. Nuclear fuel behaviour in loss-of-coolant accident (LOCA) conditions, state-of-the-art report. NEA No. 6846. NEA/CSNI/R(2009)15. ISBN 978-92-64-99091-3.

OECD/NEA, 2010. Nuclear fuel behaviour under reactivity-initiated accident (RIA) conditions, state-of-the-art report. NEA/CSNI/R(2010)1. ISBN 978-92-64-99113-2.

OECD/NEA, 2011. BEMUSE phase VI report, status report on the area, classification of the methods, conclusions and recommendations. NEA/CSNI/R(2011)4.

OECD/NEA, Working Group on Fuel Safety (WGFS), 2016. Reactivity initiated accident (RIA) fuel codes benchmark phase-II. Volume 1, simplified cases results, summary and analysis. NEA/CSNI/R(2016)6/VOL1.

OECD/NEA, Working Group on Fuel Safety (WGFS), 2017. Reactivity-initiated accident fuel-rod-code benchmark phase II: uncertainty and sensitivity analyses. NEA/CSNI/R(2017)1.

Panka, I., Keresztúri, A., 2007. Uncertainty analyses of hot channel calculations–determination of the number of failed fuel rods. Progress of Nuclear Energy, Vol. 49, pp 534-545.

Pawel, R.E., Cathcart, J.V., Campbell, J.J., 1979. The oxidation of zircaloy-4 at 900 and 1100 °C in high pressure steam. Journal of Nuclear Materials, Vol. 82, pp. 129-139.

Perez, M., Reventos, F., Batet, L., Guba, A., Tóth, I., Mieusset, T., Bazin, P., de Crécy, A., Borisov, S., Skorek, T., Glaeser, H., Joucla, J., Probst, P., Ui, A., Chung, B.D., Oh, D.Y., Pernica, R., Kyncl, M., Macek, J., Manera, A., Freixa, J., Petruzzi, A., D'Auria, F., Del Nevo, A., 2011. Uncertainty and sensitivity analysis of a LBLOCA in a PWR nuclear power plant: results of the phase V of the BEMUSE programme. Nuclear Engineering and Design, Vol. 241, pp. 4206-4222.

Plischke, E., 2010. An effective algorithm for computing global sensitivity indices (EASI). Reliability Engineering and System Safety, Vol. 95, pp. 354-360.

Plischke, E., 2012. How to compute variance-based sensitivity indicators with your spreadsheet software. Environmental Modelling & Software, Vol. 35, pp. 188-191.

Plischke, E., 2014. The course material of: The eighth summer school on sensitivity analysis of model output (SAMO 2014), Ranco, Italy, June 24 - 27, 2014; the MATLAB scripts are also available online at: www.immr.tu-clausthal.de/~epl/papers/papers.html (visited May 5, 2017).

Plischke, E., Borgonovo, E, Smith, C.L., 2013. Global sensitivity measures from given data. European Journal of Operational Research, Vol. 226, pp. 536-550.

Pourgol-Mohammad, M., Mohsen Hoseyni, S., Mojtaba Hoseyni, S., Sepanloo, K., 2016. A practical sensitivity analysis method for ranking sources of uncertainty in thermal–hydraulics applications. Nuclear Engineering and Design, Vol. 305, pp. 400-410.

Queral, C., Montero-Mayorga, J., Gonzalez-Cadelo, J., Jimenez, G., 2015. AP1000 large-break LOCA BEPU analysis with TRACE code. Annals of Nuclear Energy, Vol. 85, pp. 576-589.

Rahn, F.J., Adamantiades, A.G., Kenton, J.E., Braun, C., 1984. A guide to nuclear power technology, a resource for decision making. Wiley-Interscience Publication, John Wiley & Sons. 985 p.

Rashid, Y., Montgomery, R.O., Lyon, W.F., Yang, R., 2000. A cladding failure model for fuel rods subjected to operational and accident transients. In proceedings of: Nuclear fuel behaviour modelling at high burnup and its experimental support, technical committee meeting, Windermere, United Kingdom, June 19-23, 2000.

Roberts, K., Sanders, R., 2013. Application of uncertainty analysis to MAAP4 analyses for level 2 PRA parameter importance determination. Nuclear Engineering and Technology, Vol. 45, pp. 767-790.

Sagrado, I.C., Herranz, L.E., 2013. Impact of steady state uncertainties on RIA modeling calculations. In proceedings of: TopFuel 2013, Charlotte, North Carolina, USA, September 15-19, 2013.

Sakurai, A., Shiotsu, M., Hata, K., 1990. Correlations for subcooled pool film boiling heat transfer from large surfaces with different configurations. Nuclear Engineering and Design, Vol. 120, pp. 271-280.

Saltelli, A., Chan, K., Scott, E., 2000. Sensitivity analysis. John Wiley & Sons Inc, New York.

Saltelli, A., Ratto, M., Andres, T., Campolongo, F., Cariboni, J., Gatelli, D., Saisana, M., Tarantola, S., 2008. Global sensitivity analysis. The Primer. John Wiley & Sons, Ltd.

Secchi, P., Zio, E., Di Maio, F., 2008. Quantifying uncertainties in the estimation of safety parameters by using bootstrapped artificial neural networks. Annals of Nuclear Energy, Vol. 35, pp. 2338-2350.

Sobol', I.M., 1967. On the distribution of points in a cube and the approximate evaluation of integrals. USSR Computational Mathematics and Mathematical Physics, Vol. 7, pp. 86-112.

Sobol', I.M., 1993. Sensitivity analysis for non-linear mathematical models. Mathematical modelling and computational experiment, Vol. 1, pp. 407-414.

Stengård, J.-O., Kelppe, S., 2003. Probabilistic version of the FRAPCON-3 fuel behaviour code. VTT Project Report PRO1/T7048/02.

Studsvik Scandpower Inc., 2003. SIMULATE-3, advanced three-dimensional two-group reactor analysis code, SIMULATE-3 user's manual. Studsvik Scandpower Report SSP-01/414, Rev 3.

STUK – Radiation and Nuclear Safety Authority, 2013. Regulatory Guides on Nuclear Safety, Finland (Chapters B.3 and B.4).

Sugiyama, T., Nakamura, T., Kusagaya, K., Sasajima, H., Nagase, F., Fuketa, T., 2004. Behavior of irradiated BWR fuel under reactivity-initiated-accident conditions: results of tests FK-1, -2 and -3. JAERI Research report 2003-033.
www.iaea.org/inis/collection/NCLCollectionStore/_Public/36/116/36116816.pdf (visited May 5, 2017)

Sugiyama, T., Udagawa, Y., Fuketa, T., 2010. Evaluation of initial temperature effect on transient fuel behavior under simulated reactivity-initiated accident

conditions. Journal of Nuclear Science and Technology, Vol. 47, pp. 439-448.

Technical Program Group (TPG), 1989. Quantifying reactor safety margins; application of code scaling, applicability, and uncertainty evaluation methodology to a large-break, loss-of-coolant accident. NUREG/CR-5249, EGG-2552.

Trivedi, A.K., Srivastava, A., Lele, H.G., Kalra, M.S., Munshi, P., 2012. Uncertainty analysis of large break LOCA for pressurized heavy water reactor. Nuclear Engineering and Design, Vol. 245, pp. 180-188.

U.S.NRC Regulations, Title 10, Part 50, 1988. Domestic licensing of production and utilization facilities; § 50.46 Acceptance criteria for emergency core cooling system for light-water nuclear power reactors.

Udagawa, Y., Sugiyama, T., Amaya, M., 2014a. Heat transfer from fuel rod surface under reactivity-initiated accident conditions - NSRR experiments under varied cooling conditions -, JAEA-Data/Code 2013-021. http://jolissrch-inter.tokai-sc.jaea.go.jp/search/servlet/search?5043801 (visited May 5, 2017).

Udagawa, Y., Sugiyama, T., Amaya, M., 2014b. Reevaluation of fuel enthalpy in NSRR test for high burnup fuels. In proceedings of: TopFuel 2014, Sendai, Japan, September 14-17, 2014.

Udagawa, Y., Sugiyama, T., Suzuki, M., Amaya, M., 2013. Experimental analysis with RANNS code on boiling heat transfer from fuel rod surface to coolant water under reactivity initiated accident conditions. In proceedings of: IAEA technical meeting on modelling of water cooled fuel including design basis and severe accidents, Chengdu, China, October 28 - November 1, 2013. IAEA-TECDOC-CD-1775.

Wang, M., Qiu, S., Su, G., Tian, W., 2013. Preliminary study of parameter uncertainty influence on pressurized water reactor core design. Progress in Nuclear Energy, Vol. 68, pp. 200-209.

Wanninger, A., Seidl, M., Macián-Juan, R., 2016. Screening sensitivity analysis of a PWR fuel assembly FEM structural model. In proceedings of: TopFuel 2016, Boise, Idaho, USA, September 11-15, 2016.

Weisman, J., Bowring, R.W., 1975. Methods for detailed thermal and hydraulic analysis of water-cooled reactors. Nuclear Science and Engineering, Vol. 57, pp. 255-276.

Wilks, S.S., 1941. Determination of sample sizes for setting tolerance limits. The Annals of Mathematical Statistics, Vol. 12, pp. 91-96.

Wilks, S.S., 1942. Statistical prediction with special reference to the problem of tolerance limits. The Annals of Mathematical Statistics, Vol. 13, pp. 400-409.

Wilson, G.E., Boyack, B.E., Catton, I., Duffey, R.B., Griffith, P., Kastma, K.R., Lellouche, G.S., Levy, S., Rohatgi, U.S., Wulf, W., Zuber, N., 1990. Quantifying reactor safety margins. Part 2: characterization of important contributions to uncertainty. Nuclear Engineering and Design, Vol. 119, pp. 17-31.

Wulff, W., Boyack, B.E., Catton, I., Duffey, R.B., Griffith, P., Katsma, K.R., Lellouche, G.S., Levy, S., Rohatgi, U.S., Wilson, G.E., Zuber, N., 1990. Quantifying reactor safety margins. Part 3: assessment and ranging of parameters. Nuclear Engineering and Design, Vol. 119, pp. 33-65.

www.apros.fi (visited May 5, 2017).

Yueh, K., Karlsson, J., Stjärnsäter, J. Schrire, D., Ledergerber, G., Munoz-Reja, C., Hallstadius, L., 2016. Fuel cladding behavior under rapid loading conditions. Journal of Nuclear Materials, Vol. 469, pp. 177-186.

Zhao, H., Mousseau, V.A., 2012. Use of forward sensitivity analysis method to improve code scaling, applicability, and uncertainty (CSAU) methodology. Nuclear Engineering and Design, Vol. 249, pp. 188-196.

Zio, E., Pedroni, N., 2012. Monte Carlo simulation-based sensitivity analysis of the model of a thermal-hydraulic passive system. Reliability Engineering and System Safety, Vol. 107, pp. 90-106.

PUBLICATION I

Statistical analysis of fuel failures in accident conditions

In proceedings of: Water Reactor Fuel Performance Meeting/LWR/TopFuel, Chengdu, China, September 11-14, 2011, Paper T3-028.

2011 Water Reactor Fuel Performance Meeting
Chengdu, China, Sept. 11-14, 2011
T3-028

STATISTICAL ANALYSIS OF FUEL FAILURES IN ACCIDENT CONDITIONS

Asko Arffman*, Jukka Rintala
VTT Technical Research Centre of Finland
Tietotie 3, P.O. Box 1000, FI-02044 VTT, Finland
**asko.arffman@vtt.fi*

Abstract: A new kind of statistical fuel failure analysis procedure has been developed at VTT Technical Research Centre of Finland. For reactor safety considerations, it is essential to have a calculation tool for the evaluation of the number of fuel rods expected to fail in the course of an accident. Particularly, the safety regulations in Finland require that the number of failed fuel rods in the most limiting design basis accident scenario would be less than 10 % of all the rods. Statistical best-estimate methods have acquired an established position in this field worldwide during the past two decades. These methods are based on the selection and variation of parameters that are important in accident conditions. The accident scenario is simulated with a designated computer programme several times with different parameter values between simulations, and that way an estimation of the number of failed rods is obtained. An enormous number of simulation runs is needed in order to the results to be statistically reliable. Thus the analysis requires a lot of computer resources, and this has been a limiting factor for the breakthrough of these methods. Different approaches have been used to reduce the number of simulations.

Since 2006, a calculation system for statistical fuel failure analysis has been under development at VTT. The calculation procedure introduces neural networks as a new way to reduce the number of simulations. Neural networks are familiar from other applications in nuclear plant modelling but the concept is a novelty in this context. The developed method utilizes the results of nonparametric statistics, the Wilks' formula in particular. With the help of neural networks, the number of fuel performance code calculations can be substantially reduced from what would be necessary if all the rods in the reactor were to be simulated 59 times as required by the Wilks' formula. A neural network is trained with results from stacked fuel performance code calculations, and then the network is used as a substitute for the analysis code. Neural networks are chosen for this purpose because those are more flexible than the alternative technique, the response surfaces. The applied analysis programme is the coupled fuel performance – thermal hydraulics code FRAPTRAN-GENFLO. Here the FRAPTRAN code provides the criteria for fuel failure. The system has been successfully tested with a small-scale analysis with a loss-of-coolant accident (LOCA) scenario which is considered to be the worst design basis accident in PWRs. The system is now ready for full reactor scale applications.

Keywords: statistical analysis, Wilks' formula, neural networks, fuel failure, LOCA

1. INTRODUCTION

In safety assessments the estimation of the fraction of failing rods is conventionally based on conservative analyses, but this approach has several downsides. Sometimes it is hard to judge whether the assumptions are conservative because the phenomena in the reactor are highly nonlinear [1]. Additionally, conservative methods often lead to excessive margins and that way to economic losses. The development of statistical fuel failure analysis started worldwide when the U.S.NRC revised its rules in 1988 to allow realistic best-estimate methods complemented with uncertainty analysis alongside with the old conservative approach [2]. The so called CSAU (Code Scaling, Applicability and Uncertainty) methodology has been widely used as a standpoint for these analyses [3]. With the contribution of U.S.NRC, a group of experts developed this three-step method in 1989 to meet the new regulations.

In the first phase of CSAU, the accident scenario is divided to distinct segments by place and by the course of the accident, and then important phenomena are recognized for each place and time. The second phase consists of the evaluation of the fuel performance code and its ability to model the identified phenomena. Also the distributions of the related parameters are qualified. The third task is to combine the uncertainty distributions with a chosen method. The statistical procedure developed at VTT follows the main guidelines of this methodology.

Before the current efforts in this field at VTT, there has not been a statistical or any other systematic tool in Finland for the evaluation of the number of failing rods. The Regulatory Guides on nuclear safety set by the Finnish nuclear safety authority STUK introduce a number of design criteria that the utilized fuel has to fulfil in accident

conditions[1] [4]. The following criteria are applicable for LOCA conditions (Class 2 accident):

- less than 10 % of the rods in the reactor are allowed to be damaged
- coolability of the fuel shall be ensured
- external and internal oxidation of the cladding during the accident and the preceding normal operation shall not embrittle the cladding excessively
- limit for peak cladding temperature: 1 200 ºC
- the amount of hydrogen produced in coolant – cladding chemical reactions shall be less than 1 % of the amount of hydrogen produced if all the active cladding surrounding a rod would react with the coolant

Limits for cladding burst, collapsing and oxidation are not fixed in the regulations but those have to be experimentally determined.

The statistical calculation system has to show that the number of failing rods does not exceed the allowed limit. The premise of the current analysis is that the fuel performance code which is appropriately modelling the accident behaviour should indicate the fuel rod failure and therefore no additional failing criteria are needed. Thus the essential output from the calculations is the binary information whether the rod fails or not.

In this paper, the developed statistical procedure is presented, and description of the theoretical basis behind it is briefly summarized. The complexity of statistical fuel failure analysis is brought forth. Testing of the procedure is conducted with a proof of concept case; yet further validation with relevant power reactor applications is required in order to verify the functionality of the system.

2. METHODS FOR STATISTICAL ANALYSES

There are various approaches for the statistical fuel failure analysis. The analysis methods do not exclude each other, and they can thus be used in parallel to diminish the amount of required computer code simulations. The constant growth in computer resources has affected and will continue to affect the choice between different statistical methods.

2.1 Classification of initial parameters and definition of their distributions

The initial parameters of statistical analysis can be divided by their range to two groups: local and global. Global parameters have an effect on all the rods in the reactor, whereas local parameters bring variation to individual rods. As an example, the model parameters of a fuel performance code are global, whereas fuel manufacturing parameters are local. The division of parameters to global and local should someway be taken into account in the analysis because the fuel rods have some correlation with each other. However, the magnitude of the correlation is unknown because it is not precisely known which parameters have the biggest influence on the integrity of the rod during an accident.

Before performing the actual statistical analysis, the varied parameters have to be chosen and their distributions defined. The selection can be conducted by means of a sensitivity analysis with fuel modelling codes and by searching specific variation ranges from open literature, but much of expert judgment is still needed. Fuel manufacturing parameter ranges are usually provided by the fuel manufacturer. The choice between different statistical methods can also limit the number of parameters that can be included in the analysis. This is the case if one uses for instance response surfaces for combining the uncertainties. Typically the parameter values are normally distributed around the nominal value, but in some cases other distributions like uniform or triangular distributions are closer to reality and should be preferred.

2.2 Different approaches for reducing the number of simulations

The established methods with a view to reduce the amount of required simulation code calculations include the use of response surfaces [3, 5], grouping of the rods [6], direct Monte Carlo sampling, and applying results of tolerance interval theory [5, 7]. The last mentioned is presented in more detail in the next subsection as it is adopted as the basis of the procedure developed at VTT. Each method has its own pros and cons and none seems to be totally superior. In any case, the lack of statistical accuracy could be compensated by introducing some conservative assumptions.

The use of response surfaces is the approach of the original CSAU methodology. Response surfaces are low-order polynomial fits between initial and result parameters. With the simulations, one initial parameter at a time is varied and a connection to one or more result parameters is created. These connections are again gathered as a polynomial fit. The polynomial fit can then be used to replace the actual fuel performance code calculations, as new initial parameter values are randomly sampled and the polynomial fit is applied to predict the results. This method is useful when the relationship between initial and result parameters is simple enough, but it cannot predict for example the possible branching of the accident sequence to different directions when the safety systems are activated. In addition to that, the number of initial parameters included has to be quite small to keep the number of simulations in a reasonable measure. More enhanced methods to utilize response surfaces exist, e.g. employing a generalized regression algorithm in the procedure [8].

Another approach to the analysis is to sample the values of initial parameters from their distributions using direct Monte Carlo sampling. Here the division to global and local parameters is neglected, and that means loss of statistical reliability to some extent. Further, the number of simulations that are needed to reach a certain confidence level remains unknown.

It is also possible to group rods with characteristics like burn-up, power level and thermal hydraulic conditions. One can then pick an arbitrary amount of rods from each group

[1] The criteria are given generally for all postulated accidents. Accidents are further divided to Class 1 and 2 according to their initiating event frequency: 10^{-2} - 10^{-3} / year in Class 1, and less than that in Class 2. The criteria are set separately for the two classes.

to be included to the analysis, and that way substantially decrease the amount of simulations.

2.3 Tolerance interval method

The tolerance interval theory gives the means to determine the number of simulations that are needed for the statistical analysis when the intended probability content and confidence level are predetermined. For instance, nuclear industry corporations Westinghouse [9, 10] and Areva NP [11] both have developed their statistical methods based on the CSAU procedure with the results of nonparametric statistics chosen to be the final step to combine the uncertainty distributions.

Theoretical basis of the tolerance interval method was set by S.S. Wilks in 1941 [12]. The starting point of the problem setting is that N sets of initial parameter values are sampled from their corresponding distributions. These sets are used as simulation code inputs, and as a result there will be N values of a result parameter, accordingly. The distribution of the result parameter is an unknown function (hence the appellation nonparametric), here denoted by f(y). With tolerance interval method, the upper and lower limits in the distribution f(y) are to be chosen so that a given probability content γ would be inside those limits with a confidence level β. The above mentioned is mathematically expressed as [5, 13]:

$$P\left(\int_{L}^{U} f(y)dy > \gamma\right) = \beta \cdot \qquad (1)$$

Next, a set of result parameter values picked from the unknown distribution f(y) are arranged in ascending order. When the minimum value is marked with index r and the maximum value with index s, Equation (1) can be written:

$$\beta = 1 - \sum_{j=s-r}^{N} \binom{N}{j} \gamma^{j} (1-\gamma)^{N-j} \cdot \qquad (2)$$

In case of one-sided tolerance interval, the lower bound L is chosen to be $-\infty$ (r=0) and the upper bound U is the highest value in the random sample picked from the distribution (s=N). Thus, inserting r=0 and s=N into Equation (2), one gets the relation known as the Wilks' formula (for one sided tolerance limit):

$$\beta = 1 - \gamma^{N} . \qquad (3)$$

When this formula is applied to safety evaluations, the generally acceptable level is 95 % probability with 95 % confidence that the number of failed rods would not overstep the allowed limit. When the corresponding values are inserted into Equation (3), thus $\gamma = 0.95$ and $\beta = 0.9515$, the number of cases comes out as 59. This figure applies when there is only one result parameter but the analysis can be broadened out: if one would like to examine multiple output parameters, more calculations are needed. On the other hand, the number of calculations is independent of the number of initial parameters included to the analysis. In practice when using the Wilks' formula, one can state that when all the rods in the reactor are simulated 59 times with global variation between each of the 59 scenarios, and if the number of failed rods in the worst case is below the allowed limit, then the safety requirements are rightly met with the probability of 95 % and with the confidence level of 95 %. In other words, local variation is taken into account when simulating all the rods in the reactor, and global variation when repeating that 59 times with different global parameter values. As that kind of number of simulations is out of reach with the computer resources of today, some other method is needed alongside with the result presented above.

2.4 Neural networks

With the analysis procedure developed at VTT, neural networks are used in the same way and for the same purpose as response surfaces. Neural network approach is chosen instead of response surfaces because it is a more sophisticated tool for describing nonlinear phenomena. Compared to response surfaces, it is also more flexible because it is less confining with respect to the number of initial parameters to be included to the analysis. Naturally this approach also has its own downsides which are highlighted later on. Neural networks are used in many applications in nuclear plant modelling [14-20], but those are a novelty in fuel behaviour analyses [21, 22].

3. DEVELOPED ANALYSIS PROCEDURE

In the spirit of the CSAU methodology, the problem setting in the calculation system developed at VTT is split in distinct steps. Firstly, there are several ways to conduct the statistical analysis depending on the setup of the accident scenario and on which phenomena are to be included. It is important to decide how to take into account the propagation of modelling uncertainties throughout the calculation system. Namely, the boundary conditions of a fuel performance code come from a system code and/or from a neutronics code, and those have their own uncertainties. The source and the form of boundary conditions can thus vary, and that poses an extra challenge for the first phase of the analysis. As this first step is in a sense that ambiguous, the calculation system cannot be made fully solid but must be adapted from analysis to analysis. In this point, the possible symmetry of the accident could be made use of to reduce the number of simulations.

Secondly, the distributions of the chosen parameters are defined. In the third phase, the uncertainties are combined with the result of nonparametric statistics introduced by Wilks. There are several ways, however, to apply this result of "59 calculations" to practice.

3.1 Alternative approaches for the analysis

There are different paths that the statistical analysis could proceed depending on the setup of the analysis. As an example, let us first have a look at a situation in which the course of the accident is predetermined but no boundary conditions are calculated or known beforehand. To perform the analysis rigorously, one should calculate the boundary conditions 59 times with a system code like e.g.

APROS [23]. Then there are 59 global variations of the accident and the fluctuations in boundary conditions are taken into consideration as a source of uncertainty. Naturally, also the global parameters in the fuel modelling codes contribute to this group of 59 global variations. Next for each global case, a large number of cases with different local parameter values are calculated. The number of calculations could be for example 1000 for each global variation. In practice, simulation of the accident 59 times with a system code may be too time-consuming, and consequently the objective could be that some of the cases are left outside the analysis. This delimitation should be done in a conservative fashion but it is recognized that the conservatism is here hard to be distinguished a priori. Again, if the boundary conditions are fixed from the start, then that source of error is out of scope of the analysis and the problem setting is simplified.

As neural networks at this point lack comprehensive validation in this context, two surveys are conducted: a conservative analysis and one with neural networks. This branching into two phases is schematized in Figure 1 where the flow chart of the calculation system is presented. In the first option designated as "Phase 1", on the grounds of the above mentioned calculations, the worst global case is determined based on the highest number of failed rods. The number of failed rods in the worst global case can then be directly scaled to find out the number of failed rods in the whole reactor. This approach is on the conservative side because with a smaller number of cases, deviation of rod failure numbers grows, and thus, the biggest failure number is likely higher than what it would be if all the cases had been calculated instead of an extrapolation. And based on the tolerance interval theory, only the highest number of failed rods counts. In this case, sufficient number of cases need to be calculated to limit the deviation due to the extrapolation of the rod failure numbers. If one would like to make a more thorough analysis, one could sample the local parameter values for all the rods in the reactor and calculate all the rods in the worst global case.

Alongside with the method presented above, the same calculation results are utilized for a neural network analysis. This is designated as "Phase 2" in the flow chart. If one has calculated for example 59×1000 cases in the previous stage, one can now use these cases to train a network. This network is then used for the full analysis with both global and local parameter values sampled anew. It means that the trained network is used instead of a real fuel performance code to simulate all the rods in the reactor for 59 times. This is mathematically more justified than the conservative result because now all the simulations required by the Wilks' formula are conducted. Additionally, neural network analysis would give a wider margin to the acceptance limit as it is more realistic than the conservative approach. The Phase 2 does not require notable additional effort as neural network simulations are fast to perform. The results from Phase 1 and Phase 2 would support each other.

At this point, the neural networks are considered to be used for a complementary analysis, and the analysis based on the high number of fuel performance code simulations (Phase 1) is the primary way. Before it can be stated that neural networks are suitable for performing these kinds of analyses, it should be made sure that they work as expected in different kinds of accident scenarios. It is not at all obvious that neural networks can be utilized in all cases and therefore it is desirable to have an alternative way to perform the analysis. As the experience grows with further analyses, more can be said about how well the neural networks could be utilized to cover different scenarios.

3.2 Applied codes and programmes

In order to attain the time-dependent boundary conditions for the fuel performance code calculations, the overall progress of the accident is simulated with the system code APROS. The APROS code is developed and maintained

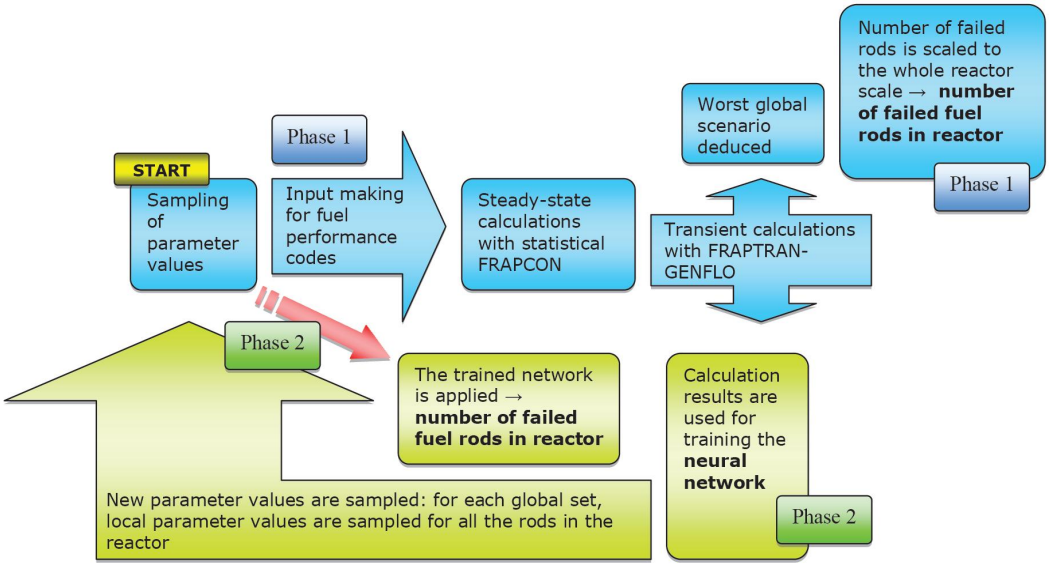

Fig. 1 Flow chart of the calculation system

jointly by VTT and Fortum. The relevant boundary conditions are coolant mass flow and enthalpy at the channel inlet, pressure at the top of the channel, and rod power including the axial power profiles. Statistical version of APROS is under development, and that will ultimately enable the propagation of uncertainties from the system code level.

The steady-state initializations of the stacked calculations are performed with the U.S.NRC/PNNL FRAPCON code (version 3.3). An advanced statistical version of FRAPCON developed at VTT in 2003 is being used. It enables the variation of selected model and fuel manufacturing parameters (cf. Table 1).

The primary calculation tool is the coupled fuel performance–thermal hydraulics code FRAPTRAN-GENFLO [24]. FRAPTRAN (version 1.3) is a single-rod fuel performance code developed by PNNL and it is designed to model accident conditions specifically [25]. The general thermal hydraulics code GENFLO has been exclusively developed at VTT. The thermal hydraulics modelling in stand-alone FRAPTRAN has been found to be unsatisfying, and therefore the coupling with an external thermal hydraulics code has been introduced. For each time-step and axial segment, GENFLO calculates the coolant temperature and clad-to-coolant heat transfer coefficients. GENFLO is fast-running due to non-iterative solution of field equations [24]. The coupled code has recently been validated against results from the Halden Project IFA-650 LOCA tests.

The cladding failure is a FRAPTRAN output, and the code's ballooning model is the one suitable for modelling the failure mode in LOCA. The model assumes that when the effective plastic strain in any axial segment of the cladding exceeds the instability strain given by the material properties package MATPRO, local non-axisymmetric cladding ballooning begins. In the current analyses, however, the calculation can be stopped and the cladding conservatively declared as having failed once the local ballooning model is called. In fact the possibility that the cladding would not fail once the instable ballooning has started is considered theoretical.

The actual calculation system consists of several small programmes that have been coded for data processing, writing inputs and steering the calculations. Some external programmes are also used, like the sampler programme SUSA (Software system for Uncertainty and Sensitivity Analysis) [26] developed by the German research organisation GRS. SUSA is utilized for generating random parameter values from specified distributions. For the conversion of the sampled data into the format used in the input generating programme, two auxiliary programmes coded in Fortran 90 are used. Parameter values are handled in Fortran NAMELIST format which makes the input files self-documenting.

A Perl script has been written to steer the stacked FRAPTRAN-GENFLO calculations in a linux cluster. Major changes to the FRAPTRAN and GENFLO codes for the purpose of the statistical analysis were avoided at this stage. So far the model parameter values cannot be varied in FRAPTRAN because those values cannot be changed via the input file without changing the source code. With the predecessor of FRAPTRAN code, FRAP-T6, one could use in-coded automated uncertainty analysis option in which input parameter values were varied. This option was removed, however, when introducing FRAPTRAN because it was not used by the U.S.NRC, not being maintained nor verified [25]. If the development of a statistical version of FRAPTRAN is considered, it would require a careful analysis of the utilized models and their uncertainties in the code. At the moment, however, the fact that the code has not been changed eases the changeover to the new 1.4 version of FRAPTRAN. Meanwhile, the new FRAPCON version 3.4 has been modified to include the capabilities for statistical analysis. Most likely these new versions of FRAPCON and FRAPTRAN will be used with the subsequent analyses.

The neural network analysis is conducted using a MATLAB built-in neural network software package, the Neural Network Toolbox™. It is a general-purpose tool for neural network analyses, and its basic use is quite simple. Of course, as always when operating with neural networks, one has to take extra care when interpreting the results. Network overfitting could become a problem. The same may occur if one uses an insufficient amount of data to train the network in relation to the number of layers and neurons in it. Generally, one can use more complex network structures and get more complicated phenomena into view if a large data set for training is used.

Two MATLAB m-files have been written in which the neural networks are operated. The m-files have been coded in such a way that the recording and opening of the network is independent of the size and configuration of the network. The applied network type is a feed-forward backpropagation network. There are a number of training functions included in the Neural Network Toolbox™ but here the default function is used. The function utilizes the Levenberg-Marquardt algorithm for training. Other training functions could also be tested in the future. The default tan-sigmoid activation function has been used after each neuron and a linear function after the output layer.

3.3 Varied parameters and their distributions

The discussion about which parameters to include to statistical analyses has continued from the start of the development of the CSAU methodology. It is hard to give any general rules for the selection as the sources of uncertainty and their relative importance vary from code to code [27]. The parameters chosen to be varied in the VTT's system are aggregated into Table 1. In some cases the lack of knowledge limits the precise definition of the corresponding uncertainty distribution. The uncertainties that are considered in statistical methods by other organizations are studied for example in the BEMUSE project [28, 29]. Appliance of those parameters with the codes and analysis here is not straightforward and needs adaptation. For example the uncertainties in thermal hydraulic parameters should be taken into consideration mainly in the system code APROS, and in addition to that, some parameter variations are possible in GENFLO. Meanwhile, fuel-related parameters are kept in their

Table 1 Varied parameters in the analysis

		distribution
Global parameters		
FRAPCON	swelling parameter	normal
	creep rate parameter	normal
	fission gas parameter	normal
	thermal conductivity parameter	normal
	cladding corrosion parameter	normal
GENFLO	basic drift flux velocity	triangular
	drift flux separation constant	triangular
	interphasial heat transfer tuning factor	triangular
	film boiling heat transfer tuning factor	triangular
	transition boiling heat transfer tuning factor	triangular
Local parameters		
	cladding outer diameter	normal
	cladding inner diameter	normal
	fuel pellet outer diameter	normal
	fuel pellet inner diameter	normal
	cold plenum length	normal
	fuel pellet density	uniform
	grain size	uniform
	flow area cross section	uniform

best-estimate values in the system code and varied only in the fuel performance codes. All in all, the discussion continues about how to take into account the inaccuracies in thermal hydraulic boundary conditions.

The thermal hydraulic parameters chosen to be varied in GENFLO are at this point the three tuning factors for heat transfer and the two drift flux model parameters. In order to gain justifiable parameter ranges, previous validation reports of GENFLO were consulted. The parameter ranges were found in some cases too wide and GENFLO failed to calculate the transient through. Therefore, adequate variation ranges had to be searched by trial and error.

The variations in fuel manufacturing parameters are expected to have little influence on the fuel failures as the tolerances are quite small. Still, at least the gas gap size has a notable effect on the cladding temperatures [27].

4. TESTING THE PROCEDURE

As a proof of concept case for testing the calculation system, a large break LOCA in Loviisa VVER-440 type reactor is used. The boundary conditions were available from a prior APROS analysis. However, preliminary calculations of a single representative rod with FRAPTRAN-GENFLO showed that the cladding temperatures do not reach high enough values to result in a fuel rod failure. This is seen in Figure 2 where the cladding outer surface temperature is presented. There is a significant difference between the cladding temperatures calculated with APROS and FRAPTRAN-GENFLO, and the most significant cause for this arose from the degree of detail in modelling of the rod in a designated fuel performance code. In FRAPTRAN-GENFLO, the conductance of the

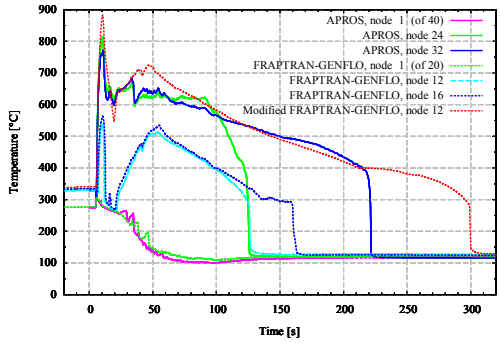

Fig. 2 Cladding surface temperatures during the accident

pellet-to-cladding gap is calculated more realistically and will be determined to be higher during the transient than the constant value (3 000 W/m²/K) used in the simple fuel rod model of APROS.

Because of the substantial volume of coolant in VVER-440 core during a LOCA, rod failures are generally estimated to be unlikely in this type of reactor. With the boundary conditions of a more typical pressurized water reactor, rod failures may be more readily present in LOCAs. In order to have enough fuel failures with the stacked calculations to be used for training the neural network, the accident had to be artificially exaggerated by assuming an elevated power level during the accident, and by decreasing the gas gap conductance in the source code. In that way, higher calculated cladding temperatures could be produced as seen in Figure 2 (marked in the figure as "modified FRAPTRAN-GENFLO").

The boundary conditions from the system code can be very demanding for the coupled fuel behaviour code. Owing to periodical pressure increase and decrease in the core region, the coolant flow tends to be reversed and go back and forth rapidly in the APROS simulation. If the coolant channel is empty for a prolonged time, GENFLO calculation fails. In these cases, careful evaluation of the boundary conditions is necessary, and resorting to filtering the boundary conditions is an option to be considered.

4.1 Performance of neural networks

After "dramatizing" the accident scenario, enough fuel failures were gained for the system testing. This was verified by preliminary calculations with FRAPTRAN-GENFLO, in which some 20 % of the 100 stacked example cases ended up with an indication of a rod failure. To test the neural networks in practice, a small-scale analysis consisting of a set of 900 stacked FRAPTRAN-GENFLO calculations was performed. Both global and local parameters presented in Table 1 were

varied. When examining the calculation results, it can be stated that the time of failure is significantly scattered due to the variation in local and/or global parameters. Also the axial location of the failure somewhat varies. This may indicate that more than one of the varied parameters has an effect on the cause of the failure. For the neural network testing, it is good to have this kind of variation in the training data. A weakness in the current neural network analysis is that one cannot point out which parameter or combination of parameters caused the rod to fail. It requires additional analysis with the real fuel performance code to find out the reason(s) for rod failures.

At this point it is interesting to learn how accurately the network predicts the cases that were not used for training the network. Also the effect of changing the neural network configuration by adding neurons and layers is a subject of interest. To test the performance of a network, the fuel performance code calculations are divided to a training set and a test set. In this case, 33 % of the cases were used as a test set. Thus the error in the test set predictions is under examination. One has to notice that the network may directly predict that the rod fails or remains intact, but the network result can as well be somewhere between these extremes. Below, a following (arbitrary) criterion is used: if the neural network prediction deviates more than 40 % from the correct result, it is considered as a missprediction. Of course the missprediction can equally be on the conservative side, thus the neural network would predict the rod to fail even though the fuel performance code shows otherwise.

Because of the intrinsic characteristics of neural networks, the performance of a network varies between simulation runs even if the training data is the same. Different network configurations were tested and as an example in Table 2, the percentages of falsely predicted rods in the test set are presented for two networks. Both networks have two hidden layers with 5 and 3 or 3 and 3 neurons. As one can see from the table, the error in predictions between simulation runs varies considerably. Still, it should be adequate that when the error is small, that particular network is recorded and used for the subsequent analysis. Thus, while a network structure with a low error fraction in its predictions is the aim, even the best structures have variation in their results. The smallest error in predictions in this case is 2.7 %, a figure that already shows quite a good accuracy.

Table 2 Examples of the percentages of falsely predicted rods in the test set with two network configurations

	5:3 –network [%]	***3:3 –network [%]***
1°	19.5	3.0
2°	4.7	4.7
3°	4.3	3.0
4°	19.2	2.7
5°	2.7	6.7
6°	4.0	3.7
7°	4.0	4.0
8°	8.1	5.1
9°	11.4	5.4
10°	2.7	11.1
11°	19.2	5.7
12°	31.6	3.7
13°	19.2	3.0
14°	6.7	5.1
15°	15.5	4.7

Among the experimentations, a small network that consists of two hidden layers with three neurons in both layers is found to have the steadiest performance. However, the most suitable network configuration should be sought each time an analysis is performed.

4.2 Duration of the analysis calculations

Statistical analysis unavoidably takes a lot of time. Statistical version of FRAPCON is fast-running but the transient calculations are slower to conduct. The duration of a single FRAPTRAN-GENFLO calculation depends among other things on the time-step length and the starting and ending times of the calculation. During the critical moments of the accident, time-step size may have to be quite small in order to gain reliable results, or for the calculation to converge. The starting time of the calculation should be some tens of seconds before the beginning of the actual transient in order to initialize the power level from low power to the steady-state power. Due to numerical reasons, time-step sizes between 0.001 s and 0.01 s may be required.

If the rod does not fail and the calculation is continued for example up to 500 seconds, the calculation time of a single FRAPTRAN-GENFLO run would be about 5 minutes. If one now calculates 59 000 cases with ten calculation nodes in the linux cluster and assumes that each calculation takes 5 minutes, it would take 21 days to finish the calculations. If the time per one calculation could be reduced for instance to 2 minutes by optimizing time-step sizes and reducing the ending time of the calculation, it would take 9 days to complete the calculations. This may be an acceptable duration for this kind of analysis.

If the 59 APROS simulations are to be conducted, it would considerably increase the duration of the analysis. A single LB-LOCA APROS run with a 3-D neutronics model can last about 2.5 days. Calculations can be further distributed to different computers.

5. CONCLUSIONS AND FUTURE WORK

A calculation system for statistical fuel failure analysis has now been developed to a point that the application to full reactor scale analyses is the next step. So far the proposed neural network approach is tested to a limited extent only and therefore two parallel analyses are suggested. Fuel performance code results are thus used in two different ways: to directly scale the number of rod failures in the worst global scenario to the whole reactor scale, and to perform a neural network analysis. If the network performs as expected, that second analysis would confirm the previous result.

The test results of the system show quite good performance with the neural network approach. All the scripts for conducting statistical analyses are now ready to be used. Depending on the setup of the analysis, for instance

on the boundary conditions and the details of the accident scenario, the scripts will be modified accordingly.

The applied simulation codes are improved according to the arising needs. Development of a statistical version of the system code APROS is about to begin. The uncertainties propagating to the fuel performance code calculations via APROS boundary conditions can then be taken into consideration. Then again, the duration of a single system code simulation is so significant that the soundness of a statistical analysis with 59 APROS simulations included is a subject to be carefully assessed. Improvements to the GENFLO code are under way. After those the boundary conditions are separately given for water and steam at the channel inlet and outlet, so as to enhance the accuracy of thermal hydraulics modelling.

When advancing to full scale applications of the statistical method, the calculation scheme can be tested also with alterations. As an example, the neural network approach may be improved if the parameter values that are used for training the network would be sampled in the first phase of the analysis from uniform distributions instead of the more realistic distributions. In that way, more calculation cases would come from the edges of the distributions now covered by only a small number of cases. Consequently, neural networks would presumably have enhanced response in the Phase 2 when realistic distributions are used. Naturally the result of Phase 1 with uniform distributions would be unrealistic, but still conservative.

Feasibility of neural networks is examined as a part of the full analysis each time it is performed. The uncertainty related to neural network predictions is an important issue to be taken into account when evaluating the final result. Likewise the conservative proportion in the network uncertainty is to be quantified (i.e. when the network incorrectly predicts the rod to fail, contrary to the result of a fuel performance code calculation). It is easy to get bad results from the analysis if there is an insufficient amount of training cases, an unsuitable network configuration, or if one encounters problems with overfitting. Despite the challenges in this approach, it is a definite advancement from the traditionally used response surface method. The presented concept for analysing fuel failures in accident conditions is the first step in Finland towards systematic statistical procedure in this field.

ACKNOWLEDGEMENTS

The work presented in this paper has been done under the auspices of the Finnish Research Programmes on Nuclear Power Plant Safety – SAFIR2010 and SAFIR2014.

REFERENCES

[1] A. Bucalossi et. al.: "Comparison Between Best-Estimate–Plus–Uncertainty Methods and Conservative Tools for Nuclear Power Plant Licensing", Nuclear Technology, Vol. 172, No. 1, pp. 29-47, 2010

[2] U.S.NRC Regulations, Title 10, Part 50: "Domestic Licensing of Production and Utilization Facilities; § 50.46 Acceptance criteria for emergency core cooling system for light-water nuclear power reactors"

[3] Technical Program Group: "Quantifying reactor safety margins; Application of Code Scaling, Applicability, and Uncertainty Evaluation Methodology to a Large-Break, Loss-of-Coolant Accident", NUREG/CR-5249, 1989

[4] STUK, Regulatory Guides on nuclear safety (YVL): "Design bases and general design criteria for nuclear fuel; YVL 6.2", Nov 1, 1999

[5] I. Panka, A. Keresztúri: "Uncertainty analyses of hot channel calculations – Determination of the number of failed fuel rods", Progress in Nuclear Energy, Vol. 49, Issue 7, pp. 534-545, 2007

[6] B. Hatala: "Quantification of fuel rod cladding failure during LOCA accident", 6th International Conference on WWER Fuel Performance, Modelling and Experimental Support, Albena, Bulgaria, Sep 19-23, 2005

[7] R. P. Martin, W. T. Nutt: "Perspectives on the application of order statistics in best-estimate plus uncertainty nuclear safety analysis", Nuclear Engineering and Design, Vol. 241, Issue 1, pp. 274-284, 2011

[8] K.-I. Ahn, B.-D. Chung, J. C. Lee: "An Assessment of Uncertainty on a LOFT L2-5 LBLOCA PCT Based on the ACE-RSM Approach: Complementary Work for the OECD BEMUSE Phase-III Program", Nuclear Engineering and Technology, Vol. 42, No. 2, 2010, 12 p.

[9] C. Frepoli: "An Overview of Westinghouse Realistic Large Break LOCA Evaluation Model", Science and Technology of Nuclear Installations, Vol. 2008, Article ID 498737, 15 p.

[10] C. Frepoli, J.S.Chiang, J.S.Petzold, D.C. Olinski: "Application And Licensing Of Westinghouse Realistic Large Break LOCA Evaluation Model (ASTRUM) for Maanshan Units 1 And 2 Nuclear Power Plant", PHYSOR 2010, Pittsburgh, Pennsylvania, USA, May 9-14, 2010

[11] R. P. Martin, L. D. O'Dell: "Development Considerations of AREVA NP Inc.'s Realistic LBLOCA Analysis Methodology", Science and Technology of Nuclear Installations, Vol. 2008, Article ID 239718, 13 p.

[12] S.S.Wilks: "Determination of Sample Sizes for Setting Tolerance Limits", The Annals of Mathematical Statistics, Vol. 12, No. 1, pp. 91-96, 1941

[13] A. Guba et al.: "Statistical aspects of best estimate method – I", Reliability Engineering and System Safety, Vol. 80, Issue 3, pp. 217-232, 2003

[14] M. G. Na et. al.: "Estimation of break location and size for loss of coolant accidents using neural networks", Nuclear Engineering and Design, Vol. 232, Issue 3, pp. 289-300, 2004

[15] T.V.Santosh et al.: "Application of artificial neural networks to nuclear power plant transient diagnosis", Reliability Engineering and System Safety, Vol. 92, Issue 10, pp. 1468-1472, 2007

[16] J. M. Gozalvez: "Sensitivity study on determining an efficient set of fuel assembly parameters in training data for designing of neural networks in hybrid generic

algorithms", Annals of Nuclear Energy, Vol. 33, Issue 5, pp. 457-465, 2006
[17]E. F. Faria, C. Pereira: "Nuclear fuel loading pattern optimization using a neural network", Annals of Nuclear Energy, Vol. 30, Issue 5, pp. 601-613, 2003
[18]J. J. Ortiz, I. Requena: "Using a multi-state recurrent neural network to optimize loading patterns in BWRs", ", Annals of Nuclear Energy, Vol. 31, Issue 7, pp. 789-803, 2004
[19]N. Pedroni et al.: "Comparison of bootstrapped artificial neural networks and quadratic response surfaces for the estimation of the functional failure probability of a thermal-hydraulic passive system", Reliability Engineering and System Safety, Vol. 95, Issue 4, pp. 386-395, 2010
[20]J. L. Montes et al.: "Local power peaking factor estimation in nuclear fuel by artificial neural networks", Annals of Nuclear Energy, Vol. 36, Issue 1, pp. 121-130, 2009
[21]F. Cadini et al.: "A model based on bootstrapped neural networks for computing the maximum fuel cladding temperature in an Rbmk-1500 nuclear reactor accident", Nuclear Engineering and Design, , Vol. 238, Issue 9, pp. 2165-2172, 2008
[22]P. Secchi et al.: "Quantifying uncertainties in the estimation of safety parameters by using bootstrapped artificial neural networks", Annals of Nuclear Energy, Vol. 35, Issue 12, pp. 2338-2350, 2008
[23]www.apros.fi
[24]A. Hämäläinen et. al.: "Coupled Code FRAPTRAN – GENFLO for Analysing Fuel Behaviour During PWR and BWR Transients and Accidents", Proceeding of a Technical Committee meeting, IAEA-TECDOC-1320, Halden, Norway, Sep 10-14, 2001
[25]U.S.NRC: "FRAPTRAN: A Computer Code for the Transient Analysis of Oxide Fuel Rods", NUREG/CR-6739, Vol. 1, PNNL-13576, 2001
[26]Gesellschaft für Anlagen- und Reaktorsicherheit (GRS) mbH: "Software System for Uncertainty and Sensitivity Analysis of Results from Computer Models; User's Guide and Tutorial", 2002
[27]M. Pourgol-Mohammad: "Thermal-hydraulics system codes uncertainty assessment: A review of the methodologies", Annals of Nuclear Energy, Vol. 36, Issues 11-12, pp. 1774-1786, 2009
[28]OECD/NEA: "BEMUSE Phase III Report, Uncertainty and Sensitivity Analysis of the LOFT L2-5 Test", NEA/CSNI/R(2007)4, Oct 11, 2007
[29]OECD/NEA: "BEMUSE Phase V Report, Uncertainty and Sensitivity Analysis of a LB-LOCA in ZION Nuclear Power Plant", NEA/CSNI/R(2009)13, Dec 21, 2009

PUBLICATION II

Statistical analysis of fuel failures in large break loss-of-coolant accident (LBLOCA) in EPR type nuclear power plant

Nuclear Engineering and Design, Vol. 285, pp. 1–14.

PUBLICATION III

Sensitivity analysis of local uncertainties in large break loss-of-coolant accident (LB-LOCA) thermo-mechanical simulations

Nuclear Engineering and Design, Vol. 305, pp. 293-302.

PUBLICATION IV

Statistical and sensitivity analysis of failing rods in EPR LB-LOCA

In proceedings of: TopFuel 2016, Boise, Idaho, USA, September 11-15, 2016, Paper 17570.

Statistical and sensitivity analysis of failing rods in EPR LB-LOCA

Asko Arkoma, Timo Ikonen

VTT Technical Research Centre of Finland Ltd, Kivimiehentie 3, FI-02044 VTT, Finland
+358 40 825 7010, asko.arkoma@vtt.fi

Abstract. A statistical fuel failure analysis procedure has been developed [1], and now applied in full scale to a large break loss-of-coolant accident (LBLOCA) scenario in EPR-type nuclear power plant. The goal is to statistically determine the number of failing fuel rods. It is also important to bring out the underlying causes for rod failures, and therefore a sensitivity analysis procedure for the preceding complex calculation chain is outlined and adopted.

In order to produce a statistically reliable estimation on the number of failing rods, a large number of simulations are required. In the analysis, single rods are simulated with the coupled fuel performance - thermal hydraulics code FRAPTRAN-GENFLO. The statistically varied factors are divided into global and local by their range of influence. Transient thermal hydraulic and power history boundary conditions and model parameters are global and affect all the rods. Fuel rod manufacturing parameters and other rod position related factors are local and are related to a certain rod. The number of global scenarios is 59 as dictated by the Wilks' formula, and 1000 randomly sampled rods are simulated in each scenario. The thermal hydraulic and transient power boundary conditions for the fuel performance code are calculated with a statistical version of the system code APROS. The steady-state irradiation histories are simulated with FRAPCON, and the steady-state power histories used as boundary conditions for FRAPCON are obtained from SIMULATE calculations. Thus, a multistage calculation chain is required to consolidate the procedure. As an outcome, in the worst global scenario, 1.4% of the simulated rods failed. It can be concluded that the Finnish safety regulations, i.e. max. 10% of the rods allowed to fail, are met.

In order to find out which input parameters have significance to the outcome of the analysis, a sensitivity analysis is done. At the moment, only the worst global scenario is considered but later on it is possible to include also the sensitivities of the global factors. Due to complexity of the existing data, first the relevant input parameters for the sensitivity analysis have to be specified. Data visualization with a cobweb graph is used for the screening. Then, selected sensitivity measures are calculated between the chosen input and output parameters. The sensitivity indices calculated are the Borgonovo's delta measure, the first order Sobol' sensitivity index, and squared Pearson correlation coefficients. The first mentioned is a novelty in this context. As an outcome, the most relevant parameters with respect to the cladding integrity were determined to be the decay heat power during the transient, the thermal hydraulic conditions in the rod's location in the reactor, and the steady-state irradiation history of the rod as represented in this analysis by the rod burnup.

Keywords: loss-of-coolant accident, statistical fuel failure analysis, sensitivity analysis, FRAPTRAN-GENFLO, EPR

INTRODUCTION

The Regulatory Guides on nuclear safety [2] set by the Finnish nuclear safety authority STUK introduce a number of design criteria that the fuel has to fulfil in accident conditions. Among others, the following criteria are applicable in LOCA conditions: less than 10% of the rods in the reactor are allowed to be damaged, and the peak cladding

temperature should not exceed 1 200 ºC. The estimation of the fraction of failing rods is traditionally based on conservative analyses but this approach has several downsides. It is hard to judge a priori whether the assumptions are conservative because the phenomena in the reactor are highly nonlinear. Therefore, a statistical calculation system has been developed and described in [1], and applied now in full reactor scale.

The tolerance interval theory [3] gives means to determine the number of simulations that are needed for the statistical analysis. The upper and lower limits in the result parameter distribution are chosen in a way that a given probability content γ would be inside those limits with a confidence level β. In the case of one-sided tolerance interval, the lower bound is chosen to be minus infinity and the upper bound is the highest value (in first order formulation) in the random sample picked from the distribution. Based on this, one can derive a well-known relation known as the Wilks' formula [4]:

$$\beta = 1 - \gamma^N. \quad (1)$$

When this formula is applied to deterministic safety evaluations, the acceptable level is a 95% probability with a 95% confidence that the number of failed fuel rods would not overstep the allowed limit [2]. When the corresponding values are inserted into Equation (1), the number of cases comes out as 59. The number of calculations is independent of the number of initial parameters included in the analysis. Furthermore, the figure is valid for one output quantity [4], and in this analysis we are interested in just one, the total number of failing rods.

The applied simulation codes are a modified version of the FRAPCON code for the steady-state simulations [5] and FRAPTRAN-GENFLO for the transient calculations [6, 7]. The thermal hydraulics boundary conditions needed for the transient analysis with FRAPTRAN-GENFLO are obtained from the system code APROS [8]. In addition to transient boundary conditions, the steady-state power histories needed in FRAPCON simulations are generated with neutronics codes.

The simulated accident scenario may be summarized as follows. As the initiating event, a double ended break in a cold leg opens. Due to pressure decrease, reactor and turbine trips follow. Simultaneously with the turbine trip, the offsite power is lost and the main recirculating coolant pumps start to coast down. The core is uncovered. The content of the accumulators is injected to the primary loop when the accumulator pressure is reached. After a delay, the diesel generators are started and the medium, and later on the low head safety injections start operation and the core is quenched.

The cause of a fuel rod failure in a LB-LOCA is the sum of many interconnected phenomena. Thermal hydraulic conditions in the rod's location during a LOCA play an important role, as well as the decay heat power during the transient. In local level, the rod's irradiation history prior to the accident and the resulting state of the rod has an effect. Also rod design parameters such as fuel enrichment and gadolinia content and tolerances in the fuel manufacturing parameters may have a contribution. To determine the relevant input factors, and to quantify their relative importance, a sensitivity analysis is done by using the data from the statistical analysis.

APPLICATION OF THE CALCULATION SYSTEM

The initial parameters of the statistical analysis can be divided into two groups by their range. Global parameters have an effect on all the rods in the reactor, whereas local parameters bring variation only to individual rods. For example, the model parameters of a fuel performance code are global, whereas fuel manufacturing parameters are local. The above mentioned 59 simulation cases are constructed in a way that selected model parameters in the codes, and the fuel performance codes' boundary conditions are different between the scenarios. The values for fuel manufacturing parameters are random sampled from their distributions; those have the same values in each global scenario. The uncertainties related to the neutronics calculations used to produce the base irradiation pin power histories are left outside the study; that may be considered in future studies.

In practice, when using the Wilks' formula, one can state that when all the rods in the reactor are simulated 59 times with variations between each of the 59 scenarios, and if the number of failed rods in the worst case is below the allowed limit, then the safety requirements are rightly met with the probability of 95% and with the confidence level of 95%. As that kind of number of transient fuel performance code simulations, i.e. 59 times the 63 865 rods in EPR,

is out of reach with the computer resources of today, some other method or approach is needed alongside in order to reduce the amount of simulations.

In our approach, a limited number of random sampled rods are simulated for each global scenario. The number of simulations is chosen to be 1000, in order to keep the computation time still reasonable (less than two weeks with 25-32 simultaneous simulations in cluster), and yet the number to be sufficient. In order to be able to pinpoint the worst global scenario unambiguously, the same rods are simulated in each global scenario. The number of failed rods in the worst global case can then be directly scaled to find out the number of failed rods in the whole reactor. This approach is on the conservative side because with a smaller number of cases, the deviation of the number of failures grows. Therefore, the highest failure number is likely to be higher than it would have been if all the cases had been calculated. In a thorough analysis, the rest of the rods among the global scenarios may be taken into account by fitting a neural network for each global scenario by using the data from the 1000 simulated rods per scenario, as explained in [9]. The trained network may then be applied to reduce the deviation resulting from the extrapolation.

In the LOCA scenario considered in this paper, the accident occurs after the 4^{th} cycle. At the end of cycle 4, there are five different assembly types in the core. These types vary in U-235 enrichment, the number of Gd rods in the assembly, and the Gd_2O_3 content in the Gd rods. About half of the assemblies have been in the core only for the cycle 4. The rest have been irradiated for two cycles: one bundle during the cycles 1 and 4, and all the others during the cycles 3 and 4. The cycle lengths for cycles 1, 3 and 4 are 18, 24 and 24 months, respectively.

Codes in the Calculation System

The calculation system is presented in Figure 1. The primary calculation tool is the coupled fuel performance–thermal hydraulics code FRAPTRAN-GENFLO. FRAPTRAN (version 1.4) is a single-rod transient fuel performance code developed by PNNL for U.S.NRC [5]. FRAPTRAN has been coupled with general thermal hydraulics code GENFLO [10], developed at VTT, to improve the thermal hydraulics modeling in LOCA. For each time-step and axial segment, GENFLO calculates the coolant temperature and the clad-to-coolant heat transfer coefficients. GENFLO contains a five-equation thermal hydraulics model (two energy and mass equations, one momentum equation) with drift-flux phase separation. The code is able to simulate the long-lasting reversed core flow which is possible in EPR. The default LOCA cladding failure criterion in FRAPTRAN is applied in rod failure predictions. The ballooning model of FRAPTRAN assumes that local non-axisymmetric cladding ballooning begins when the effective plastic strain in any axial segment of the cladding exceeds the instability strain given by the material properties package MATPRO. The rod is considered to fail when the indicator for the rod failure is triggered.

The steady-state initializations of the transient calculations are performed with the U.S.NRC/PNNL FRAPCON code (version 3.4), with statistical features introduced at VTT [11]. For the FRAPCON simulations, the steady-state power histories of all the rods in the reactor are needed. SIMULATE 3 [12] was used to simulate the core and to obtain the power histories. In order to obtain the time-dependent transient boundary conditions for the fuel performance code calculations, the progress of the accident was simulated 59 times with the system code APROS, developed jointly by VTT and Fortum. The relevant boundary conditions obtained from APROS are the enthalpy and the mass flows of both liquid and vapor at the channel inlet and outlet, the coolant pressure and the rod power evolution. Also axial power profiles are provided by APROS. The applied dynamic one-dimensional two-phase flow model of APROS simulates the behavior of a system containing liquid and gas phases, covering all heat transfer modes. The system is governed by six partial differential equations, from which pressures, void fractions and phase velocities and enthalpies are solved. The phases are coupled to each other with empirical friction and heat transfer terms.

Varied Parameters

As a first step of a statistical analysis, the varied parameters have to be chosen and their distributions defined. The parameters chosen to be varied in the VTT's system are collected into Table 1. The parameters that are important regarding the whole core are varied in APROS, and those that are important in fuel behavior analysis are varied in fuel performance codes. Generally, the parameters affecting the thermal hydraulics are varied in APROS. However,

the parameters now varied in GENFLO cannot be currently varied in APROS and therefore those are taken into consideration in GENFLO. Meanwhile, fuel-related parameters are kept at their best-estimate values in APROS and varied only in the fuel performance codes. Selected model parameters are varied in FRAPCON. The lack of the current analysis is that no model parameters are varied in FRAPTRAN; this deficiency is mended in future analyses.

TABLE 1. Varied parameters and their distributions.

Global parameters	*Distribution*[1]	*Min.*	*Max.*	*Global scenario #47*[2]
APROS				
Containment pressure [MPa]	N (0.250)	0.200	0.300	0.263
Pump1 inertia [kgm^2]	N (5210.0)	5157.9	55262.1	5247.2
Pump2,3,4 inertia [kgm^2]	N (5210.0)	5105.8	5314.2	5164.9
Decay heat of normal [%]	N (100.0)	92.0	108.0	95.1
Accu2,3,4 pressure [MPa]	N (4.9800)	4.7800	5.1800	4.9484
Accu2,3,4 level [m]	N (4.4600)	4.3600	4.5600	4.5124
Emergency water temperature [°C]	N (50.0)	10.0	50.0	21.4
Emergency water flow [%]	N (100.00)	95.00	105.00	97.47
CCFL parameter	N (1.0000)	0.6900	1.0350	0.9232
Discharge coefficient, RPV side	N (0.8750)	0.7500	1.0000	0.8202
Discharge coefficient, pump side	N (0.8750)	0.7500	1.0000	0.9383
Upper plenum temperature [°C]	N (336.0)	331.0	341.0	332.9
FRAPCON				
Swelling parameter	N (1.0; 0.000144)	not defined		0.995770
Creep rate parameter	N (1.0; 0.25)	0.6	1.1	0.881100
Fission gas parameter	N (0.0; 0.25)	-1	1	0.363080
Thermal conductivity parameter	N (1.0; 0.01)	not defined		1.015300
Cladding corrosion parameter	N (1.0; 0.0004)	0.6	1.4	1.016000
GENFLO				
Basic drift flux velocity	Tri (1.2)	1.13	1.2	1.154200
Drift flux separation constant	Tri (1.1)	1.1	1.2	1.122200
Interphasial heat transfer tuning factor	Tri (0.3)	0.1	0.33	0.183950
Film boiling heat transfer tuning factor	Tri (0.2)	0.08	0.22	0.187390
Transition boiling heat transfer tuning factor	Tri (0.2)	0.18	0.22	0.192250
Local parameters (FRAPCON)	N			
Cladding inner diameter, Fuel pellet diameter, Cladding wall thickness, Cold plenum length, Fuel pellet density, Bottom plenum volume, Internal fill pressure				

[1]N=Normal (μ,σ^2) or (μ); Tri=Triangular (mode) *[2]Values in global scenario #47 that revealed to be the worst case*

The parameters and their ranges used in the APROS analysis are based mainly on the BEMUSE data [13, 14] but also other publically available data has been used [15, 16]. The varied model parameters and their ranges in FRAPCON and GENFLO are based on previous analyses done at VTT. Normal distribution is used for the fuel manufacturing parameters, but the exact values are proprietary information. Sampling of parameter values is conducted with the SUSA software developed by the German research organization GRS [17].

Boundary conditions from system code APROS

In APROS, the reactor core is divided into 20 axial nodes for the solution of thermal hydraulics and neutronics. The core is divided into 17 thermal hydraulic channels. The locations of the thermal hydraulic channels in relation to the fuel bundles are presented in Figure 1. As there are no shrouds around the fuel assemblies in EPR, there are cross flows in the core. It is important to take the cross flows into account in the simulations as those balance the flows between bundles with various power levels. However, a single FRAPTRAN-GENFLO simulation is done for a closed subchannel, and the cross flows cannot explicitly be taken into account. However, as the core is divided in APROS into thermal hydraulic channels consisting of several bundles instead of only one bundle per channel, the cross flows are being taken into account in the boundary conditions produced for FRAPTRAN-GENFLO.

The linear power histories and thermal hydraulic boundary conditions are available for 17 channels except the inlet enthalpy for liquid and vapor which are given for eight sectors. The eight sectors take into account the asymmetric temperature distribution in the core resulting from the break in one of the cold legs. The axial power profiles are available for all the 241 bundles. The same static beginning-of-transient axial power profiles are used in all the 59

global scenarios. The linear power histories available for the channels are further refined for each bundle by using a normalized multiplier defined from an APROS output file. The multiplying coefficients are defined using the average power in an APROS channel:

$$coeff_{bundle} = P_{bundle} \frac{total\ number\ of\ bundles\ in\ APROS\ channel}{P_{channel}}. \quad (2)$$

Channel power is obtained by adding up the bundle powers in that particular coolant channel. An approximation has to be made regarding the transient power evolutions in fuel rods: as the transient pin power is not known but only the bundle power, the latter is used in FRAPTRAN-GENFLO simulations as pin power. Similarly, bundle axial power profile is used as pin axial profile.

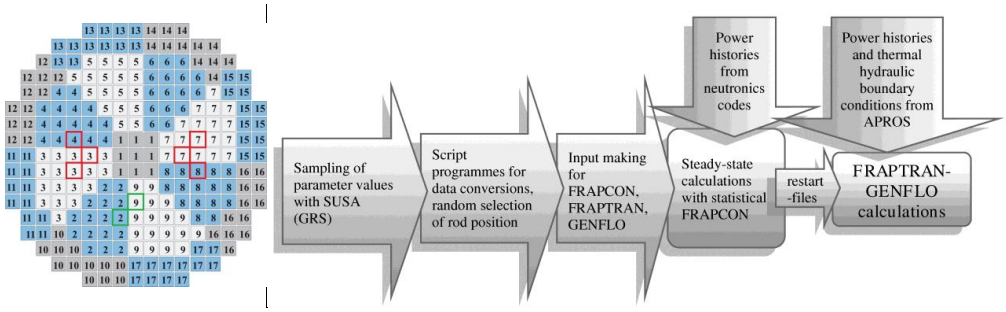

FIGURE 1. Division of the core into 17 coolant channels in APROS, altered from [9] (left). Calculation system flowchart (right).

RESULTS OF THE STATISTICAL ANALYSIS

The numbers of rods that failed in each global scenario are shown in Figure 2. The highest number of failures, 14 rods, occurred in global scenario 47. Thus in the worst case, 1.4% of the rods failed. In each scenario, the same 1000 rods were simulated, and consequently in many cases, the same rods failed in various global scenarios. Some of the simulations were not successfully terminated; in scenario #3, total of 62 simulations ended with an error, 58 of which were due to GENFLO. With respect to errors, this was the worst case. If all the erroneous simulations were conservatively assumed to stand for a rod failure, the total portion would be 6.6%, and the safety criterion is still easily met.

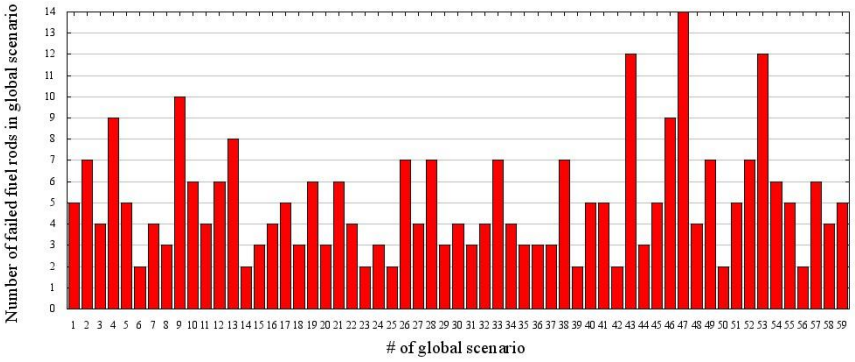

FIGURE 2. Numbers of failed fuel rods in each global scenario; 1000 rods were simulated per scenario.

The global parameter values applied in scenario 47 are presented in Table 1. The evolutions of selected output parameters in the global scenario 47 are plotted in Figure 3. The curves corresponding to the failed rods are indicated with markers. In each scenario, the highest peak cladding temperatures occurred always soon after the beginning of the accident, and were at the same level in all global variations, little below or above 900 ºC. The requirement concerning the highest peak cladding temperature, 1 200 ºC, is thereby met.

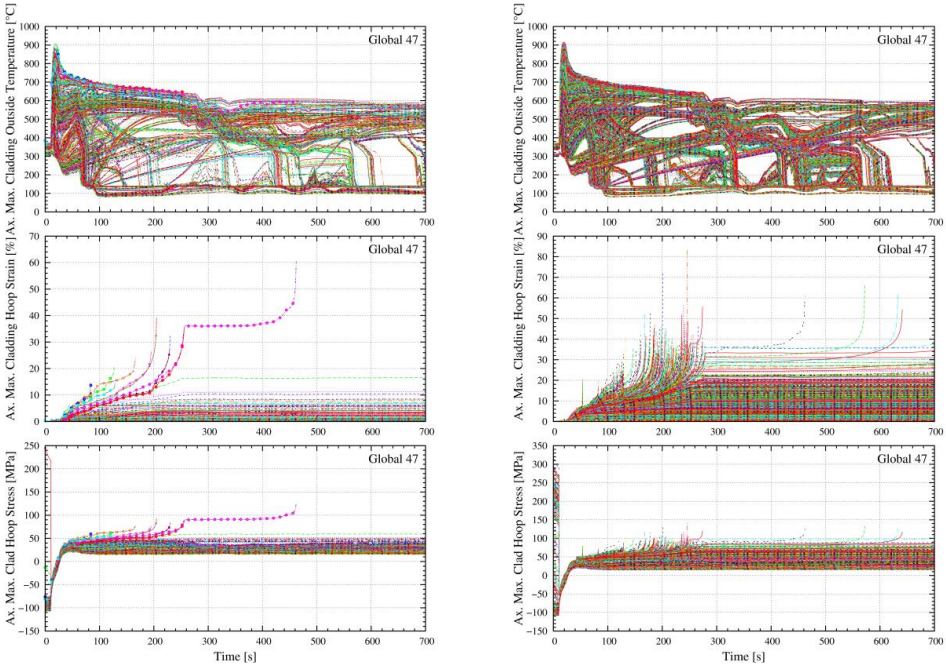

FIGURE 3. Evolutions of key output parameters in FRAPTRAN-GENFLO simulations in the worst global scenario with respect to the number of failing fuel rods. First, 1000 rods were simulated (left hand side), and then all the rods that had been in reactor during cycles 3 and 4 (right hand side).

Compared to the previously published results [9], the numbers of failed rods in almost all the scenarios are few units higher. The reason is that different cladding yield strength correlation in FRAPTRAN is applied between the analyses. The default model is used in this paper, and the older model from [18] was applied in the previous calculations [9]. The model from [18] was previously used as it had proved to give the best results in modeling Halden IFA-650 LOCA series with FRAPTRAN-GENFLO [19]. In addition, a bug in FRAPTRAN was corrected between the two analyses: in previous simulations, false indications of rod failures were given by the low-temperature PCMI cladding failure model during the high temperature phase in LOCA.

Among the analyzed global scenarios, all the failed rods had been in reactor during the 3rd and 4th cycle. In other words, no failures were simulated in the rods that had been in reactor only during the 4th cycle, or during the 1st and 4th cycle. Therefore, by applying the boundary conditions and the global parameter values of the worst global scenario (in terms of the number of failed rods), all the rods in the loading pattern that had been in reactor during 3rd and 4th cycle were simulated with FRAPTRAN-GENFLO. In this smart sample, 1.96% of rods were simulated to end up in fuel rod failure, and 0.44% of simulations crashed. Thus even in a whole reactor scale, taking account the most limiting rods, the safety criterion is met. The evolutions of the output parameters are presented in Figure 3.

SENSITIVITY ANALYSIS

A sensitivity analysis was done using the data of all those rods in the reactor that had been in core during 3rd and 4th cycle. In this analysis only one global scenario, i.e. the worst case is considered. The effect and importance of various local parameters, i.e. the location related parameters and the sampled fuel manufacturing parameters, to the outcome of chosen output parameters is studied. In the future, also global parameters may be addressed in the analysis.

The number of sensitivity analysis methods that are suitable to this problem is limited because the dataset is given, which excludes methods that take advantage of efficient sampling techniques [20]. In addition, the influential input parameters are highly correlated. This results from the facts that, firstly, the phenomena in a nuclear reactor are highly interlinked. Secondly, the data used for the sensitivity analysis originates from a complex calculation system consisting of several codes. If parameters are selected from successive phases of the calculation chain, their effect may be taken into account more than once when performing the sensitivity analysis. The analysis is further complicated by the differences in the level of detail in modeling in various codes.

Because the data used in the sensitivity analysis is complex, even defining the input parameters is not trivial. In the first phase, all the potentially important sampled or calculated input parameters of the LOCA analysis are distinguished. To help sorting out the relevant parameters, a cobweb graph [21] is used to visualize the input variables that lead to high hoop strains in the LOCA calculations. Finally, sensitivities are quantified by calculating various sensitivity indices.

Data pre-processing

Part of the data is scalar while some is in the form of time series. The latter include transient power histories, thermal hydraulic boundary conditions, and steady-state power histories. In order to perform the sensitivity analysis, the time series data needs to be simplified. Some of the thermal hydraulic boundary conditions of the 17 coolant channels vary significantly during the transient, and therefore condensing the boundary conditions into scalars was not attempted. Instead, the 17 thermal hydraulic boundary conditions are treated by the sequence number of the particular channel in the APROS model. When comparing the steady-state power histories of the rods during both of the cycles, it is seen that within a cycle the power evolution is quite steady. The exceptions are the gadolinia rods in which the power increases during the first cycle. Due to the simplicity of the histories, average values for power are calculated for each rod for both cycles.

The decay heat during the transient is directly proportional to the initial power prior to the transient, and therefore the transient power histories may be represented by the initial steady-state power values obtained from APROS. However, in the subsequent sensitivity analysis, the power coefficients for the bundles are considered instead of the actual transient power. This choice is made because that way the channel power may be grouped together with the thermal hydraulics boundary conditions, which are also given per channel. The normalized bundle power coefficients are calculated through Equation (2).

The rod failure criterion in FRAPTRAN for ballooning in LOCA is based on empirical stress and strain limits. In the sensitivity analysis, maximum values relative to time and axial position of the cladding plastic hoop strain, hoop stress and outer surface temperature are used instead. This makes the analysis more general and independent of the particular failure criterion adopted in FRAPTRAN. The continuous output is also easier to analyze statistically than the binary failed/non-failed output of the rod failure model.

Methods for visual and quantitative sensitivity analysis

A cobweb graph [21] is used for visualizing and screening the input variables that lead to extreme values of a selected output parameter. In the graph, the values of the input parameters have been scaled to the range 0...1, and the values associated with single simulations are connected with lines. The simulations that exceed a certain criterion are plotted with a different color than the rest of the simulations. In the LOCA analysis, the cladding ballooning is a key result and may be represented by the cladding plastic hoop strain. Therefore, the simulations in which the plastic hoop strain is equal or exceeds a chosen limit, fixed in this analysis to be 20%, are highlighted in the cobweb graph.

The sensitivity indices calculated for the data are the Borgonovo's delta measure [22, 23] and the first order Sobol' sensitivity index [24]. These sensitivity indices can be evaluated from pre-existing data. The first order Sobol' sensitivity index is chosen for its simplicity, and the Borgonovo's delta is used as it is a more comprehensive, moment-independent measure. Also, squared Pearson correlation coefficients, i.e. the R^2 values [25], are calculated for comparison whenever possible. Traditionally in sensitivity analysis of LOCA, various correlation coefficients are applied as sensitivity measures [26, 27]. However, the present work involves data presented as ordinal numbers

(the coolant channel number) that cannot be analyzed with correlation coefficients. The Borgonovo's delta is defined for the input variable X_i as [22]:

$$\delta_i = 0.5\, E_{X_i}\left[\int |f_Y(y) - f_{Y|X_i}(y)|dy\right]. \quad (3)$$

The term in the square brackets is the shift between the probability density function of an output and the probability density function of a conditional output with the value of X_i fixed. E_{Xi} stands for expectation value. The numerical estimation of δ_i is done using a Gaussian kernel estimator with Kolmogorov-Smirnov filtering to reduce spurious correlations [23]. The sensitivity index S_i for an input parameter X_i and output Y is formally defined as the ratio between the variance of the conditional expectation value and unconditional variance as:

$$S_i = var\left[E[Y|X_i]\right] / var[Y]. \quad (4)$$

Usually the calculation of S_i is done with a specific sampling design [20], which is very efficient but in the case of pre-existing data cannot be used. Instead, the numerical estimation of S_i follows the discrete cosine transformation method [28, 29]. With both sensitivity measures S_i and δ_i, the range of the indices is 0-1; zero means that the output is independent of the input parameter in question. The indices are calculated with two MATLAB scripts [30].

RESULTS OF THE SENSITIVITY ANALYSIS

The cobweb graph is shown in Figure 4. Parameter values of all the rods that have been irradiated during cycles 3 and 4 are plotted with red color and the simulations with equal to or higher than 20% plastic hoop strain are plotted with black. Enrichment and gadolinia content are not shown in figure due to confidentiality reasons.

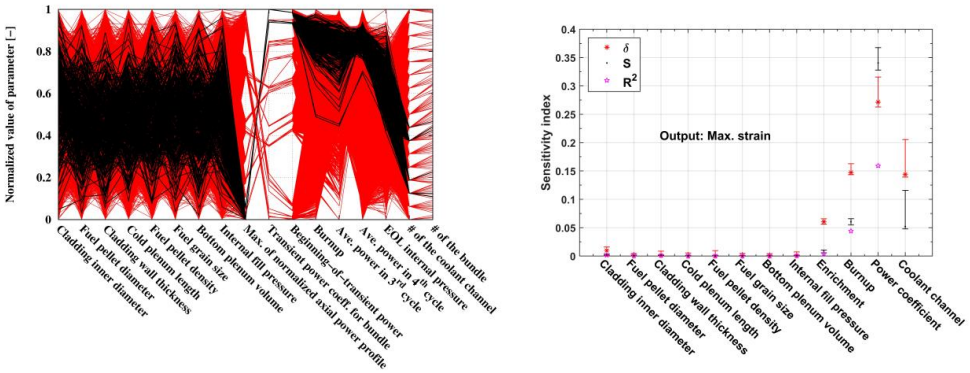

FIGURE 4. Cobweb graph used for screening the most important input parameters (left). Calculated sensitivity indices (right).

The following conclusions are made based on the cobweb graph:

- Tolerances in fuel manufacturing parameters do not significantly affect the transient strain.
- Average steady-state power during the 4th cycle is more correlated to high strains than the 3rd cycle power.
- High burnup is related to high strain, but the range of burnups in the high strain rods is fairly large.
- The range of end-of-life internal pressures resulting in high strains is large, but high strains are not reached in rods with the end-of-life internal pressure in the lower third.
- The distinction between the beginning-of-transient power and the transient power coefficients for the bundles is seen: highest strains are achieved with the highest power coefficients but not with the highest beginning-of-transient powers. Strong correlation with the high hoop strain is seen in both.
- High strains are associated to distinct coolant channels and bundles.

When comparing the cobweb graph with the locations of the bundles and coolant channels in the core (Figure 1), one can see that the rods with the highest permanent hoop strain (> 20%) are located in bundles that are situated in the middle circle of coolant channels in APROS model, namely in channels 3, 4, 7 and 8. Again, these rods are located in six bundles, marked with red squares in Figure 1 (according to FRAPTRAN, a few rods failed also in two more bundles with less than 20% strain, marked with green squares in Figure 1). This is explained by the fact that

the powers in the outer circle channels are a lot lower compared to the middle circle and the central channel. In the central channel, the highest powers do not reach the level of those in the middle circle channels, and therefore the hoop strains are not high in that channel.

Next, the parameters to be included to the quantitative sensitivity analysis are chosen. The cobweb graph showed that the rod manufacturing tolerances are quite insignificant but the indices for those are calculated for comparison. Some of the input parameters are screened out due to strong correlation with each other, while some dependent parameters cannot be excluded, e.g. burnup and transient power. These are screened out: gadolinia content, as it is associated with the U-235 enrichment; end-of-life internal pressure, strongly correlated with burnup; average steady-state power in both cycles, correlated with burnup and decay heat; beginning-of-transient power, partly included in the channel number through the average channel power.

The sensitivity indices are presented in Figure 4 for chosen inputs and the output maximum strain. It is seen that the most relevant parameters, in order of importance, are the decay heat power during the transient represented by the bundle power coefficient, the steady-state irradiation history of the rod represented by the rod burnup, and the thermal hydraulic boundary conditions plus the coolant channel power in the rod's location as represented by the coolant channel number. Also fuel enrichment has a non-zero effect. Meanwhile, the tolerances in fuel manufacturing parameters have practically negligible effect, even though the delta indices are not exactly zero. As the inputs are not independent, caution should be used with further interpretation of the indices. Similar study is done for the two other outputs, maximum stress and temperature, and the conclusions are the same [31].

The effect of coolant channel thermal hydraulics is hard to sort out from the effect of coolant channel power, and the effect may only be seen indirectly. Based on high power, at least some of the rods located in channel 5 should reach high strains but that is not observed. Furthermore, the coolant channel power in that channel is higher than in those where the high strains are reached. According to the cobweb graph and the calculated sensitivity indices, the explanation for the lower strains in that channel remains to be searched from among the rod burnup and the coolant channel thermal hydraulics. Similar burnups are observed in channel 5 as in the channels where the strains are high, which excludes the burnup as the sole explaining factor. Therefore, it may be concluded that the thermal hydraulic effects dominate over the effect of the coolant channel power.

CONCLUSION

Using a calculation system for statistical fuel failure analysis, the number of failed fuel rods in LB-LOCA in an EPR was estimated. The number of failing fuel rods in 59 simulated global scenarios ranged from 2 to 14 rods per 1000 simulations. Thus, in the worst case, 1.4% of the simulated rods failed. It can be concluded that according to the statistical analysis performed, the requirement that less than 10% of the rods may fail in a LB-LOCA is met. Also, the highest peak cladding temperatures in all global variations were around 900 ºC, and the requirement concerning the highest peak cladding temperature, 1 200 ºC, is thereby met.

A sensitivity analysis was done in order to discover the most influential input parameters in the worst global scenario. Both visual and numerical methods were applied. A cobweb graph was used both to visually interpret the data and to perform final screening of the input variables. For example, the rod manufacturing parameters were identified as almost non-influential already using the cobweb graph. The burnup, the power coefficient during the transient and the coolant channel number were chosen for further numerical analysis. For comparison, the manufacturing parameters were also chosen to be included in the last stage. The results of the numerical analysis gave support to the conclusions made concerning the importance of the three key parameters.

ACKNOWLEDGMENTS

The work presented in this paper has been done under the auspices of The Finnish Research Programme on Nuclear Power Plant Safety 2015 – 2018 (SAFIR2018). The statistical fuel failure analysis has been done for the Finnish nuclear safety authority STUK. The statistical procedure has been developed in the Finnish Research Programmes on Nuclear Power Plant Safety – SAFIR2010 and SAFIR2014.

REFERENCES

[1] Arffman, A. (currently Arkoma, A.), Rintala, J., "Statistical Analysis of Fuel Failures in Accident Conditions", in proceedings of *Water Reactor Fuel Performance Meeting*, Chengdu, China, September 11-14, 2011, paper T3-028, (2011).

[2] Radiation and Nuclear Safety Authority (STUK), "Regulatory Guides on nuclear safety", chapters B.3 and B.4, (2013).

[3] U.S.NRC, "FRAPCON-3.4: A Computer Code for the Calculation of Steady-State Thermal-Mechanical Behavior of Oxide Fuel Rods for High Burnup", NUREG/CR-7022, **1**, PNNL-19418, (2011).

[4] Wilks, S.S., "Determination of Sample Sizes for Setting Tolerance Limits", *The Annals of Mathematical Statistics*, **12**(1), 91-96, (1941).

[5] Guba, A., Makai, M., Pál, L., "Statistical aspects of best estimate method – I", *Reliability Engineering and System Safety*, **80**(3), 217-232, (2003).

[6] Hämäläinen, A., Stengård, J.-O., Miettinen, J., Kyrki-Rajamäki, R., "Coupled Code FRAPTRAN – GENFLO for Analysing Fuel Behaviour During PWR and BWR Transients and Accidents", in proceeding of *Technical Committee meeting*, Halden, Norway, September 10–14, 2001, IAEA-TECDOC-1320, (2001).

[7] U.S.NRC, "FRAPTRAN: A Computer Code for the Transient Analysis of Oxide Fuel Rods", NUREG/CR-7023, **1**, (2011).

[8] www.apros.fi (visited 26.4.2016).

[9] Arkoma, A., Hänninen, M., Rantamäki, K., Kurki, J., Hämäläinen, A., "Statistical analysis of fuel failures in large break loss-of-coolant accident (LB-LOCA) in EPR type nuclear power plant", *Nuclear Engineering and Design*, **285**, 1–14, (2015)

[10] Miettinen, J., Hämäläinen, A., "GENFLO - A General Thermal Hydraulic Solution for Accident Simulation" VTT Research Notes 2163, ISBN 951-38-6083-3, ISSN 1455-0865, (2002).

[11] Stengård, J.-O., Kelppe, S., "Probabilistic Version of the FRAPCON-3 Fuel Behaviour Code", VTT Project Report PRO1/T7048/02, (2003).

[12] Studsvik Scandpower Inc., "SIMULATE-3, Advanced Three-Dimensional Two-Group Reactor Analysis Code, SIMULATE-3 User's Manual", Studsvik Scandpower Report SSP-01/414 Rev 3, (2003).

[13] OECD/NEA, "BEMUSE Phase V Report, Uncertainty and Sensitivity Analysis of a LB-LOCA in ZION Nuclear Power Plant", NEA/CSNI/R(2009)13, (2009).

[14] OECD/NEA, "BEMUSE Phase III Report, Uncertainty and Sensitivity Analysis of the LOFT L2-5 Test", NEA/CSNI/R(2007)4, (2007).

[15] Freixa, J., Kim, T.-W., Manera, A., "Post-test thermal-hydraulic analysis of two intermediate LOCA tests at the ROSA facility including uncertainty evaluation", in proceedings of *The 14th International Topical Meeting on Nuclear Reactor Thermal hydraulics, NURETH-14*, Toronto, Canada, September 25-30, 2011, paper NURETH14-470, (2011).

[16] Freixa, J., Kim, T.-W., Manera, A., "Thermal-Hydraulic Analysis of an Intermediate LOCA Test at the ROSA facility including Uncertainty Evaluation", in proceedings of *The 8th International Topical Meeting on Nuclear Thermal-Hydraulics, Operation and Safety (NUTHOS-8)*, Shanghai, China, October 10-14, 2010, paper N8P0242, (2010).

[17] Kloos, M., "SUSA Version 3.6, User's Guide and Tutorial, Software for Uncertainty and Sensitivity Analyses", Gesellschaft für Anlagenund Reaktorsicherheit (GRS) mbH, (2008).

[18] Pacific Northwest National Laboratory, "FRAPCON-3: Modifications to Fuel Rod Material Properties and Performance Models for High-Burnup Application", NUREG/CR-6534, **1**, PNNL-11513, (1997).

[19] Manngård, T., Stengård, J.-O., "Evaluation of the Halden IFA-650 loss-of-coolant accident experiments 5, 6 and 7", Strålsäkerhetsmyndigheten (Swedish Radiation Safety Authority) report number 2014:19, ISSN: 2000-0456, (2014).

[20] Saltelli, A., Ratto, M., Andres, T., Campolongo, F., Cariboni, J., Gatelli, D., Saisana, M., Tarantola, S., "Global Sensitivity Analysis", The Primer. John Wiley & Sons, Ltd., (2008).

[21] Cooke, R. M., van Noortwijk, J. M., "Generic graphics for uncertainty and sensitivity analysis", in proceedings of *ESREL '99 - The 10th European Conference on Safety and Reliability*, Munich, Germany, 1999, 1187-1192, (2000).

[22] Borgonovo, E., "A new uncertainty importance measure", *Reliability Engineering and System Safety*, **92**, 771-784, (2007).

[23] Plischke, E., Borgonovo, E., Smith, C. L., "Global sensitivity measures from given data", *European Journal of Operational Research*, **226**, 536–550, (2013).

[24] Sobol', I.M., "Sensitivity analysis for non-linear mathematical models", *Mathematical modelling and computational experiment*, **1**, 407-414, (1993).

[25] Draper, N., Smith, H., "Applied Regression Analysis", John Wiley & Sons Ltd, (1998).

[26] Abdelghany, J.M., Martin, R.P., "Uncertainty Analysis for Containment Response of U.S. EPR™ Reactor to Large Break Loss-of-Coolant Accidents", in proceedings of *ICAPP '10*, San Diego, U.S.A, June 12-17, 2010, Paper 10131, (2010).

[27] Glaeser, H., "GRS Method for Uncertainty and Sensitivity Evaluation of Code Results and Applications", *Science and Technology of Nuclear Installations*, Article ID 798901, (2008).

[28] Plischke, E., "An Effective Algorithm for Computing Global Sensitivity Indices (EASI)", *Reliability Engineering & Systems Safety*, **95**, 354-360, (2010).

[29] Plischke, E., "How to compute variance-based sensitivity indicators with your spreadsheet software", *Environmental Modelling & Software*, **35**, 188-191, (2012).

[30] SAMO, 2014. The course material of The Eighth Summer School on Sensitivity Analysis of Model Output (SAMO 2014), Italy, June 24 - 27, 2014; also available online at: www.immr.tu-clausthal.de/~epl/papers/papers.html (visited 26.4.2016)

[31] Arkoma, A., Ikonen, T., "Sensitivity analysis of local uncertainties in large break loss-of-coolant accident (LB-LOCA) thermo-mechanical simulations", *Nuclear Engineering and Design*, **305**, 293–302, (2016).

PUBLICATION V

Evaluation and adaptation of the RIA code SCANAIR for modelling BWR fuel and conditions

In proceedings of: TopFuel 2012, Manchester, United Kingdom, September 2-6, 2012, Paper A0089.

EVALUATION AND ADAPTATION OF THE RIA CODE SCANAIR FOR MODELLING BWR FUEL AND CONDITIONS

A. ARFFMAN
VTT Technical Research Centre of Finland
Tietotie 3, FI-02044 – Finland

A. MOAL, V. GEORGENTHUM
Institut de Radioprotection et de Sûreté Nucléaire
Centre d'études de Cadarache, 13115 – France

ABSTRACT

The SCANAIR code, developed by the Institut de Radioprotection et de Sûreté Nucléaire (IRSN), is designed for modelling the behaviour of a single fuel rod in fast transient and accident conditions during a reactivity initiated accident (RIA) in pressurized water reactor (PWR). In SCANAIR, the available fuel material properties and the thermal-hydraulics (TH) model are for PWR fuel and coolant conditions, respectively, but the code does not have similar models for boiling water reactor (BWR) to be applied in BWR RIA, the rod drop accident (RDA). Thus, the code lacks material properties of Zircaloy-2 (Zry-2) which is the cladding material in BWR fuel rod. Up until now, the only Zry-2 models implemented into the code are the laws for yield stress (YS) and ultimate tensile stress (UTS) of irradiated cladding from a bibliographic study, and the laws have not been validated with SCANAIR. New YS and UTS laws are now fitted based on PROMETRA mechanical tests and implemented into SCANAIR.

1. Introduction

The main issues to be considered in order to be able to model BWR RDA with SCANAIR are firstly the Zry-2 cladding material properties and behaviour (elastic, plastic and viscoplastic models), and secondly the BWR thermal hydraulics modelling in RIA conditions.

In this paper, the needs for the adaptation of the material properties and the TH model in SCANAIR to be sufficient for BWR fuel and conditions are discussed. The ring tensile tests for fresh and irradiated Zry-2 cladding made as part of the French PROMETRA [1] programme are utilized in fitting new YS and UTS correlations in order to more accurately model the cladding plastic behaviour. After implementing these laws into the V_7_2 version of the code, comparative SCANAIR simulations are performed by applying the old and new correlations to BWR fuel tests LS-1 and FK-1 performed in the NSRR facility in Japan at room temperature and atmospheric pressure conditions. The effect of the new models on cladding strain energy density (SED) and failure propensity is investigated. In this context, the adequacies of the code's cladding failure models regarding Zry-2 are also evaluated.

2. Zircaloy-2 material properties

As the cladding strain rates in an RIA can be around 1 s^{-1}, the cladding mechanical properties tests have to be specifically designed for reaching high strain rates. The French PROMETRA (TRAnsient MEchanical PROperties) programme is internationally the most extensive series of mechanical tests on cladding materials of PWR fuel rod under RIA loading conditions but there have not been tests on Zry-2 cladding until the recent tests utilized here. Other mechanical tests

on Zry-2 reported in open literature are GNF mechanical test on Zry-2 under RIA conditions at room temperature [2], NFD and Studsvik tests on irradiated and un-irradiated Zry-2 [3].

The integral effect test data on BWR fuel mainly comes from the NSRR facility. The test series made in NSRR on irradiated fuel consist of TS series (5 tests), FK series (11) and two LS tests, all in stagnant water. The LS-2 test was conducted in the newish high temperature, high pressure (HTHP) capsule of NSRR, and all the other tests were performed at room temperature and atmospheric pressure (RTAP). Tests on BWR fuel have also been made in SPERT facility (in USA, 10 tests during 1969-1970 on low burn-up fuel, RTAP). The rodlets tested in SPERT were of different design than the current BWR fuel rods.

Zry-2 cladding elastic behaviour, enthalpy, conductivity and thermal expansion are reported to be similar to those of Zircaloy-4 (Zry-4) [4]. Also the transition between alpha and beta phase is similar to Zry-4. There is no viscoplastic model available in open literature specifically for Zry-2 in RIA conditions but it is expected that the high temperature viscoplastic behaviour of Zry-2 is similar to Zry-4 as the differences in the heat treatment during the manufacturing process no longer play any role at high temperatures.

In contrast to the stress relieved annealing (SRA) typical for Zry-4 cladding, the heat treatment of Zry-2 is typically recrystallization annealing (RXA). This difference affects the ductility of the cladding: in RXA cladding, there are more radially oriented grains, and as the hydrides preferably precipitate along the grain boundaries, the RXA cladding has more radial hydrides [5]. It is especially the radial hydrides that make the cladding vulnerable to a pellet-cladding mechanical interaction (PCMI) induced rupture when there is a strong tensile stress in the circumferential direction.

3. Coolant modelling in BWR RDA

The thermal-hydraulics model in SCANAIR is one dimensional, single-phase model with mass and energy balance equations, and therefore the bulk boiling in BWRs cannot be taken into account. The clad-to-coolant heat exchange modelling is based on a boiling curve approach with correlations describing different boiling regimes. The model has been developed using the data from the separate effect programme PATRICIA studying the PWR conditions (280 °C inlet, 15.5 MPa, 5 m/s). In addition, the TH model has been accommodated to model stagnant water in RTAP conditions using the test results from the NSRR facility. Then again, the coefficients of the TH model have not been fitted for any other (intermediate) combination of temperature and pressure than RTAP and PWR conditions. The pressure and the temperature in BWR hot zero power (HZP) conditions (240 °C, 7 MPa) are close to the NSRR HTHP capsule (280 °C, 7 MPa) with the difference in the coolant velocity (2 m/s in BWR HZP [5]). The coefficients of the TH model may be tuned for these conditions using the test results from NSRR HTHP capsule but more instrumented tests are needed in order to do so.

On the other hand, the cold zero power (CZP; ~20-30 °C, 0.1 MPa) is considered to be the worst initial state of an RIA in BWR's because of the highest reactivity addition and the high content of undissolved radial hydrides in the cladding [5]. The coolant conditions in RTAP capsule of NSRR resemble the coolant state at BWR CZP conditions. Still, there is some difference in the coolant flow velocity as there is flow in BWR CZP conditions (0.7 m/s [5]) whereas in NSRR capsule the coolant is stagnant. However, if the flow rate is less than 1 m/s it should not have an effect to the maximum cladding surface temperature (though it has a significant effect on the film boiling duration). Then again, the initial cladding temperature in CZP conditions in BWR RDA is reported to be closer to 80 °C than to room temperature [6]. This may require some fine adjustment to be done for the TH model parameters, but more importantly the elevated

temperature affects the ductility of the cladding: the brittle to ductile transition is possible already at temperatures close to 80 °C [6].

4. New yield stress and UTS correlations

The PROMETRA data on Zry-2 originates from 12 tensile tests on ring specimens of irradiated cladding, and from 9 tests on fresh cladding specimens. The irradiated cladding material (LK3 with inner liner) has been base-irradiated 7 cycles up to the discharge burn-up of ~58 MWd/kg$_U$ during the years 1998-2005.

The corresponding PROMETRA test matrix is presented in Tab 1. The strain rate in the tests has been 1.0 s^{-1} but one test with both fresh and irradiated specimen has been done with a strain rate of 0.001 s^{-1}. Not a significant strain rate effect can be seen with the irradiated specimens.

Tab 1: PROMETRA test matrix for Zry-2 cladding ring tensile tests.

		Furnace heating					Induction heating	
T [°C]		25	50	150	280	480	600	800
strain rate [s^{-1}]	Fresh fuel							
		1			0.001	1	1	1
		1					1	1
								1
	Irradiated fuel							
			1	1	1	1	1	1
			1	1	0.001	1	1	1

With the fresh fuel samples, it should be noted that when including the measurement point of deviant (0.001 s^{-1}) strain rate, the best-fit curve may be significantly different compared to if this point would be excluded. Thus more measurements at the temperature range 200-300 °C are needed in order to verify the corresponding values of YS and UTS. Here the point is excluded from the fits. With the irradiated samples, the transition from furnace heating to induction heating may induce too low values with two measurements prior to the transition. The same samples also showed macroscopic deformation. These measurements are excluded from the fits.

As there are no measurement points above 800 °C for Zry-2, points from Zry-4 mechanical tests are added to the high temperature region when fitting the correlations. In SCANAIR, the values of YS and UTS are limited to stay at or above 50.0 MPa in order to ease the convergence so in practice this inclusion has no effect as regards the simulation results.

4.1 Fitting the new correlations

Different forms of correlations are tested in order to find the best fit with the measured points. First, the same formulation is tried as with the irradiated Zry-4, M5 and Zirlo claddings [1], presented in Eq. (1). This is also the correlation for Zry-2 YS and UTS already in SCANAIR:

$$\sigma[\mathrm{MPa}] = \frac{a + b \cdot T[^{\circ}\mathrm{C}]}{1 + e^{c(T[^{\circ}\mathrm{C}] - d)}}. \qquad (1)$$

The other correlations that were tested are a second-order polynomial for the fresh fuel points, and a linear fit for the irradiated case. The most suitable correlations (in terms of the higher coefficient of determination, R^2) are: Eq. (1) for the irradiated Zry-2 YS and UTS, and the polynomial fit for the fresh Zry-2 YS and UTS. However, to be consistent, Eq. (1) is used also with fresh Zry-2 as the differences in R^2 values between the polynomial fit and Eq. (1) are not

significant (polynomial: R^2=0.9642 (UTS), =0.9740 (YS); Eq. (1): R^2=0.9486 (UTS), =0.9681 (YS)). With irradiated samples, linear fit is found to be almost as good as the formulation in Eq. (1). The fitted curves and the trial fits as well as the previous correlations are presented in Fig 1.

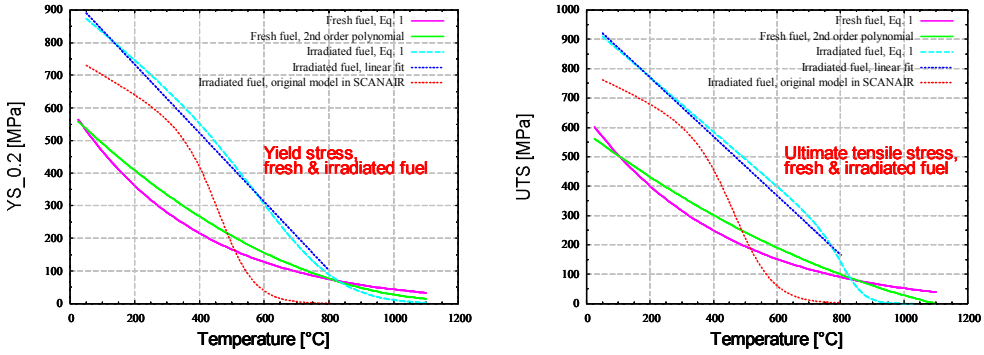

Fig 1: $YS_{0.2}$ (left hand side) and UTS (right hand side) of fresh and irradiated Zry-2.

4.2 Testing the changes by simulating NSRR tests LS-1 and FK-1 with SCANAIR

The NSRR test LS-1 [8] (reactivity insertion 4.6 $; pulse full width at half maximum 4.4 ms; targeted fuel enthalpy 126 cal/g; enthalpy at failure 53 cal/g; time of failure 240.6 ms) and FK-1 [9] (4.6 $; 4.4 ms; 130 cal/g; survived) have been conducted on irradiated BWR fuel (69 and 45 MWd/kg_U, respectively). With the LS-1 test, according to the base-irradiation calculation with VTT-ENIGMA (amended version of v5.9b), the gap is closed prior to the transient, while with FK-1 there is a gap of 76 µm (according to FRAPCON v3.4). The gap size has a very large impact on the calculated SED as can be seen in Fig 2 (left hand side, small figure). If the gap is closed, the calculated cladding mechanical SED increases by about 3 MJ/m³ when using the new correlations. If the gap is open (FK-1), the maximum mechanical SED remains unchanged. With both cases, there is not a significant impact on cladding outer temperatures whether one uses the old or the new correlations.

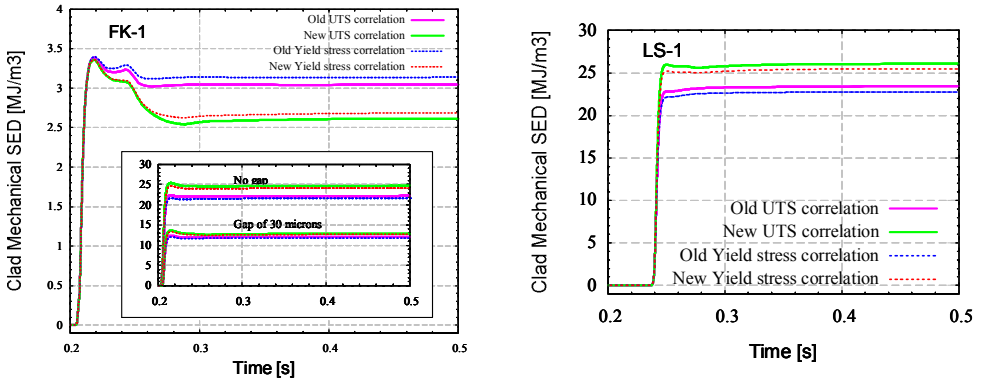

Fig 2: Cladding mechanical SED in FK-1 and LS-1 tests with the old and the new YS and UTS correlations in SCANAIR.

5. Cladding failure criteria for Zry-2 cladding

There are three different approaches in SCANAIR for predicting cladding failure: fracture mechanical model CLARIS for the PCMI type failure, strain limit based model for post burn-out ballooning failure, and a model based on calculating the strain energy density (SED) which is then compared to the critical SED (CSED) given as an input to the code. The ballooning type of failure is more relevant with fresh fuel but the problem is that there are no up-to-date tests on fresh BWR fuel in open literature for the development and validation of a ballooning type RIA failure criterion in SCANAIR.

5.1 Fracture mechanical model CLARIS

As the CLARIS model is developed for the failure predictions of PWR fuel, several additions and changes would be needed in order to apply it to BWR fuel. The J-integral database needs to be re-calculated with the CAST3M code using BWR fuel geometry (the J-integral values in CLARIS database are evaluated using three different values for the cladding thickness: 470, 520 and 570 μm, but the BWR cladding is thicker than this). The material properties of Zry-2 need to be implemented into CLARIS. The general approach in CLARIS is based on the assumption that the cladding outer brittle (hydrided) zone depth can be evaluated, but the hydride morphology is different in Zry-2 cladding than in Zry-4 (less hydrides in total, but more radial hydrides which are more detrimental). Also the fracture toughness values used in CLARIS differ between Zry-2 and -4 claddings. Because all of these factors would cause inaccuracy to the results, it is better for the moment to apply the CSED criterion for the PCMI failure predictions of BWR fuel instead of CLARIS.

5.2 Strain Energy Density

The new CSED criterion for Zry-2 by EPRI is presented in Eq. (2) [6, 7]. It is based on two open-end burst test series at room temperature [2], and thus the correlation is valid only for the PCMI phase.

$$\mathrm{CSED}[\mathrm{MJ/m^3}] = 35.89\,\mathrm{e}^{-0.0114\mathrm{H[ppm]}} + 2.09\,. \qquad (2)$$

In Eq. (2), H designates the total hydrogen content absorbed into the cladding. When the hydrogen content is not known, it can be estimated from the cladding outer oxide layer thickness with a correlation. For the FK-1 and LS-1 tests, the calculated CSEDs according to Eq. (2) are 17.9 (max. hydrogen content 72 ppm [10]) and 3.3 MJ/m³ (hydrogen content 300 ppm [8]), respectively, which means that FK-1 is correctly predicted to survive the transient, and LS-1 to fail (cf. Fig 3). Eq. (2) is applicable to be used with these tests as the cladding temperatures remain near the room temperature during the early phase of the PCMI. With LS-1, the calculated enthalpy at failure is 50 cal/g and the time of failure is 240.1 ms; thus those are in good agreement with the measurements.

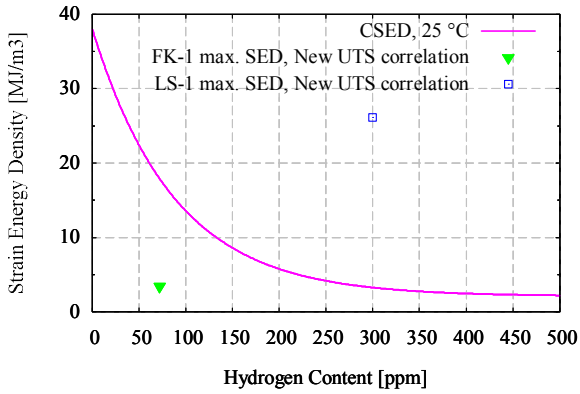

Fig 3: CSED according to Eq. (2), and the maximum values of SED for FK-1 and LS-1 according to the SCANAIR calculation.

6. Summary and Conclusions

New yield stress and UTS correlations are fitted based on the PROMETRA mechanical tests, and implemented into SCANAIR. The failure predictions with SED are found to be very sensitive to the gap size calculated by the irradiation code. Compared to the source of uncertainty resulting from that, the new YS and UTS correlations have only a minor significance to the failure predictions.

7. References

[1] B. Cazalis et al.: “The PROMETRA Program: Fuel Cladding Mechanical Behavior Under High Strain Rate”, Nuclear Technology Vol. 157, March 2007

[2] M. Nakatsuka: “Mechanical Properties of High Burnup BWR Fuel Cladding Tubes Under Simulated RIA conditions”, Proceedings of the 2004 International Meeting on LWR Fuel Performance, Orlando, Florida, September 19-22, 2004, Paper 1017

[3] L.O. Jernkvist: “A Strain-based Clad Failure Criterion for Reactivity Initiated Accidents in Light Water Reactors”, SKI Report 2004:32, August 2004

[4] D. T. Hagrman (editor): “SCDAP/ RELAP5/MOD3.1 Code Manual Volume IV: MATPRO – A Library of Materials Properties for Light-Water-Reactor Accident Analysis”, NUREG/CR-6150, EGG-2720, Volume IV, November 1993

[5] NEA WGFS: “Nuclear Fuel Behaviour under Reactivity-initiated Accident (RIA) Conditions”, State-of-the-art Report, NEA/CSNI/R(2010)1, ISBN 978-92-64-99113-2

[6] “Fuel Reliability Program: Proposed RIA Acceptance Criteria”, EPRI, Palo Alto, CA: 2010, 1021036

[7] W. Liu et al.: “Analysis of High Burnup Fuel Failures at Low Temperatures in RIA Tests Using CSED”, Proceedings of 2010 LWR Fuel Performance/TopFuel/WRFPM, Orlando, Florida, USA, September 26-29, 2010, Paper 131

[8] T. Sugiyama et al.: “Failure of high burnup fuels under reactivity-initiated accident conditions”, Annals of Nuclear Energy 36 (2009), p. 380–385

[9] T. Nakamura et al.: “Boiling Water Reactor Fuel Behavior Under Reactivity-Initiated-Accident Conditions At Burnup Of 41 To 45 GWd/tonne U”, Nuclear Technology ,Vol. 129, Feb. 2000, p. 141-151

[10] T. Nakamura et al.: “High-Burnup BWR Fuel Behavior Under Simulated Reactivity-Initiated Accident Conditions”, Nuclear Technology ,Vol. 138, June 2002, p. 246-259

PUBLICATION VI

Extending the reactivity initiated accident (RIA) fuel performance code SCANAIR for boiling water reactor (BWR) applications

Nuclear Engineering and Design, Vol. 322, pp. 192–203.

Aalto-DD 26/2018
VTT SCIENCE 170

From the nuclear fuel point of view, there are two main types of postulated design basis accidents in current light water reactors: loss-of-coolant accidents (abbreviated as LOCA) and reactivity initiated accidents (RIA). Both of these accidents are addressed in this thesis by computational modelling of single fuel rods.

The Regulatory Guides on nuclear safety in Finland require that less than 10% of the rods fail in LOCA. In order to demonstrate the fulfilment of this criterion, a statistical methodology is developed and applied to a postulated LOCA in an EPR type reactor. To show the factors affecting rod failures, a sensitivity analysis procedure is outlined and applied to the statistical analysis data.

The ability to model fuel behaviour in RIA in all types of nuclear reactors in Finland, i.e. PWRs, BWRs and VVERs, is of considerable importance. However, the simulation tool currently available is not able to consider BWR RIAs. Therefore, the modelling code is here evaluated and adapted for BWRs.

ISBN 978-952-60-7846-5 (printed)
ISBN 978-952-60-7847-2 (pdf)
ISSN-L 1799-4934
ISSN 1799-4934 (printed)
ISSN 1799-4942 (pdf)

978-951-38-8617-2 (printed)
978-951-38-8616-5 (pdf)
2242-119X
2242-119X (printed)
2242-1203 (pdf)

Aalto University
School of Science
Department of Applied Physics
www.aalto.fi

BUSINESS + ECONOMY

ART + DESIGN + ARCHITECTURE

SCIENCE + TECHNOLOGY

CROSSOVER

DOCTORAL DISSERTATIONS